

Dynamics in Quantum Spin Glass Systems

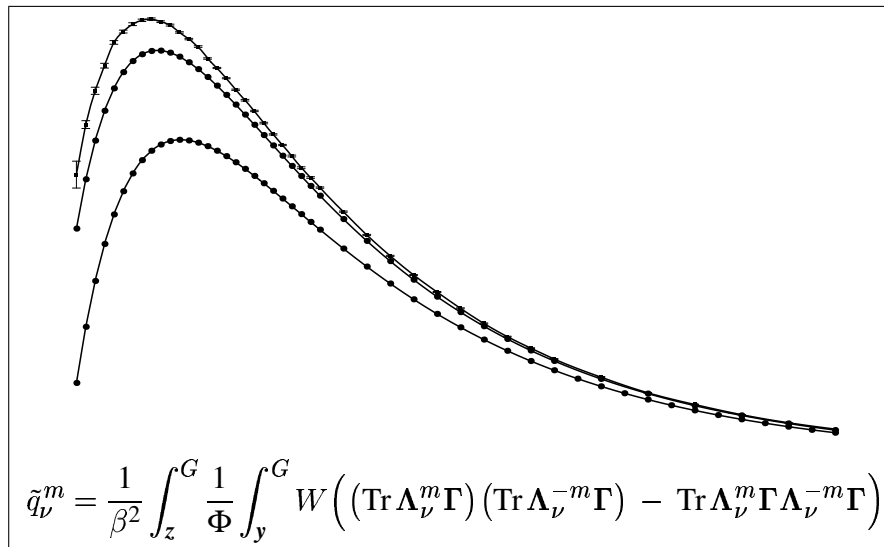
Dissertation zur Erlangung des
naturwissenschaftlichen Doktorgrades
der Bayerischen Julius-Maximilians-Universität
Würzburg

vorgelegt von

Michael Bechmann

aus

Berlin



Würzburg 2004

Eingereicht am 4. November 2004
bei der Fakultät für Physik und Astronomie

Erster Gutachter: Prof. Dr. Reinhold Oppermann

Zweiter Gutachter: Priv. Doz. Dr. Michael Potthoff

der Dissertation.

Erster Prüfer: Prof. Dr. Reinhold Oppermann

Zweiter Prüfer: Prof. Dr. Jean Geurts

der mündlichen Prüfung.

Tag der mündlichen Prüfung: 24. November 2004

to Nina

Contents

Abstract	1
Zusammenfassung	2
Introduction	3
1 The dynamical self-consistency problem	4
1.1 Model definition	4
1.2 The Popov-Fedotov-Trick	5
1.3 The dynamical spin glass decoupling scheme	7
1.3.1 Disorder average	8
1.3.2 First decoupling step and effective action	9
1.3.3 The dynamical saddle point	9
1.3.4 Second decoupling step: Non-interacting fermions	11
1.3.5 The free energy	13
1.4 The dynamical self-consistency equations	14
1.4.1 Extremization of the free energy	14
1.4.1.1 Equation for \tilde{q}_ν^0	15
1.4.1.2 Equation for q_ν	15
1.4.1.3 Equation for $\tilde{q}_\nu^{m \neq 0}$	16
1.4.1.4 Final formulation of the self-consistency equations	17
1.4.2 Explicit construction of the spin-spin correlations	18
1.4.2.1 Equation for q_ν	18
1.4.2.2 Equation for \tilde{q}_ν^m	19
1.4.3 Conclusion and summary of the dynamical self-consistency problem . .	20
2 The Heisenberg spin glass	24
2.1 The spin-static approximation	25
2.1.1 Spin-static self-consistency equations	25

2.1.1.1	The spin-static weight function	26
2.1.1.2	The general anisotropic case	27
2.1.1.3	The isotropic special case	28
2.1.2	Calculation of dynamical quantities	28
2.1.3	Selected results for the isotropic Heisenberg spin glass	29
2.1.3.1	The model on the spin space	29
2.1.3.2	The model on the Fock space	30
2.1.4	Some comments on other model variants	31
2.2	The dynamical approximation	32
2.2.1	A new systematic approximation scheme	32
2.2.2	Implementation notes and some technical details	33
2.2.3	Dynamical results for the isotropic Heisenberg spin glass on the spin space	35
2.2.3.1	Solutions in the paramagnetic phase	35
2.2.3.2	Determination of the critical temperature	35
2.2.3.3	The specific heat	38
2.2.4	Dynamical results for the isotropic Heisenberg spin glass on the Fock space	40
2.3	The perturbative $\tilde{q}_{m \neq 0}$ -expansion	40
2.3.1	Diagrammatic expansion of Φ	42
2.3.2	Results for the isotropic Heisenberg spin glass on the spin space	43
2.3.2.1	Asymptotics of the dynamical approximation scheme at large orders M	44
2.3.2.2	The static susceptibility	44
2.3.2.3	The specific heat	45
2.3.2.4	Fulfillment of the sum rule (1.41)	45
2.4	Summary and conclusion	47
3	The itinerant fermionic spin glass	49
3.1	Model definition	50
3.2	The dynamical CPA approach	50
3.3	The itinerant fermionic Ising spin glass	52
3.3.1	General solution strategies	54
3.3.2	Spin-static approximation	56
3.3.2.1	Results at finite temperature	56
3.3.2.2	The limit of zero temperature	57
	Saddle point integration of y_0	59
	Self-consistency equations.	60
	Results at zero temperature.	60
3.3.3	Dynamical solutions	61
3.3.3.1	The phase diagram in the T - t plane	61
3.3.3.2	Location of the quantum critical point	63
3.3.4	Summary and conclusion	64

A Appendix	65
A.1 Derivation of a general formula for a class of Matsubara frequency sums	65
A.2 Derivatives of the weight function W	66
A.3 Derivation of an expression for the internal energy	68
A.4 Expansions of the self-consistency equations in powers of small q_ν	69
A.4.1 The q_ν -equation and critical temperatures	69
A.4.2 The \tilde{q}_ν^m -equation	71
A.5 Computation of the critical exponent (3.43)	71
Bibliography	74
Lebenslauf	78

Abstract

This thesis aims at a description of the equilibrium dynamics of quantum spin glass systems. To this end a generic fermionic $SU(2)$, spin $1/2$ spin glass model with infinite-range interactions is defined in the first part. The model is treated in the framework of imaginary-time Grassmann field theory along with the replica formalism. A dynamical two-step decoupling procedure, which retains the full time dependence of the (replica-symmetric) saddle point, is presented. As a main result, a set of highly coupled self-consistency equations for the spin-spin correlations can be formulated.

Beyond the so-called spin-static approximation two complementary systematic approximation schemes are developed in order to render the occurring integration problem feasible. One of these methods restricts the quantum-spin dynamics to a manageable number of bosonic Matsubara frequencies. A sequence of improved approximants to some quantity can be obtained by gradually extending the set of employed discrete frequencies. Extrapolation of such a sequence yields an estimate of the full dynamical solution. The other method is based on a perturbative expansion of the self-consistency equations in terms of the dynamical correlations.

In the second part these techniques are applied to the isotropic Heisenberg spin glass both on the Fock space (HSG_F) and, exploiting the Popov-Fedotov trick, on the spin space (HSG_S). The critical temperatures of the paramagnet to spin glass phase transitions are determined accurately. Compared to the spin-static results, the dynamics causes slight increases of T_c by about 3% and 2%, respectively. For the HSG_S the specific heat $C(T)$ is investigated in the paramagnetic phase and, by way of a perturbative method, below but close to T_c . The exact $C(T)$ -curve is shown to exhibit a pronounced non-analyticity at T_c and, contradictory to recent reports by other authors, there is no indication of maximum above T_c .

In the last part of this thesis the spin glass model is augmented with a nearest-neighbor hopping term on an infinite-dimensional cubic lattice. An extended self-consistency structure can be derived by combining the decoupling procedure with the dynamical CPA method. For the itinerant Ising spin glass numerous solutions within the spin-static approximation are presented both at finite and zero temperature. Systematic dynamical corrections to the spin-static phase diagram in the plane of temperature and hopping strength are calculated, and the location of the quantum critical point is determined.

Zusammenfassung

Die vorliegende Arbeit beschäftigt sich mit der Gleichgewichtsdynamik in Quanten-Spinalglassystemen. Dazu wird im ersten Teil ein allgemeines fermionisches $SU(2)$, Spin $1/2$ Spinalglassmodell mit langreichweitiger Wechselwirkung definiert. Das Modell wird im Rahmen der Grassmann-Feldtheorie und mithilfe des Replikatricks behandelt. Es wird ein dynamisches zweistufiges Entkopplungsverfahren vorgestellt, welches die volle Zeitabhängigkeit des (replika-symmetrischen) Sattelpunktes berücksichtigt. Als ein Hauptergebnis kann ein Satz von gekoppelten Selbstkonsistenzgleichungen für die Spin-Spin-Korrelationen formuliert werden.

Über die spin-statische Näherung hinaus werden zwei komplementäre systematische Approximationsverfahren entwickelt, die das auftretende Integrationsproblem beherrschbar machen. Eine dieser Methoden beschränkt die Quantenspindynamik auf eine handhabbare Anzahl bosonischer Matsubara Frequenzen. Unter schrittweiser Hinzunahme weiterer diskreter Frequenzen ergibt sich eine Sequenz verfeinerter Näherungen einer beliebigen Größe. Durch Extrapolation kann die voll dynamische Lösung bestimmt werden. Die andere Methode fußt auf einer Störungsentwicklung der Selbstkonsistenzgleichungen in den dynamischen Korrelationen.

Im zweiten Teil werden diese Techniken angewandt auf das isotrope Heisenberg-Spinalglass sowohl auf dem Fockraum (HSG_F), als auch, unter Verwendung des Popov-Fedotov-Tricks, auf dem Spinraum (HSG_S). Die kritischen Temperaturen der Spinalglass-Phasenübergänge werden genau ermittelt. Verglichen mit den spin-statischen Ergebnissen führt die Dynamik zu leichten Erhöhungen von T_c um jeweils 3% bzw. 2%. Für das HSG_S wird die spezifische Wärme in der paramagnetischen Phase und dicht unterhalb T_c untersucht. Es wird gezeigt, daß die exakte $C(T)$ -Kurve eine Nicht-Analytizität an T_c aufweist. Dagegen finden sich keine Anzeichen eines Maximums oberhalb von T_c , was im Widerspruch zu Beobachtungen anderer Autoren steht.

Im letzten Teil dieser Arbeit wird das Spinalglassmodell um einen Hüpfsterm auf einem unendlich-dimensionalen kubischen Gitter ergänzt. Durch Kombination des Entkopplungsverfahrens und der dynamischen CPA-Methode kann eine erweiterte Selbstkonsistenzstruktur gewonnen werden. Für das itinerante Ising-Spinalglass werden innerhalb der spin-statischen Näherung zahlreiche Lösungen bei endlichen Temperaturen als auch bei $T = 0$ präsentiert. Es werden systematische dynamische Korrekturen zum spin-statischen Phasendiagramm in der Ebene von Temperatur und Hüpfstärke berechnet, woraus der quantenkritische Punkt bestimmt wird.

Introduction

During the last three decades, the theory of spin glasses has been attracting much attention. This may have two reasons. The first is its clear relevance to science. Several classes of disordered magnetic materials which manifestly exhibit spin glass behavior have been discovered by now, and numerous experiments elucidated the intriguing physical properties of these systems [31, 5, 13]. Furthermore, an adequate description of the spin glass state required new and unusual concepts in statistical mechanics. Applicable to a wide range of complex systems, these concepts have spread over many other fields of research, for instance optimization theory [29], information processing [33], or the theory of neural networks [20], to mention only a few of the most prominent examples.

A second reason for the sustaining interest in spin glass systems certainly is the big challenge they have been and continue to be offering to us. The phenomenon of non-trivial ergodicity breaking encountered in the spin glass state entails very intricate theories already at the mean field level. This point can be illustrated by the case of the fully connected Ising spin glass, the famous Sherrington-Kirkpatrick model. Despite it certainly is the most comprehensively studied and best understood genuine spin glass model, a closed exact solution in the low temperature phase could not be found yet and is still subject of intense research.

Quantum spin glass models provide yet another difficulty which arises from their inherent quantum-spin dynamics. The mean field approach to translationally invariant models of ferromagnets or antiferromagnets leads to self-consistency equations for suitably defined magnetizations, i.e. static quantities. In contrast, in the presence of disorder the corresponding self-consistency structure involves time (resp. frequency) dependent local spin-spin correlations. The resulting coupling of infinitely many dynamical degrees of freedom obstructs simple mean field solutions for quantum spin glass models even in their paramagnetic phases. This technical difficulty initially motivated the work presented in this thesis.

In the first chapter, a mean field theory for quantum spin glasses shall be formulated. Subsequently, the resulting dynamical self-consistency problem shall be tackled both analytically and numerically within especially developed systematic approximation schemes. Chapter 2 is concerned with Heisenberg spin glass variants, and the last part is dedicated to an itinerant fermionic Ising spin glass.

1

The dynamical self-consistency problem

The aim of this chapter is to establish a technical framework for the description of the equilibrium dynamics in infinite-range spin 1/2 quantum spin glass systems. To this end a generic Hamiltonian for the magnetic part of fermionic spin glass systems allowing for arbitrary global anisotropy shall be considered. It includes various physically interesting special cases, some of which will be studied in the course of this work. As the Fock space is effectively reduced to the spin space by the Popov-Fedotov chemical potential [39], the general fermionic formulation readily accounts for genuine spin models, too.

The model is treated within imaginary-time Grassmann-field theory along with the replica formalism to handle the disorder. By means of an exact two-step decoupling procedure, which retains the full dynamics of the problem, the effective action can be reduced to that of non-interacting fermions in a self-induced dynamical potential. The applied method is a quantum version of the basic decoupling scheme originally introduced in the context of the classical Ising spin glass [47, 26]. In particular, the method is the dynamical generalization of the spin-static formalism for fermionic spin glass models developed in Ref. [35].

Using a replica-symmetric Ansatz, the general self-consistency problem for the spin glass order parameter and the dynamical replica-diagonal spin-spin correlations shall be formulated. The resulting set of highly coupled self-consistency equations constitutes a central issue of this thesis. Therefore, a rather detailed derivation will be given.

1.1 Model definition

The magnetic part of fermionic spin glass systems can be described quite generally by the basic grand-canonical Hamiltonian

$$\hat{\mathcal{K}}_{\text{SG}} = \frac{1}{2} \sum_{i \neq j} \hat{\mathbf{S}}_i \mathbf{J}_{ij} \hat{\mathbf{S}}_j - \mathbf{h} \sum_i \hat{\mathbf{S}}_i - \mu \sum_i \hat{n}_i \quad (1.1)$$

with a global external magnetic field \mathbf{h} pointing in arbitrary direction and a chemical potential μ . The indices i and j label the sites of the system. In terms of the usual fermionic construc-

tion operators $a_{i\sigma}^\dagger$ and $a_{i\sigma}$, which create and destroy, respectively, a particle at site i with spin projection $\sigma = \{\uparrow, \downarrow\}$, the number operators read

$$\hat{n}_i = \sum_{\sigma} a_{i\sigma}^\dagger a_{i\sigma}. \quad (1.2)$$

Using the Pauli matrices σ_ν with $\nu = \{x, y, z\}$, the spatial components of the spin 1/2 operators are given by

$$\hat{S}_i^\nu = \sum_{\sigma\sigma'} a_{i\sigma}^\dagger \sigma_{\sigma\sigma'}^\nu a_{i\sigma'}, \quad (1.3)$$

where the conventional pre-factor $\hbar/2$ has been dropped for convenience. In this work the spin-pair interaction matrices are restricted to diagonal shape,

$$\mathbf{J}_{ij} = \begin{pmatrix} J_{ij}^x & 0 & 0 \\ 0 & J_{ij}^y & 0 \\ 0 & 0 & J_{ij}^z \end{pmatrix}, \quad (1.4)$$

i.e. there are no direct interactions between different spin components. The coupling constants $J_{ij}^\nu = J_{ji}^\nu$ are defined to be uncorrelated real random numbers drawn from the symmetric Gaussian distribution

$$P_\nu(J_{ij}^\nu) = \frac{1}{\sqrt{2\pi}\hat{J}_\nu} \exp\left(-\frac{1}{2}\left(\frac{J_{ij}^\nu}{\hat{J}_\nu}\right)^2\right). \quad (1.5)$$

The assumption of infinitely ranged interactions is expressed by the fact that the disorder distribution (1.5) is independent of the distance between two interacting spins at sites i and j . For such a model to be sensible it is essential to adapt the disorder variances to the size of the system according to

$$\hat{J}_\nu = \frac{1}{\sqrt{N}} J_\nu, \quad (1.6)$$

where N is the total number of spins and the J_ν are fixed model parameters. It will turn out that the scaling (1.6) ensures the free energy to be an extensive thermodynamic quantity.

Each spatial direction is governed by an individual parameter J_ν . Thus, the present model allows for arbitrary global anisotropy. In particular, the choice $J_\nu = 0$ entirely removes all couplings of spin components in ν -direction from the Hamiltonian (1.1). In this sense the general model includes the Ising and XY cases.

1.2 The Popov-Fedotov-Trick

There exists a strikingly simple fermionic representation of spin 1/2 systems. A spin Hamiltonian $\hat{\mathcal{H}}_S$, defined on the spin space, can be mapped onto a corresponding Hamiltonian $\hat{\mathcal{H}}_F$ on the Fock space by expressing the spin operators in terms of the fermionic construction operators according to eq. (1.3). A problem arises from the different dimensionalities of the vector spaces the two Hamiltonians act on. There are two possible orientations for each individual

spin, which amounts to a total of 2^N states available to a system of N spins. The Fock space of the corresponding fermionic system, however, is generated by 4^N many-particle states each of which is built up from four basic local states. Associated with the i^{th} site there are the two magnetic (physical) states

$$|\uparrow\rangle_i = a_{i\uparrow}^\dagger |0\rangle_i \quad \text{and} \quad |\downarrow\rangle_i = a_{i\downarrow}^\dagger |0\rangle_i \quad (1.7)$$

and, contrary to the spin space, the two non-magnetic (non-physical) states

$$|0\rangle_i \quad \text{and} \quad |\uparrow\downarrow\rangle_i = a_{i\uparrow}^\dagger a_{i\downarrow}^\dagger |0\rangle_i. \quad (1.8)$$

It was first shown by Popov and Fedotov in 1988 that this problem can be resolved easily by introducing the imaginary and temperature dependent chemical potential [39]

$$\mu_{\text{PF}} = -\frac{i\pi}{2}T. \quad (1.9)$$

Following the original proof of this statement one may write

$$\hat{\mathcal{H}}_{\text{F}} = \hat{\mathcal{H}}_{\text{F},\kappa} + \hat{\mathcal{H}}_{\text{F},\bar{\kappa}}, \quad (1.10)$$

where $\hat{\mathcal{H}}_{\text{F},\kappa}$ contains all contributions of the spin operators at some arbitrarily chosen site κ , and $\hat{\mathcal{H}}_{\text{F},\bar{\kappa}}$ is the entire remaining part. Hence, the particle number operator can be written

$$\hat{N} = \sum_i \hat{n}_i = \hat{N}_{\bar{\kappa}} + \hat{n}_{\kappa}. \quad (1.11)$$

The trace operation decomposes in a similar fashion:

$$\text{Tr} = \text{Tr}_{\bar{\kappa}} \text{Tr}_{\kappa} = \text{Tr}_{\bar{\kappa}} (\text{Tr}_{\kappa,\text{m}} + \text{Tr}_{\kappa,\text{nm}}). \quad (1.12)$$

Here the labels ‘‘m’’ and ‘‘nm’’ denote partial traces over the magnetic and non-magnetic local states (1.7, 1.8), respectively. With these definitions the grand-canonical fermionic partition function can be manipulated into

$$\begin{aligned} Z_{\text{F}} &= \text{Tr} e^{-\beta(\hat{\mathcal{H}}_{\text{F}} - \mu_{\text{PF}}\hat{N})} \\ &= \text{Tr} e^{-\beta\hat{\mathcal{H}}_{\text{F}}} e^{\mu_{\text{PF}}\hat{N}} \\ &= \text{Tr}_{\bar{\kappa}} \text{Tr}_{\kappa,\text{m}} e^{-\beta\hat{\mathcal{H}}_{\text{F}}} e^{\mu_{\text{PF}}\hat{N}} + \text{Tr}_{\bar{\kappa}} e^{-\beta\hat{\mathcal{H}}_{\text{F},\bar{\kappa}}} e^{\mu_{\text{PF}}\hat{N}_{\bar{\kappa}}} \text{Tr}_{\kappa,\text{nm}} e^{\beta\mu_{\text{PF}}\hat{n}_{\kappa}}. \end{aligned} \quad (1.13)$$

In the second and third line the facts

$$[\hat{S}_i^\nu, \hat{n}_j]_- = 0 \quad \text{and} \quad \hat{S}_i^\nu |0\rangle_i = \hat{S}_i^\nu |\uparrow\downarrow\rangle_i = 0 \quad (1.14)$$

have been used, respectively. Since

$$\text{Tr}_{\kappa,\text{nm}} e^{\beta\mu_{\text{PF}}\hat{n}_{\kappa}} = {}_{\kappa}\langle 0 | e^{-i\pi\hat{n}_{\kappa}/2} | 0 \rangle_{\kappa} + {}_{\kappa}\langle \uparrow\downarrow | e^{-i\pi\hat{n}_{\kappa}/2} | \uparrow\downarrow \rangle_{\kappa} = 1 - 1 = 0, \quad (1.15)$$

the second term on the right hand side of eq. (1.13) vanishes. In the magnetic local states (1.7) site κ is occupied by exactly one particle and hence

$$Z_{\text{F}} = -i \text{Tr}_{\bar{\kappa}} \text{Tr}_{\kappa,\text{m}} e^{-\beta\hat{\mathcal{H}}_{\text{F}}} e^{\mu_{\text{PF}}\hat{N}_{\bar{\kappa}}}. \quad (1.16)$$

The same procedure can be repeated now for all remaining sites \bar{k} . Thus, the contributions of the non-magnetic states to the partition function cancel each other while the action of the magnetic states introduces a factor $-i$ for each site. Altogether, this reasoning leads to

$$Z_F = (-i)^N \text{Tr}_m e^{-\beta \hat{\mathcal{H}}_F} = (-i)^N \text{Tr} e^{-\beta \hat{\mathcal{H}}_S} = (-i)^N Z_S. \quad (1.17)$$

Up to a unimportant constant factor, the partition function of the spin system is indeed equal to the grand-canonical partition function of the corresponding fermionic system with the chemical potential μ_{PF} defined by eq. (1.9). All physical properties of the spin system can be derived from the partition function (including appropriate generating fields as required) and can therefore be calculated within this fermionic representation.

The Popov-Fedotov trick makes the whole apparatus for fermionic many-particle systems readily applicable to spin models, and particularly it provides a standard diagram technique. The chemical potential (1.9) merely causes a shift of the fermionic Matsubara frequencies. Thus, spin 1/2 systems are characterized by the ‘‘semionic’’ Matsubara frequencies

$$s_n = \left(2n + \frac{1}{2}\right) \pi T. \quad (1.18)$$

The method has been generalized to arbitrary spin quantum numbers [52].

For the time being, the chemical potential in the generic model (1.1) remains unspecified. Later in this work it will be fixed appropriately to study specific physically relevant model variants.

1.3 The dynamical spin glass decoupling scheme

Within the formalism of continuous imaginary-time Grassmann field theory [32] the grand-canonical partition function of a single instance of the system (1.1) with a particular configuration of the random interactions \mathbf{J}_{ij} (1.4) is expressed in terms of a functional integral over anti-commuting fields ψ :

$$Z(\mathbf{J}_{ij}) = \int \mathcal{D}\psi \exp(-\mathcal{A}_0(\psi) - \mathcal{A}_J(\psi, \mathbf{J}_{ij})). \quad (1.19)$$

The two action parts are given by

$$\mathcal{A}_0(\psi) = \sum_i \int_0^\beta d\tau \bar{\Psi}_i^\tau ((\partial_\tau - \mu) \mathbb{1}_2 - \mathbf{h}\boldsymbol{\sigma}) \Psi_i^\tau, \quad (1.20)$$

$$\mathcal{A}_J(\psi, \mathbf{J}_{ij}) = \frac{1}{2} \sum_{i \neq j} \sum_\nu J_{ij}^\nu \int_0^\beta d\tau S_{\nu i}^\tau S_{\nu j}^\tau, \quad (1.21)$$

where $\Psi = (\psi_\uparrow, \psi_\downarrow)^\text{T}$ is a Grassmann spinor,

$$S_\nu = \bar{\Psi} \boldsymbol{\sigma}_\nu \Psi \quad (1.22)$$

denotes the Grassmann representation of a spin variable, and $\boldsymbol{\sigma} = (\boldsymbol{\sigma}_x, \boldsymbol{\sigma}_y, \boldsymbol{\sigma}_z)^\text{T}$ is the vector composed of the three Pauli matrices.

1.3.1 Disorder average

As the model is assumed to have quenched disorder one needs to average physical quantities rather than the partition function¹. An important example is the free energy which is related to the partition function (1.19) of an individual sample by

$$F(\mathbf{J}_{ij}) = -T \ln Z(\mathbf{J}_{ij}). \quad (1.23)$$

The disorder average of physical quantities can be accomplished by means of the famous replica trick. In the probably most prominent case of the free energy it relies on the identity

$$\ln x = \lim_{n \rightarrow 0} \frac{x^n - 1}{n}. \quad (1.24)$$

Using this representation of the logarithm in eq. (1.23) one obtains (henceforth, the symbol $[\]_{\text{dis}}$ denotes the disorder average)

$$[F(\mathbf{J}_{ij})]_{\text{dis}} = -T \lim_{n \rightarrow 0} \frac{[Z(\mathbf{J}_{ij})^n]_{\text{dis}} - 1}{n}. \quad (1.25)$$

The quantity

$$Z(\mathbf{J}_{ij})^n = \prod_{a=1}^n Z(\mathbf{J}_{ij}) = \int \mathcal{D}\psi \exp\left(-\sum_{a=1}^n (\mathcal{A}_0(\psi_a) + \mathcal{A}_J(\psi_a, \mathbf{J}_{ij}))\right) \quad (1.26)$$

can be interpreted as the partition function of a super-system comprising n exact copies (replicas) of the original system. These replicas are well separated and there is no direct interaction between them. However, the replicas are not independent of each other because the disorder configuration is the very same for all replicas.

The disorder average of eq. (1.26) amounts to an integration over the coupling constants J_{ij}^ν weighted with their Gaussian probability distribution (1.5). Recalling the Hubbard-Stratonovich integral identity

$$\exp\left(\frac{x^2}{4a^2}\right) = \frac{a}{\sqrt{\pi}} \int_{-\infty}^{\infty} d\xi \exp(-a^2 \xi^2 \pm \xi x) \quad (1.27)$$

one easily finds

$$\begin{aligned} [\exp(-\mathcal{A}_{J,n})]_{\text{dis}} &= \left(\prod_{i < j} \prod_{\nu} \int_{-\infty}^{\infty} dJ_{ij}^{\nu} P(J_{ij}^{\nu}) \right) \exp\left(-\sum_{a=1}^n \mathcal{A}_J(\psi_a, J_{ij})\right) \\ &= \exp\left(\frac{1}{4N} \sum_{\nu} J_{\nu}^2 \sum_{i \neq j} \sum_{ab} \int_0^{\beta} \int_0^{\beta} d\tau d\tau' S_{\nu ia}^{\tau} S_{\nu ja}^{\tau} S_{\nu ib}^{\tau'} S_{\nu jb}^{\tau'}\right) \end{aligned} \quad (1.28)$$

with an obvious definition of $\mathcal{A}_{J,n}$. Here the scaling (1.6) has been taken into account already.

¹A detailed discussion of quenched vs. annealed averages can be found in Ref. [13].

1.3.2 First decoupling step and effective action

In order to facilitate the functional integration over the Grassmann fields the effective four-spin, or eight-fermion interaction in eq. (1.31) has to be manipulated into a bi-linear form of the Grassmann fields. This requires a two-step decoupling procedure [35, 3] which shall be discussed in the following.

First, the site sum of the four-spin products in eq. (1.31) can be rewritten as

$$\sum_{i \neq j} S_{via}^\tau S_{vja}^\tau S_{vib}^{\tau'} S_{vjb}^{\tau'} = \left(\sum_i S_{via}^\tau S_{vib}^{\tau'} \right)^2 - \sum_i \left(S_{via}^\tau S_{vib}^{\tau'} \right)^2. \quad (1.29)$$

The second contribution is of order $O(N)$ smaller than the first one, and is therefore it is negligible in the limit of a infinitely large system. Now the leading contribution can be decoupled by means of site-global, time and replica dependent Hubbard-Stratonovich fields according to eq. (1.27). This operation yields

$$[\exp(-\mathcal{A}_{J,n})]_{\text{dis}} = \text{const.} \int \mathcal{D}Q \exp(-\mathcal{A}_{J,\text{eff}}(\psi, Q)) \quad (1.30)$$

with the effective action

$$\mathcal{A}_{J,\text{eff}}(\psi, Q) = \sum_\nu J_\nu^2 \sum_{ab} \int_0^\beta \int_0^\beta d\tau d\tau' \left(\frac{1}{4} N \left(Q_{\nu ab}^{\tau\tau'} \right)^2 - \frac{1}{2} \sum_i S_{via}^\tau Q_{\nu ab}^{\tau\tau'} S_{vib}^{\tau'} \right). \quad (1.31)$$

Comparison of the actions (1.21, 1.31), both being of fourth order in the Grassmann fields, reveals the progress accomplished so far. The disorder average and the subsequent first decoupling step result in an effective single-site problem. As a drawback, the method generates inter-replica couplings.

1.3.3 The dynamical saddle point

The further evaluation of eq. (1.30) relies on the elimination of the spin glass fields $Q_{\nu ab}^{\tau\tau'}$ by means of a saddle point integration which becomes exact in the limit $N \rightarrow \infty$. A common way to proceed would be the assumption of a replica-symmetric and spin-static (i.e. $\tau\tau'$ -independent) saddle point [35, 34]. The main issue of this thesis is, however, the role played by the quantum dynamics, and hence the full time dependence shall be retained.

General saddle point equations can be derived by imposing the stationarity condition to the replicated and disorder averaged partition function. Using the symbol $\langle \rangle_{\text{th}}$ for the thermal (quantum-statistical) average, the saddle point values of the spin glass fields can be formally expressed in terms of the corresponding averaged spin products at some arbitrarily chosen lattice site, say $i = s$:

$$Q_{\nu a \neq b}^{\tau\tau'} \Big|_{\text{s.p.}} = \left[\left\langle S_{\nu sa}^\tau S_{\nu sb}^{\tau'} \right\rangle_{\text{th}}^{a \neq b} \right]_{\text{dis}} = \left[\left\langle S_{\nu sa}^0 \right\rangle_{\text{th}} \left\langle S_{\nu sb}^0 \right\rangle_{\text{th}} \right]_{\text{dis}}, \quad (1.32 \text{ a})$$

$$Q_{\nu aa}^{\tau\tau'} \Big|_{\text{s.p.}} = \left[\left\langle S_{\nu sa}^\tau S_{\nu sa}^{\tau'} \right\rangle_{\text{th}} \right]_{\text{dis}} = \left[\left\langle S_{\nu sa}^{|\tau-\tau'|} S_{\nu sa}^0 \right\rangle_{\text{th}} \right]_{\text{dis}}. \quad (1.32 \text{ b})$$

Clearly, the inter-replica correlations (1.32 a) are independent of time because the replicas are decoupled before the disorder average or, in other words, the fermions can not propagate between distinct replications of the system. All quantum-dynamical behavior of the model originates from the replica-diagonal spin-spin correlations. Since the Grassmann representations of the spin operators in (1.32 b) commute, the dynamical saddle point depends on the absolute difference of the two time arguments only.

The work presented here is based on the choice of a replica-symmetric saddle point possessing the appropriate time dependence according to eqs. (1.32):

$$Q_{\nu a \neq b}^{\tau \tau'} \Big|_{\text{s.p.}} =: q_{\nu}, \quad (1.33 \text{ a})$$

$$Q_{\nu aa}^{\tau \tau'} \Big|_{\text{s.p.}} =: \tilde{q}_{\nu}^{|\tau - \tau'|}. \quad (1.33 \text{ b})$$

In the following, the theory shall be developed in the discrete frequency space. The Fourier transformations of the saddle point functions $\tilde{q}_{\nu}^{|\tau - \tau'|}$ and of the Grassmann fields are used in the form

$$\Psi^{\tau} = T \sum_{l=-\infty}^{\infty} \Psi^l \exp(-iz_l \tau), \quad (1.34)$$

$$\tilde{q}_{\nu}^{|\tau - \tau'|} = \sum_{m=-\infty}^{\infty} \tilde{q}_{\nu}^m \exp(-i\omega_m (\tau - \tau')), \quad (1.35)$$

where z_l and ω_m denote the usual fermionic and bosonic Matsubara frequencies, respectively. The real Fourier coefficients $\tilde{q}_{\nu}^m = \tilde{q}_{\nu}(\omega_m)$ are the central quantities in the further formulation of the theory. These parameters obey the symmetry relation

$$\tilde{q}_{\nu}^m = \tilde{q}_{\nu}^{-m}, \quad (1.36)$$

and they are intimately related to the local dynamical spin susceptibility:

$$\chi_{\nu}^m = \chi_{\nu}(\omega_m) = \beta (\tilde{q}_{\nu}^m - q_{\nu} \delta_{m,0}). \quad (1.37)$$

Substituting the Fourier decompositions of the time-dependent quantities (1.34, 1.35) into eq. (1.31) and performing the time integrations one arrives at the effective saddle point action (the vector notation of the arguments shall symbolize dependence on all parameters q_{ν} and \tilde{q}_{ν}^m)

$$\mathcal{A}_{J,\text{sp}}(\psi, \mathbf{q}, \tilde{\mathbf{q}}) = -nNS(\mathbf{q}, \tilde{\mathbf{q}}) - \frac{1}{2\beta^2} \sum_{i\nu} J_{\nu}^2 \left(q_{\nu} \sum_{a \neq b} \mathcal{S}_{\nu ia}^{m=0} \mathcal{S}_{\nu ib}^{m=0} + \sum_{m=-\infty}^{\infty} \tilde{q}_{\nu}^m \sum_{a=1}^n \mathcal{S}_{\nu ia}^m \mathcal{S}_{\nu ia}^{-m} \right), \quad (1.38)$$

where the special notation

$$\mathcal{S}_{\nu ia}^m = \sum_{l=-\infty}^{\infty} \bar{\Psi}_{ia}^{l+m} \sigma_{\nu} \Psi_{ia}^l \quad (1.39)$$

and the abbreviation

$$S(\mathbf{q}, \tilde{\mathbf{q}}) = \frac{\beta^2}{4} \sum_{\nu} J_{\nu}^2 \left(q_{\nu}^2 - \sum_{m=-\infty}^{\infty} (\tilde{q}_{\nu}^m)^2 \right) \quad (1.40)$$

have been introduced. Irrelevant terms of order $O(n^2)$, which do not contribute in the replica limit, have been ignored.

A general property of the model variant on the spin space can be established by considering the replica-diagonal spin-spin correlation (1.32 b) at equal times $\tau = \tau'$. From the property of the Pauli matrices $\sigma_{\nu}^2 = \mathbb{1}_2$ and the fact that for the spin model the trace is effectively restricted to magnetic states (see Sec. 1.2) directly follows $\tilde{q}_{\nu}^{\tau=\tau'} = 1$. By the Fourier transformation (1.35) one obtains the important sum rule

$$\sum_{m=-\infty}^{\infty} \tilde{q}_{\nu}^m = 1 \quad (1.41)$$

for all model variants on the spin space.

1.3.4 Second decoupling step: Non-interacting fermions

In order to decouple the static part, i.e. the $m = 0$ part of the saddle point action (1.38) the inter-replica interactions may be rewritten as

$$\sum_{a \neq b} \mathcal{S}_{\nu ia}^{m=0} \mathcal{S}_{\nu ib}^{m=0} = \left(\sum_{a=1}^n \mathcal{S}_{\nu ia}^{m=0} \right)^2 - \sum_{a=1}^n (\mathcal{S}_{\nu ia}^{m=0})^2. \quad (1.42)$$

The first term on the right hand side of eq. (1.42) is decoupled by a replica-global Hubbard-Stratonovich field $z_{\nu i}$, whereas the second term is treated together with the \tilde{q}_{ν}^0 -contribution to the action (1.38) using a replica-local field $y_{\nu ia,0}$.

The decoupling of the dynamical (i.e. $m \neq 0$) interactions is facilitated by the algebraic identity

$$\mathcal{S}_{\nu ia}^m \mathcal{S}_{\nu ia}^{-m} = \frac{1}{4} (\mathcal{S}_{\nu ia}^m + \mathcal{S}_{\nu ia}^{-m})^2 + \frac{1}{4} (i \mathcal{S}_{\nu ia}^m - i \mathcal{S}_{\nu ia}^{-m})^2. \quad (1.43)$$

For the two squares on the right hand side of eq. (1.43) the two individual replica-local decoupling fields $y_{\nu ia,m}^+$ and $y_{\nu ia,m}^-$ are used, where the superscripts correspond to the respective signs inside the brackets. Making explicit use of the symmetry relation (1.36) the second decoupling step altogether leads to

$$\begin{aligned} \exp(-\mathcal{A}_{J,\text{sp}}) &= \exp(nNS(\mathbf{q}, \tilde{\mathbf{q}})) \int_{\mathbf{z}} \int_{\mathbf{y}}^G \times \\ &\exp \left(\frac{1}{\beta} \sum_{i a \nu} J_{\nu} \left((\sqrt{q_{\nu}} z_{\nu i} + \sqrt{\tilde{q}_{\nu}^0 - q_{\nu}} y_{\nu ia,0}) \mathcal{S}_{\nu ia}^{m=0} + \right. \right. \\ &\left. \left. \sum_{m>0} \sqrt{\frac{\tilde{q}_{\nu}^m}{2}} \left(y_{\nu ia,m}^+ (\mathcal{S}_{\nu ia}^m + \mathcal{S}_{\nu ia}^{-m}) + i y_{\nu ia,m}^- (\mathcal{S}_{\nu ia}^m - \mathcal{S}_{\nu ia}^{-m}) \right) \right) \right). \end{aligned} \quad (1.44)$$

A comment on the employed shorthand notation for the Gaussian integrations is due. The basic Gaussian integral operator is defined by

$$\int_x^G f(x) = \frac{1}{\sqrt{2\pi}} \int_{-\infty}^{\infty} dx \exp\left(-\frac{x^2}{2}\right) f(x). \quad (1.45)$$

Multiple Gaussian integrations over all z -type (replica-global) and y -type (replica-local) fields, which occur in the expression to be integrated, shall be denoted by the vector symbols \mathbf{z} and \mathbf{y} , respectively. In eq. (1.44), for instance, the explicit meaning of these abbreviations is

$$\int_{\mathbf{z}}^G = \prod_{i\nu} \int_{z_{\nu i}}^G, \quad (1.46 \text{ a})$$

$$\int_{\mathbf{y}}^G = \prod_{ia\nu} \int_{y_{\nu ia,0}}^G \prod_{m>0} \int_{y_{\nu ia,m}^+}^G \int_{y_{\nu ia,m}^-}^G. \quad (1.46 \text{ b})$$

By means of the two-step dynamical decoupling procedure described above the effective spin glass interaction in eq. (1.28) has been reduced to a bi-linear form of the Grassmann fields in eq. (1.44). In order to perform the Grassmann path integral it is convenient to slightly reorganize the action by introducing the real effective static magnetic fields

$$H_{\nu ia}^{m=0} = h_{\nu} + J_{\nu} \left(\sqrt{q_{\nu}} z_{\nu i} + \sqrt{\tilde{q}_{\nu}^0 - q_{\nu}} y_{\nu ia,0} \right) \quad (1.47)$$

and the complex effective dynamical magnetic fields

$$H_{\nu ia}^{m \neq 0} = \begin{cases} J_{\nu} \sqrt{\frac{1}{2} \tilde{q}_{\nu}^m} \left(y_{\nu ia,m}^+ + i y_{\nu ia,m}^- \right), & m > 0, \\ (H_{\nu ia}^{-m})^*, & m < 0. \end{cases} \quad (1.48)$$

Using the definition

$$\mathbf{v}_{ia}^m = \sum_{\nu} \sigma_{\nu} H_{\nu ia}^m \quad (1.49)$$

the disorder averaged partition function of the n -fold replicated system finally acquires the compact form

$$[Z^n]_{\text{dis}} = \int_{\mathbf{z}}^G \int_{\mathbf{y}}^G \mathcal{D}\psi \exp(-\mathcal{A}_{\text{eff}}), \quad (1.50)$$

where the complete effective action reads

$$\mathcal{A}_{\text{eff}} = -nNS(\mathbf{q}, \tilde{\mathbf{q}}) - \frac{1}{\beta} \sum_{ia} \sum_{ll'} \bar{\Psi}_{ia}^l \left((iz_l + \mu) \mathbb{1}_2 \delta_{ll'} + \mathbf{v}_{ia}^{l-l'} \right) \Psi_{ia}^{l'}. \quad (1.51)$$

According to eq. (1.51) the original problem has been mapped onto an ensemble of non-interacting fermions which are subject to a complex replica and spin dependent effective random potential \mathbf{V}_{ia} . In the (tensor) product space of the space spanned by the fermionic Matsubara

frequencies and the two-dimensional spin space, the effective potential is a matrix of block-Toeplitz structure:

$$\mathbf{V}_{ia} = \begin{pmatrix} \ddots & & & & \ddots \\ & \mathbf{v}_{ia}^0 & \mathbf{v}_{ia}^{-1} & \mathbf{v}_{ia}^{-2} & \mathbf{v}_{ia}^{-3} \\ & \mathbf{v}_{ia}^1 & \mathbf{v}_{ia}^0 & \mathbf{v}_{ia}^{-1} & \mathbf{v}_{ia}^{-2} \\ & \mathbf{v}_{ia}^2 & \mathbf{v}_{ia}^1 & \mathbf{v}_{ia}^0 & \mathbf{v}_{ia}^{-1} \\ & \mathbf{v}_{ia}^3 & \mathbf{v}_{ia}^2 & \mathbf{v}_{ia}^1 & \mathbf{v}_{ia}^0 \\ & \ddots & & & \ddots \end{pmatrix}. \quad (1.52)$$

From the definitions (1.48, 1.49) it follows the relation $\mathbf{v}_{ia}^{-m} = (\mathbf{v}_{ia}^m)^\dagger$ and hence the hermiticity of the dynamical effective potential, $\mathbf{V}_{ia} = \mathbf{V}_{ia}^\dagger$.

Due to the site-global decoupling (1.30), made possible by the assumed infinite-range interactions, there are no couplings between different sites any more. Indeed, the partition function (1.50) can be expressed as a product of identical site-local contributions, and therefore it represents a single-site problem. Henceforth, the site index i will be dropped (until now it has been kept anticipating the treatment of the itinerant spin glass model in Chap. 3).

1.3.5 The free energy

The replicas in eq. (1.51) are joined only by the replica-global fields z_ν . In respect to the Grassmann integration they are independent of each other, and thus their contributions factorize. According to an algebraic standard identity the result of the Grassmann integration in eq. (1.50) is exactly the determinant of the matrix generating the bi-linear form of the Grassmann fields in the exponent [32]. For each replica this matrix is given by (up to a trivial factor $1/\beta$)

$$\Gamma_a^{-1} = \mathbf{G}_0^{-1} + \mathbf{V}_a, \quad (1.53)$$

where

$$\left(\mathbf{G}_0^{-1} \right)_{ll'} = (iz_l + \mu) \delta_{ll'} \mathbb{1}_2 \quad (1.54)$$

is the inverse of the Green's function of the non-magnetic system (i.e. $J_\nu \equiv 0$ and $h_\nu \equiv 0$). The Green's function Γ defined by eq. (1.53) inherits the non-diagonality in frequency space from the potential (1.52) and can thus be viewed as an auxiliary object only. It can be interpreted as a full propagator of the effective ensemble of non-interacting fermions subjected to a particular configuration of the magnetic fields (1.47, 1.48). Meaningful physical results, however, always involve properly weighted averages over these effective fields.

For the determinant mentioned above to be finite and sensible a suitable regularization is necessary. This need is an inherent feature of the continuous-time formalism employed here. In the present context, regularization means that the partition function is evaluated relatively to an (preferably exactly solvable) reference system. The simplest choice is the system described by the trivial Hamiltonian operator

$$\mathcal{H}_{\text{reg}} = 0, \quad (1.55)$$

the partition function

$$Z_{\text{reg}} = \text{Tr} e^{-\beta \mathcal{H}_{\text{reg}}} = 4^N, \quad (1.56)$$

and the corresponding free Green's function

$$(\mathbf{G}_{\text{reg}}^{-1})_{ll'} = iz_l \delta_{ll'} \mathbb{1}_2. \quad (1.57)$$

Finally, the result of the Grassmann integration for any replica a can be written as

$$W(\mathbf{q}, \tilde{\mathbf{q}}, \mathbf{z}, \mathbf{y}_a) = \det(\Gamma_a^{-1} / \mathbf{G}_{\text{reg}}^{-1}). \quad (1.58)$$

Using the definition

$$\Phi(\mathbf{q}, \tilde{\mathbf{q}}, \mathbf{z}) = \int_{\mathbf{y}_a}^G W(\mathbf{q}, \tilde{\mathbf{q}}, \mathbf{z}, \mathbf{y}_a) \quad (1.59)$$

the partition function takes the form

$$[Z^n]_{\text{dis}} = Z_{\text{reg}} \exp(nNS(\mathbf{q}, \tilde{\mathbf{q}})) \int_{\mathbf{z}}^G \Phi(\mathbf{q}, \tilde{\mathbf{q}}, \mathbf{z})^{nN}. \quad (1.60)$$

In this expression the replicas do not appear explicitly any more. After analytical continuation of the integer n to non-integer values the replica limit $n \rightarrow 0$ can be taken according to eq. (1.25). This yields the disorder averaged free energy per site

$$\beta f(\mathbf{q}, \tilde{\mathbf{q}}) = 2 \ln 2 - S(\mathbf{q}, \tilde{\mathbf{q}}) - \int_{\mathbf{z}}^G \ln \Phi(\mathbf{q}, \tilde{\mathbf{q}}, \mathbf{z}). \quad (1.61)$$

Unfortunately, the determinant eq. (1.58) and hence the functional Φ (1.59) can be evaluated analytically only within the spin-static approximation (see Sec. 2.1.1.1). For a general dynamical treatment one has to retain the matrix structure of the theory.

1.4 The dynamical self-consistency equations

In this section the general dynamical self-consistency equations shall be derived in two different ways. Within the first method the free energy (1.61) is extremized with respect to the saddle point values q_ν and \tilde{q}_ν^m . As an alternative to this standard method the spin-spin correlations (1.32) are constructed explicitly making use of Wick's theorem.

1.4.1 Extremization of the free energy

For the (formal) integration over the spin glass fields it has been assumed in Sec. 1.3.3 that there exists a saddle point (1.33) in the $Q_{\nu ab}^{\tau\tau'}$ -dependence of the effective action (1.31). After Grassmann integration and replica limit, the saddle point can now be determined requiring stationarity of the free energy (1.61). This leads to conditional equations which involve derivatives of the functional Φ (1.59) with respect to the parameters q_ν and \tilde{q}_ν^m . It appears convenient to express these equations in terms of derivatives of the weight function W (1.58) with respect to the effective magnetic fields (1.47, 1.48) in a first step. As the replica limit has been taken already to obtain the expression for the free energy, the replica indices are superfluous and will be dropped in this section.

1.4.1.1 Equation for \tilde{q}_ν^0

To start with the simplest case of the static replica-diagonal spin-spin correlations, from eqs. (1.61, 1.40) follows

$$\frac{\partial}{\partial \tilde{q}_\nu^0} \beta f \stackrel{!}{=} 0 \quad \Rightarrow \quad \tilde{q}_\nu^0 = \frac{2}{\beta^2 J_\nu^2} \int_z \frac{1}{\Phi} \frac{\partial}{\partial \tilde{q}_\nu^0} \Phi. \quad (1.62)$$

Since the parameters \tilde{q}_ν^0 appear in the static magnetic fields H_ν^0 only one can write

$$\frac{\partial}{\partial \tilde{q}_\nu^0} \Phi = \int_y^G \underbrace{\frac{J_\nu}{2\sqrt{\tilde{q}_\nu^0 - q_\nu}} y_{\nu,0}}_{\partial H_\nu^0 / \partial \tilde{q}_\nu^0} \frac{\partial}{\partial H_\nu^0} W. \quad (1.63)$$

Integration by parts, i.e. using the identity

$$\int_x^G x g(x) = \int_x^G \frac{\partial}{\partial x} g(x), \quad (1.64)$$

yields

$$\begin{aligned} \frac{\partial}{\partial \tilde{q}_\nu^0} \Phi &= \int_y^G \frac{J_\nu}{2\sqrt{\tilde{q}_\nu^0 - q_\nu}} \frac{\partial}{\partial y_{\nu,0}} \frac{\partial}{\partial H_\nu^0} W \\ &= \int_y^G \frac{J_\nu}{2\sqrt{\tilde{q}_\nu^0 - q_\nu}} \underbrace{J_\nu \sqrt{\tilde{q}_\nu^0 - q_\nu}}_{\partial H_\nu^0 / \partial y_{\nu,0}} \frac{\partial}{\partial H_\nu^0} \frac{\partial}{\partial H_\nu^0} W. \end{aligned} \quad (1.65)$$

The second step is correct because W depends on $y_{\nu,0}$ via H_ν^0 only. For the moment one finds the intermediate result

$$\tilde{q}_\nu^0 = \frac{1}{\beta^2} \int_z^G \frac{1}{\Phi} \int_y^G \frac{\partial}{\partial H_\nu^0} \frac{\partial}{\partial H_\nu^0} W. \quad (1.66)$$

1.4.1.2 Equation for q_ν

In the case of the spin glass order parameters the stationarity condition leads to

$$\frac{\partial}{\partial q_\nu} \beta f \stackrel{!}{=} 0 \quad \Rightarrow \quad q_\nu = -\frac{2}{\beta^2 J_\nu^2} \int_z^G \frac{1}{\Phi} \frac{\partial}{\partial q_\nu} \Phi. \quad (1.67)$$

Again, the components q_ν appear in the static magnetic fields H_ν^0 only. Thus, the calculation is similar to that in the previous section:

$$\begin{aligned} \int_z^G \frac{1}{\Phi} \frac{\partial}{\partial q_\nu} \Phi &= \int_z^G \frac{1}{\Phi} \int_y^G \underbrace{\frac{J_\nu}{2} \left(\frac{1}{\sqrt{q_\nu}} z_\nu - \frac{1}{\sqrt{\tilde{q}_\nu^0 - q_\nu}} y_{\nu,0} \right)}_{\partial H_\nu^0 / \partial q_\nu} \frac{\partial}{\partial H_\nu^0} W \\ &= -\frac{\beta^2 J_\nu^2}{2} \tilde{q}_\nu^0 + \int_z^G \frac{J_\nu}{2\sqrt{q_\nu}} \frac{\partial}{\partial z_\nu} \frac{1}{\Phi} \int_y^G \frac{\partial}{\partial H_\nu^0} W \end{aligned}$$

$$\begin{aligned}
&= \int_z^G \frac{J_\nu}{2\sqrt{q_\nu}} \frac{-1}{\Phi^2} \left(\frac{\partial}{\partial z_\nu} \Phi \right) \int_y^G \frac{\partial}{\partial H_\nu^0} W \\
&= - \int_z^G \frac{J_\nu}{2\sqrt{q_\nu}} \underbrace{\frac{J_\nu \sqrt{q_\nu}}{\partial H_\nu^0 / \partial q_\nu}}_{\frac{1}{\Phi^2}} \left(\int_y^G \frac{\partial}{\partial H_\nu^0} W \right)^2.
\end{aligned} \tag{1.68}$$

One obtains

$$q_\nu = \frac{1}{\beta^2} \int_z^G \frac{1}{\Phi^2} \left(\int_y^G \frac{\partial}{\partial H_\nu^0} W \right)^2. \tag{1.69}$$

1.4.1.3 Equation for $\tilde{q}_\nu^{m \neq 0}$

Due to the symmetry relation (1.36), \tilde{q}_ν^m and \tilde{q}_ν^{-m} may be understood as a single independent parameter of the free energy. Hence, the stationarity condition is

$$\frac{\partial}{\partial \tilde{q}_\nu^m} \beta f \stackrel{!}{=} 0 \quad \Rightarrow \quad \tilde{q}_\nu^m = \frac{1}{\beta^2 J_\nu^2} \int_z^G \frac{1}{\Phi} \frac{\partial}{\partial \tilde{q}_\nu^m} \Phi. \tag{1.70}$$

Without loss of generality $m > 0$ is assumed in this section. Each of the parameters \tilde{q}_ν^m appears in the two dynamical magnetic fields H_ν^m and H_ν^{-m} defined in eq. (1.48):

$$\begin{aligned}
\frac{\partial}{\partial \tilde{q}_\nu^m} \Phi &= \int_y^G \left(\underbrace{\frac{J_\nu}{2^{\frac{3}{2}} \sqrt{\tilde{q}_\nu^m}} (y_{\nu,m}^+ + i y_{\nu,m}^-)}_{\partial H_\nu^m / \partial \tilde{q}_\nu^m} \frac{\partial}{\partial H_\nu^m} + \underbrace{\frac{J_\nu}{2^{\frac{3}{2}} \sqrt{\tilde{q}_\nu^m}} (y_{\nu,m}^+ - i y_{\nu,m}^-)}_{\partial H_\nu^{-m} / \partial \tilde{q}_\nu^m} \frac{\partial}{\partial H_\nu^{-m}} \right) W \\
&= \frac{J_\nu}{2^{\frac{3}{2}} \sqrt{\tilde{q}_\nu^m}} \int_y^G \left(\frac{\partial}{\partial y_{\nu,m}^+} \left(\frac{\partial}{\partial H_\nu^m} + \frac{\partial}{\partial H_\nu^{-m}} \right) + i \frac{\partial}{\partial y_{\nu,m}^-} \left(\frac{\partial}{\partial H_\nu^m} - \frac{\partial}{\partial H_\nu^{-m}} \right) \right) W \\
&= \frac{J_\nu}{2^{\frac{3}{2}} \sqrt{\tilde{q}_\nu^m}} \int_y^G \left(\underbrace{\frac{J_\nu \sqrt{\tilde{q}_\nu^m}}{2}}_{\partial H_\nu^{\pm m} / \partial y_{\nu,m}^+} \left(\frac{\partial^2}{\partial H_\nu^{m2}} + \frac{\partial^2}{\partial H_\nu^{-m2}} + 2 \frac{\partial}{\partial H_\nu^m} \frac{\partial}{\partial H_\nu^{-m}} \right) + \right. \\
&\quad \left. i \underbrace{i J_\nu \sqrt{\tilde{q}_\nu^m}}_{\pm \partial H_\nu^{\pm m} / \partial y_{\nu,m}^-} \left(\frac{\partial^2}{\partial H_\nu^{m2}} + \frac{\partial^2}{\partial H_\nu^{-m2}} - 2 \frac{\partial}{\partial H_\nu^m} \frac{\partial}{\partial H_\nu^{-m}} \right) \right) W \tag{1.71}
\end{aligned}$$

In the last line all but the mixed derivative terms cancel. This yields

$$\tilde{q}_\nu^m = \frac{1}{\beta^2} \int_z^G \frac{1}{\Phi} \int_y^G \frac{\partial}{\partial H_\nu^m} \frac{\partial}{\partial H_\nu^{-m}} W \tag{1.72}$$

which is consistent with expression (1.66) for the zero frequency components.

1.4.1.4 Final formulation of the self-consistency equations

In order to complete the derivation of the self-consistency equations the required derivatives of the determinant W with respect to the effective magnetic fields have to be evaluated. This can be achieved by means of the matrix identity

$$\det \mathbf{M} = \exp \operatorname{Tr} \ln \mathbf{M}. \quad (1.73)$$

Application of this identity to W , eq. (1.58), yields

$$\frac{\partial}{\partial H_\nu^m} W = W \frac{\partial}{\partial H_\nu^m} \operatorname{Tr} \ln (\mathbf{\Gamma}^{-1} / \mathbf{G}_{\text{reg}}^{-1}) = W \frac{\partial}{\partial H_\nu^m} \operatorname{Tr} \ln (\mathbb{1} + \mathbf{G}_0 \mathbf{V}). \quad (1.74)$$

In the second step it has been used that \mathbf{G}_0 as well as \mathbf{G}_{reg} are independent of H_ν^m . The further treatment of eq. (1.74) relies on the expansion of the \ln in terms of matrix powers of $\mathbf{G}_0 \mathbf{V}$ according to the series expansion

$$\ln (\mathbb{1} + \mathbf{M}) = \sum_{k=1}^{\infty} \frac{(-1)^{k+1}}{k} \mathbf{M}^k. \quad (1.75)$$

Exploiting the cyclic invariance of the trace operation one finds

$$\begin{aligned} \frac{\partial}{\partial H_\nu^m} W &= W \operatorname{Tr} \sum_{k=1}^{\infty} \sum_{i=1}^k \frac{(-1)^{k+1}}{k} (\mathbf{G}_0 \mathbf{V})^{i-1} \left(\mathbf{G}_0 \frac{\partial}{\partial H_\nu^m} \mathbf{V} \right) (\mathbf{G}_0 \mathbf{V})^{k-i} \\ &= W \operatorname{Tr} \sum_{k=0}^{\infty} (-1)^k \underbrace{\left(\frac{\partial}{\partial H_\nu^m} \mathbf{V} \right)}_{=: \mathbf{\Lambda}_\nu^m} (\mathbf{G}_0 \mathbf{V})^k \mathbf{G}_0 \\ &= W \operatorname{Tr} \mathbf{\Lambda}_\nu^m \mathbf{\Gamma}. \end{aligned} \quad (1.76)$$

The constant auxiliary matrix $\mathbf{\Lambda}_\nu^m$ introduced in the second line selects the proper directional and frequency contributions. Due to the construction of the effective potential matrix \mathbf{V} defined by eqs. (1.52, 1.49) the only non-vanishing entries of $\mathbf{\Lambda}_\nu^m$ are σ_ν -blocks along the m^{th} sub-diagonal:

$$(\mathbf{\Lambda}_\nu^m)_{ll'} = \sigma_\nu \delta_{l+m, l'}, \quad \mathbf{\Lambda}_\nu^m = \begin{pmatrix} 0 & \cdots & 0 \\ \vdots & 0 & \\ \sigma_\nu & 0 & \vdots \\ \vdots & \sigma_\nu & 0 \\ 0 & \cdots & \sigma_\nu & \cdots & 0 \end{pmatrix}, \quad \mathbf{\Lambda}_\nu^{-m} = \mathbf{\Lambda}_\nu^{m\dagger}. \quad (1.77)$$

Combining eqs. (1.69, 1.76) one arrives at the self-consistency equation for the replica-symmetric spin glass order parameters

$$q_\nu = \frac{1}{\beta^2} \int_z \frac{1}{\Phi^2} \left(\int_y W \operatorname{Tr} \mathbf{\Lambda}_\nu^0 \mathbf{\Gamma} \right)^2. \quad (1.78)$$

A general calculation of multiple effective field derivatives of W will be presented in App. A.2. At second order the general expression reads

$$\frac{\partial}{\partial H_{\nu'}^{m'}} \frac{\partial}{\partial H_{\nu}^m} W = W (\text{Tr } \Lambda_{\nu}^m \Gamma) (\text{Tr } \Lambda_{\nu'}^{m'} \Gamma) - W \text{Tr } \Lambda_{\nu}^m \Gamma \Lambda_{\nu'}^{m'} \Gamma. \quad (1.79)$$

This result can be substituted into eq. (1.72) which yields the self-consistency equation for the dynamical spin-spin correlations

$$\tilde{q}_{\nu}^m = \frac{1}{\beta^2} \int_{\mathbf{z}}^G \frac{1}{\Phi} \int_{\mathbf{y}}^G W \left((\text{Tr } \Lambda_{\nu}^m \Gamma) (\text{Tr } \Lambda_{\nu}^{-m} \Gamma) - \text{Tr } \Lambda_{\nu}^m \Gamma \Lambda_{\nu}^{-m} \Gamma \right). \quad (1.80)$$

Note that this equation includes the zero frequency components (1.66) as a special case.

1.4.2 Explicit construction of the spin-spin correlations

In addition to the variational procedure of the previous section an alternative method to derive the self-consistency equations (1.78, 1.80) shall be presented, which turns out to be particularly useful in the context of the itinerant spin glass model discussed in Chap. 3. Here the spin-spin correlations (1.32) are expressed in terms of the frequency-dependent Grassmann fields and evaluated by applying Wick's theorem.

Recalling the Grassmann representation of the spin operators (1.22) and the Fourier transformation (1.34) of the Grassmann fields, one can express the Fourier components of the spin products in the saddle point condition (1.32) by

$$\frac{1}{\beta^2} \int_0^{\beta} \int_0^{\beta} d\tau d\tau' S_{\nu a}^{\tau} S_{\nu a}^{\tau'} \exp(i\tau\omega_m + i\tau'\omega_{m'}) = \frac{1}{\beta^4} \sum_{ll'} \bar{\Psi}_a^l \sigma_{\nu} \Psi_a^{l+m} \bar{\Psi}_b^{l'} \sigma_{\nu} \Psi_b^{l'+m'}. \quad (1.81)$$

In the following the field-theoretic representation of the auxiliary Green's function (1.53) will be employed. An individual matrix element is defined by

$$(\Gamma_a)_{\sigma\sigma'}^{ll'} = \frac{1}{\beta} \left\langle \psi_{a\sigma}^l \bar{\psi}_{a\sigma'}^{l'} \right\rangle_{\mathcal{A}_{\text{eff}}} = \frac{1}{\beta} \frac{\int \mathcal{D}\psi \psi_{a\sigma}^l \bar{\psi}_{a\sigma'}^{l'} \exp(-\mathcal{A}_{\text{eff},a})}{\int \mathcal{D}\psi \exp(-\mathcal{A}_{\text{eff},a})}, \quad (1.82)$$

where the effective action is given by eq. (1.51) (superfluous site indices have been dropped), and $\mathcal{A}_{\text{eff},a}$ denotes the contributions from replica a only.

1.4.2.1 Equation for q_{ν}

In order to derive the self-consistency equation for the time-independent spin glass order parameters q_{ν} one considers the static case of the spin product (1.81), i.e. $m = m' = 0$, for distinct replicas. The dynamical components must average to zero for $a = b$. Within the dynamical decoupling formalism presented here, the sequence of quantum-statistical average and disorder average, as indicated schematically in eq. (1.32 a), assumes the explicit form

$$q_{\nu} = \frac{1}{\beta^4} \lim_{n \rightarrow 0} \int_{\mathbf{z}}^G \int_{\mathbf{y}}^G \sum_{ll'} \sum_{\sigma_1 \dots \sigma_4} (\sigma_{\nu})_{\sigma_1 \sigma_2} (\sigma_{\nu})_{\sigma_3 \sigma_4} \times \int \mathcal{D}\psi \psi_{a\sigma_2}^l \bar{\psi}_{a\sigma_1}^l \psi_{b\sigma_4}^{l'} \bar{\psi}_{b\sigma_3}^{l'} \exp(-\mathcal{A}_{\text{eff}}) \Big|_{a \neq b}. \quad (1.83)$$

Note that the usual denominator $[Z^n]_{\text{dis}}$ becomes trivial in the replica limit and has thus been dropped. Since the action \mathcal{A}_{eff} (1.51) is diagonal in replica space, the Grassmann path integral in eq. (1.83) factorizes. The contributions from the special replicas a and b are basically given by the Green's function (1.82), where the denominator gives rise to a weight factor (1.58). Using the auxiliary matrix (1.77), the frequency- and spin sums in (1.83) can be brought into the compact formulation

$$\begin{aligned} \sum_{l=-\infty}^{\infty} \sum_{\sigma\sigma'} (\sigma_\nu)_{\sigma\sigma'} (\Gamma_a)_{\sigma'\sigma}^{ll} &= \sum_{l=-\infty}^{\infty} \sum_{\sigma} (\sigma_\nu (\Gamma_a)_{ll})_{\sigma\sigma} \\ &= \text{Tr} \Lambda_\nu^0 \Gamma_a =: A_{a,\nu}^0. \end{aligned} \quad (1.84)$$

Each of the remaining replicas $c \neq \{a, b\}$ contributes a weight factor W_c . The n -fold regularization, which has to be added formally according to eq. (1.58), reduces to unity in the replica limit. A suitable arrangement of the replica-local (y -type) integrations leads together with eq. (1.59) to

$$\begin{aligned} q_\nu &= \frac{1}{\beta^2} \lim_{n \rightarrow 0} \int_z^G \left(\int_{y_a}^G W_a A_{a,\nu}^0 \right) \left(\int_{y_b}^G W_b A_{b,\nu}^0 \right) \prod_{c \neq \{a,b\}} \int_{y_c}^G W_c \Big|_{a \neq b} \\ &= \frac{1}{\beta^2} \int_z^G \left(\int_y^G W A_\nu^0 \right)^2 \underbrace{\lim_{n \rightarrow 0} \Phi^{n-2}}_{\Phi^{-2}}. \end{aligned} \quad (1.85)$$

In the second line the replica indices do not appear explicitly any more and thus the limit $n \rightarrow 0$ can be taken which correctly reproduces the earlier result eq. (1.78).

1.4.2.2 Equation for \tilde{q}_ν^m

In the case of the replica-diagonal correlations (1.32 b) their special time dependence has to be taken into account. As a consequence of this symmetry only the Fourier components (1.81) with $m = -m'$ can survive the average procedure. The dynamical saddle point components can thus be expressed by

$$\begin{aligned} \tilde{q}_\nu^m &= \frac{1}{\beta^4} \lim_{n \rightarrow 0} \int_z^G \int_y^G \sum_{ll'} \sum_{\sigma_1 \dots \sigma_4} (\sigma_\nu)_{\sigma_1 \sigma_2} (\sigma_\nu)_{\sigma_3 \sigma_4} \times \\ &\quad \int \mathcal{D}\psi \underbrace{\psi_{a\sigma_2}^{l+m} \bar{\psi}_{a\sigma_1}^l}_{\text{---}} \underbrace{\psi_{a\sigma_4}^{l'-m} \bar{\psi}_{a\sigma_3}^{l'}}_{\text{---}} \exp(-\mathcal{A}_{\text{eff}}). \end{aligned} \quad (1.86)$$

The four Grassmann fields in eq. (1.86) all carry the same replica index. When Wick's theorem is applied, there are hence two different ways to contract the fields, as indicated, contrary to the situation met in expression (1.83). In the case of the upper contraction the frequency- and spin

sums yield

$$\begin{aligned}
& \sum_{ll'} \sum_{\sigma_1 \dots \sigma_4} (\sigma_\nu)_{\sigma_1 \sigma_2} (\sigma_\nu)_{\sigma_3 \sigma_4} (\Gamma_a)_{\sigma_2 \sigma_1}^{l+m,l} (\Gamma_a)_{\sigma_4 \sigma_3}^{l'-m,l'} \\
&= \left(\sum_{l=-\infty}^{\infty} \sum_{\sigma_1} (\sigma_\nu (\Gamma_a)_{l+m,l})_{\sigma_1 \sigma_1} \right) \left(\sum_{l=-\infty}^{\infty} \sum_{\sigma_3} (\sigma_\nu (\Gamma_a)_{l'-m,l'})_{\sigma_3 \sigma_3} \right) \\
&= (\text{Tr } \Lambda_\nu^{-m} \Gamma_a) (\text{Tr } \Lambda_\nu^m \Gamma_a) =: A_{a,\nu}^m A_{a,\nu}^{-m}, \tag{1.87}
\end{aligned}$$

while the lower contraction leads to

$$\begin{aligned}
& \sum_{ll'} \sum_{\sigma_1 \dots \sigma_4} (\sigma_\nu)_{\sigma_1 \sigma_2} (\sigma_\nu)_{\sigma_3 \sigma_4} (\Gamma_a)_{\sigma_2 \sigma_3}^{l+m,l'} (\Gamma_a)_{\sigma_4 \sigma_1}^{l'-m,l} \\
&= \sum_{ll'} \sum_{\sigma_1 \sigma_3} (\sigma_\nu (\Gamma_a)_{l+m,l'})_{\sigma_1 \sigma_3} (\sigma_\nu (\Gamma_a)_{l'-m,l})_{\sigma_3 \sigma_1} \\
&= \sum_{l=-\infty}^{\infty} \sum_{\sigma_1} (\Lambda_\nu^{-m} \Gamma_a \Lambda_\nu^m \Gamma_a)_{\sigma_1 \sigma_1}^{ll} \\
&= \text{Tr } \Lambda_\nu^m \Gamma_a \Lambda_\nu^{-m} \Gamma_a =: B_{a,\nu}^m. \tag{1.88}
\end{aligned}$$

The latter contribution comes with a negative sign according to the Feynman rule for closed loops. Repeating the arguments of Sec. 1.4.2.1 one finally arrives at

$$\begin{aligned}
\tilde{q}_\nu^m &= \frac{1}{\beta^2} \lim_{n \rightarrow 0} \int_z^G \left(\int_{y_a}^G W_a (A_{a,\nu}^m A_{a,\nu}^{-m} - B_{a,\nu}^m) \right) \prod_{b \neq a} \int_{y_b}^G W_b \\
&= \frac{1}{\beta^2} \int_z^G \left(\int_y^G W (A_\nu^m A_\nu^{-m} - B_\nu^m) \right) \underbrace{\lim_{n \rightarrow 0} \Phi^{n-1}}_{\Phi^{-1}}. \tag{1.89}
\end{aligned}$$

In the replica limit this result exactly coincides with eq. (1.80).

1.4.3 Conclusion and summary of the dynamical self-consistency problem

In the first chapter of this thesis a quite general SU(2), spin 1/2 fermionic spin glass model with infinite-range interactions and arbitrary global anisotropy has been defined by eqs. (1.1–1.6). The model has been treated with standard techniques for disordered many-particle systems. A replica-symmetric, but rigorous quantum-dynamical decoupling procedure has led to an single-site problem of non-interacting particles which are subject to an effective frequency dependent potential. Finally, a set of highly coupled self-consistency equations has been derived which constitutes the centerpiece of this thesis, and most of the material presented in the following chapters is based on it. Therefore, this self-consistency structure, including all auxiliary quantities, shall be summarized in this section to provide a quick overview for future reference.

Within the present formulation of the theory, the self-induced potential \mathbf{V} is a Toeplitz matrix in the space of the fermionic Matsubara frequencies,

$$(\mathbf{V})_{ll'} = \mathbf{v}_{l-l'}, \tag{1.90}$$

where the entries \mathbf{v}_m themselves are 2×2 matrices in spin space and read

$$\mathbf{v}_m = \sum_{\nu} \sigma_{\nu} H_{\nu}^m. \quad (1.91)$$

The effective magnetic fields are constructed from the external field, the saddle point parameters q_{ν} and \tilde{q}_{ν}^m which have been introduced in eqs. (1.33, 1.35), and the corresponding real z - and y -type decoupling fields according to

$$H_{\nu}^{m=0} = h_{\nu} + J_{\nu} \left(\sqrt{q_{\nu}} z_{\nu} + \sqrt{\tilde{q}_{\nu}^0 - q_{\nu}} y_{\nu,0} \right) \quad (1.92)$$

and

$$H_{\nu}^{m \neq 0} = \begin{cases} J_{\nu} \sqrt{\frac{1}{2} \tilde{q}_{\nu}^m} (y_{\nu,m}^{+} + i y_{\nu,m}^{-}), & m > 0, \\ (H_{\nu}^{-m})^*, & m < 0. \end{cases} \quad (1.93)$$

One straight-forwardly defines the auxiliary Green's function matrix

$$\Gamma^{-1} = \mathbf{G}_0^{-1} + \mathbf{V} \quad (1.94)$$

which describes the propagation of the effectively non-interacting particles in the space of spin projection and fermionic frequency. Here

$$\left(\mathbf{G}_0^{-1} \right)_{ll'} = (i z_l + \mu) \delta_{ll'} \mathbb{1}_2 \quad (1.95)$$

is the diagonal Green's function matrix of the free system.

The evaluation of any physical quantity generally involves Gaussian integrations over all decoupling fields that occur in eqs. (1.92, 1.93). In this final formulation the previously introduced integral operators acquire the explicit meaning

$$\int_{\mathbf{z}}^G = \prod_{\nu} \int_{z_{\nu}}^G, \quad (1.95 \text{ a})$$

$$\int_{\mathbf{y}}^G = \prod_{\nu} \int_{y_{\nu,0}}^G \prod_{m>0} \int_{y_{\nu,m}^{+}}^G \int_{y_{\nu,m}^{-}}^G, \quad (1.95 \text{ b})$$

where the basic Gaussian integral has been defined by eq. (1.45). For a particular configuration of these integration variables the determinant

$$W(\mathbf{q}, \tilde{\mathbf{q}}, \mathbf{z}, \mathbf{y}) = \det(\Gamma^{-1} / \mathbf{G}_{\text{reg}}^{-1}) \quad (1.96)$$

is found to play the role of a weight factor. A suitable choice for the regularization required for concrete numerical calculations is

$$\left(\mathbf{G}_{\text{reg}}^{-1} \right)_{ll'} = i z_l \delta_{ll'} \mathbb{1}_2. \quad (1.97)$$

Integrating out all y -type variables one yields

$$\Phi(\mathbf{q}, \tilde{\mathbf{q}}, \mathbf{z}) = \int_{\mathbf{y}}^G W(\mathbf{q}, \tilde{\mathbf{q}}, \mathbf{z}, \mathbf{y}) \quad (1.98)$$

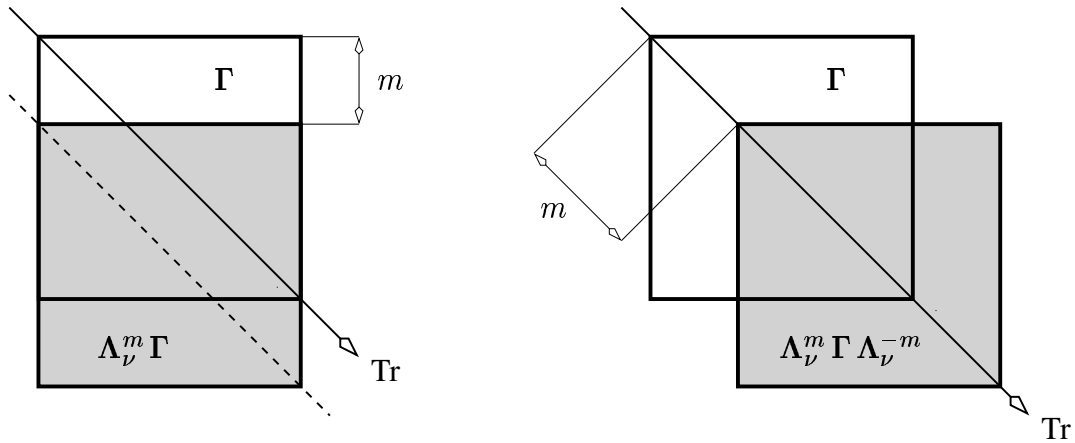


Figure 1.1: Construction of the integrand in the self-consistency equation (1.99 b) for the parameters \tilde{q}_ν^m . Left: The action of the auxiliary matrix Λ_ν^m (1.77) is to move down the elements of the matrix Γ (1.94) by m blocks. Thus, the first contribution to the integrand is a product of the sums over the m^{th} sub- and super-diagonals of the matrix Γ . Right: The second part is the trace of the matrix product of two factors Γ , which are shifted against each other about m blocks along the diagonal. This term contributes for $m \neq 0$ even in the spin-static approximation (see Sec. 2.1.2)

which can be viewed as a functional of $\tilde{q}_\nu^m = \tilde{q}_\nu(\omega_m)$.

This set of equations is completed by the self-consistency equations for the spin glass order parameters q_ν and the frequency dependent replica-diagonal spin-spin correlations \tilde{q}_ν^m . Two different ways of derivation, extremization of the free energy (Sec. 1.4.1) and explicit construction of the spin-spin correlations (1.4.2), have been presented. Both methods consistently yield the compact expressions

$$q_\nu = \frac{1}{\beta^2} \int_z^G \frac{1}{\Phi^2} \left(\int_y^G W \text{Tr} \Lambda_\nu^0 \Gamma \right)^2, \quad (1.99 \text{ a})$$

$$\tilde{q}_\nu^m = \frac{1}{\beta^2} \int_z^G \frac{1}{\Phi} \int_y^G W \left((\text{Tr} \Lambda_\nu^m \Gamma) (\text{Tr} \Lambda_\nu^{-m} \Gamma) - \text{Tr} \Lambda_\nu^m \Gamma \Lambda_\nu^{-m} \Gamma \right), \quad (1.99 \text{ b})$$

where the auxiliary matrix Λ_ν^m has been defined in eq. (1.77). Due to the static nature of the spin glass order parameters merely a sum over the frequency-diagonal elements of Γ appears in eq. (1.99 a). The construction of the integrand in eq. (1.99 b), however, involves the frequency off-diagonal elements, too, as illustrated in Fig. 1.1.

The self-consistency structure defined by eqs. (1.90 – 1.99) applies to many different models of physical interest, on the Fock space as well as on the spin space. These can be specified by an appropriate choice of the model parameters J_ν and h_ν in eqs. (1.92, 1.93) and the chemical potential μ in eq. (1.95).

Any attempt to solve this self-consistency structure faces the fundamental problem of the infinitely many quantities \tilde{q}_ν^m each of which effectuates corresponding Gaussian integrations via eqs. (1.92, 1.93). In order to determine the dynamical behavior of quantum spin glass systems

this integration problem has to be tamed. Suitable approximation schemes are required and shall be developed and applied in the following chapters.

Studying specific models in the following chapters, the focus shall be mainly on the respective paramagnetic phases including phase boundaries, where the replica-symmetric approach (1.33 a) is believed to be correct. In order to investigate the low temperature spin glass phase it will be necessary to extend the self-consistency structure to allow for Parisi replica symmetry breaking (RSB). This can be done straight-forwardly. However, the numerical treatment of RSB problems provides a substantial challenge, already for spin-static models [38], and even much more so in combination with quantum dynamics.

Another open problem left for future work is to perform the zero temperature limit of the presented self-consistency equations. With lowering the temperature the Matsubara frequencies move together, and a sensible frequency-continuous formulation of the matrix structure at $T = 0$ has to be found. A zero temperature theory would be particularly desirable in the context of model variants which undergo zero temperature phase transitions, such as the Ising spin glass at a critical transverse field, or the isotropic Heisenberg spin glass on the Fock space at a critical real chemical potential (see Sec. 2.1.3.2). In the respective (quantum) paramagnetic phases RSB would be of no relevance.

2

The Heisenberg spin glass

Soon after Sherrington and Kirkpatrick developed their classical mean-field theory for the Ising spin glass model [47, 26], also the infinite-range Heisenberg spin glass (HSG) model, being the natural quantum generalization of the SK-model, began to attract increased attention. The quantum-dynamical self-consistency problem was first formulated by Bray and Moore in 1980 [6], who predicted the existence of a low-temperature spin glass phase for all spin quantum numbers S . The corresponding generalized TAP-equations were derived by Sommers [48, 49]. Effects of external fields and anisotropy were also investigated [18, 27]. However, in most of these works explicit calculations relied on the so-called spin-static approximation, which completely neglects quantum-dynamical correlations.

Later, theorists have been looking at the quantum-dynamical problem posed by the infinite-range HSG from different angles. Grempel and Rozenberg, for instance, employed a Quantum Monte Carlo method to solve the effective single site problem numerically for the case $S = 1/2$. They examined the paramagnetic phase and confirmed its instability towards spin glass order at a finite transition temperature [19]. Arrachea and Rozenberg considered fully connected finite clusters of $S = 1/2$ spins and applied a numerical technique combining exact diagonalization and direct disorder averages. Thus theoretical difficulties due to both the replica as well as the imaginary-time formalism could be avoided on the expense of strong finite size effects. In a different analytical approach Sachdev et. al. extended the symmetry group of the spin operators and investigated the $SU(N)$ -generalization of the model [46]. The instrumental limit $N \rightarrow \infty$ permits exact solutions in the paramagnetic as well as in the glassy phase, and a rich phase diagram in the $T - S$ plane could be constructed [15, 16].

Despite of almost twenty five years of research on the infinite-range HSG model our current understanding of this system is far from being complete. Among the many unresolved problems, two shall be primarily dealt with in this chapter. The first is the question pertaining to the exact location of the paramagnet to spin glass phase transition. A precise determination of the critical temperature is not only of theoretical interest, but it would provide an important practical benchmark for numerical treatments in the future. The second main issue addressed is the shape of the specific heat curve at and above T_c . Experiments with real HSG materials exhibit a broad maximum of the specific heat above T_c [5, 31]. It will be shown that the present model does not

account for this feature, which is in contradiction to what has been claimed recently by other authors [1].

In the first section of this chapter the general self-consistency structure summarized in Sec. 1.4.3 shall be re-formulated within the spin-static approximation. The solutions of this simplified set of equations define a frame of reference for the dynamical calculations presented in the subsequent sections. In order to capture the effects of the quantum-spin dynamics inherent to the system two different new approximation schemes are developed, both of which systematically improve the spin-static results. The basic concept of the so-called dynamical approximation scheme, introduced in Sec. 2.2.1, is to treat the quantum-dynamical correlations on a restricted set of discrete bosonic Matsubara frequencies. The complementary approximation technique of Sec. 2.3 is based on a diagrammatic expansion of the self-consistency equations in powers of the dynamical correlations themselves.

2.1 The spin-static approximation

In the realm of quantum spin glasses the spin-static approximation is widely used. The term expresses the idea to disregard the imaginary-time dependence of the saddle point 1.32. Providing a simple but very instructive special case of the self-consistency structure defined by eqs. (1.92 – 1.99 b), the spin-static approximation is a good starting point for the quantum-dynamical calculations in the following sections.

2.1.1 Spin-static self-consistency equations

Within the dynamical formalism of Chap. 1 the spin-static approximation can be introduced most naturally via the effective potential (1.90) employing the decomposition

$$\mathbf{V} = \mathbf{V}_{\text{stat}} + \mathbf{V}_{\text{dyn}}. \quad (2.1)$$

Here the first term denotes the part diagonal in (fermionic) frequency space,

$$(\mathbf{V}_{\text{stat}})_{ll'} = \mathbf{v}_0 \delta_{ll'}, \quad (2.2)$$

which is composed of the static magnetic fields (1.92), whereas \mathbf{V}_{dyn} comprises all off-diagonal blocks made up by the complex dynamical fields (1.93). Now the spin-static approximation consists in neglecting the dynamical contributions to the effective potential, i.e. one presumes $\mathbf{V} \simeq \mathbf{V}_{\text{stat}}$.

The matrix \mathbf{V}_{stat} is block-diagonal and so is the static auxiliary Green's function

$$\Gamma_{\text{stat}}^{-1} = \mathbf{G}_0^{-1} + \mathbf{V}_{\text{stat}}, \quad (\Gamma_{\text{stat}})_{ll'} = \gamma_l \delta_{ll'}, \quad (2.3)$$

where the blocks along the diagonal are given by

$$\gamma_l^{-1} = (iz_l + \mu) \mathbb{1}_2 + \mathbf{v}_0, \quad \gamma_l = \frac{(iz_l + \mu) \mathbb{1}_2 + \mathbf{v}_0}{(iz_l + \mu)^2 - H_0^2}. \quad (2.4)$$

2.1.1.1 The spin-static weight function

Due to this simple structure of the matrix Γ_{stat} the weight function W as well as the integrands of the self-consistency equations (1.99) can be evaluated analytically. Indeed, the determinant (1.96) factorizes into 2×2 determinants for each fermionic Matsubara frequency:

$$\begin{aligned} W_{\text{stat}} &= \det \left(\Gamma_{\text{stat}}^{-1} / \mathbf{G}_{\text{reg}}^{-1} \right) = \prod_{l=-\infty}^{\infty} \det \left(\frac{1}{iz_l} \gamma_l^{-1} \right) \\ &= \prod_{\sigma=\pm} \exp \sum_{l=-\infty}^{\infty} \ln \frac{iz_l + x_{\sigma}}{iz_l}, \end{aligned} \quad (2.5)$$

where the abbreviation

$$x_{\pm} = \mu \pm H_0 \quad (2.6)$$

has been used. H_0 is the absolute value of the static magnetic field vector,

$$H_0 = \sqrt{\sum_{\nu} (H_{\nu}^0)^2}. \quad (2.7)$$

Recalling the symmetry relation $z_{-l-1} = -z_l$, the negative frequency terms can be removed from the sum in eq. (2.5). Care has to be taken, however, because this frequency sum does not converge absolutely since

$$\ln \frac{iz_l + x_{\sigma}}{iz_l} = \frac{x_{\sigma}}{iz_l} + O(z_l^{-2}). \quad (2.8)$$

This problematic contribution may be separated from the rest, and thus one obtains

$$W_{\text{stat}} = \prod_{\sigma=\pm} \exp \left(\underbrace{\sum_{l=0}^{\infty} \ln \frac{z_l^2 + x_{\sigma}^2}{z_l^2}}_{\ln \cosh(\frac{1}{2}\beta x_{\sigma})} + \sum_{l=-\infty}^{\infty} \frac{\mu}{iz_l} \right). \quad (2.9)$$

The first sum in eq. (2.9) can be evaluated elementary by virtue of the residue theorem. The second sum requires the use of a convergence factor which leads to the standard result [12]

$$\lim_{\eta \rightarrow 0} \sum_{l=-\infty}^{\infty} \frac{\exp(iz_l \eta)}{iz_l} = \frac{\beta}{2}. \quad (2.10)$$

Altogether one arrives at the spin-static weight function

$$W_{\text{stat}} = \frac{1}{2} \exp(\beta \mu) C(\mu, H_0) \quad (2.11)$$

with the characteristic function

$$C(\mu, H_0) = \cosh(\beta \mu) + \cosh(\beta H_0). \quad (2.12)$$

Note that inserting this result into eq. (1.60) and taking the limit $J_{\nu} \rightarrow 0$ the partition function of the non-interacting system is reproduced exactly ¹.

¹The second series in eq. (2.9) is ambiguous and can be evaluated to zero by suitable rearrangement. Then the correct result (2.11) can be obtained using a more complicated and particularly μ -dependent regularization [35].

2.1.1.2 The general anisotropic case

One way to proceed would be to extremize the spin-static free energy obtained by substituting the expression (2.11) into eqs. (1.98, 1.61). Nevertheless, here the spin-static self-consistency equations shall be viewed as a special case of the general equations (1.99). Taking this route, the two expressions

$$A_\nu^m = \text{Tr} \Lambda_\nu^m \Gamma_{\text{stat}} \quad (2.14 \text{ a})$$

$$B_\nu^m = \text{Tr} \Lambda_\nu^m \Gamma_{\text{stat}} \Lambda_\nu^{-m} \Gamma_{\text{stat}} \quad (2.14 \text{ b})$$

have to be computed explicitly. At zero (bosonic) frequency, i.e. for $m = 0$, these terms evaluate to

$$\begin{aligned} A_\nu^0 &= \sum_{l=-\infty}^{\infty} \text{Tr}_\sigma \sigma_\nu \gamma_l \\ &= -2H_\nu^0 \sum_{l=-\infty}^{\infty} \frac{1}{(iz_l + \mu)^2 - H_0^2} = \beta \frac{H_\nu^0 \sinh(\beta H_0)}{H_0 C(\mu, H_0)} \end{aligned} \quad (2.15)$$

and

$$\begin{aligned} B_\nu^0 &= \sum_{l=-\infty}^{\infty} \text{Tr}_\sigma \sigma_\nu \gamma_l \sigma_\nu \gamma_l \\ &= 2 \sum_{l=-\infty}^{\infty} \frac{1}{(iz_l + \mu)^2 - H_0^2} + 4(H_\nu^0)^2 \sum_{l=-\infty}^{\infty} \frac{1}{((iz_l + \mu)^2 - H_0^2)^2} \\ &= \frac{\beta^2}{\beta H_0} \left(\frac{(H_\nu^0)^2}{H_0^2} - 1 \right) \frac{\sinh(\beta H_0)}{C(\mu, H_0)} - \beta^2 \frac{(H_\nu^0)^2}{H_0^2} \frac{1 + \cosh(\beta\mu) \cosh(\beta H_0)}{C(\mu, H_0)^2}. \end{aligned} \quad (2.16)$$

Here the symbol Tr_σ denotes the trace over the two spin states. The occurring Matsubara sums can be performed easily either using *Mathematica*[®] or by means of the general formula for this type of sums which will be derived in Sec. A.1. In terms of the expressions (2.11, 2.15, 2.16) and defining

$$\Phi_{\text{stat}} = \int_{y_0}^G W_{\text{stat}}, \quad (2.17)$$

the spin-static self-consistency equations read

$$q_\nu = \frac{1}{\beta^2} \int_z^G \frac{1}{\Phi_{\text{stat}}^2} \left(\int_{y_0}^G W_{\text{stat}} A_\nu^0 \right)^2, \quad (2.19 \text{ a})$$

$$\tilde{q}_\nu^0 = \frac{1}{\beta^2} \int_z^G \frac{1}{\Phi_{\text{stat}}} \int_{y_0}^G W_{\text{stat}} \left((A_\nu^0)^2 - B_\nu^0 \right). \quad (2.19 \text{ b})$$

Compared to the general dynamical counterparts (1.99) the spin-static approximation brings about tremendous simplifications. On one hand the Gaussian integrations extend over the six static decoupling fields z_ν and $y_{\nu,0}$ only (as indicated by the notation y_0). On the other hand the matrix structure of the integrands has disbanded.

2.1.1.3 The isotropic special case

The matter further simplifies if global isotropy is given. This means first that the disorder distribution (1.5) does not depend on the spatial direction ν , and second that there is no external magnetic field applied, i.e.

$$J_\nu = J \quad \text{and} \quad h_\nu = 0. \quad (2.20)$$

From these assumptions immediately follows that the spin-spin correlations eqs. 1.32 are independent of direction, too, as expressed by

$$q_\nu = q \quad \text{and} \quad \tilde{q}_\nu^m = \tilde{q}_m. \quad (2.21)$$

Due to this global symmetry the Gaussian \mathbf{y}_0 -integrations can be carried out analytically, and the \mathbf{z} -integrations can be reduced to a single radial integration. A lengthy but straightforward calculation yields [35]

$$q = \frac{1}{3c^2} \int_r^G \left(\frac{b^2 \cosh(cr) + \frac{c^2 r^2 - b^2}{cr} \sinh(cr)}{\cosh(cr) + \frac{b^2}{cr} \sinh(cr) + \cosh(\beta\mu) \exp\left(-\frac{b^2}{2}\right)} \right)^2, \quad (2.23 \text{ a})$$

$$\tilde{q}_0 = \frac{1}{3} \int_r^G r^2 \frac{\cosh(cr) + \frac{2+b^2}{cr} \sinh(cr)}{\cosh(cr) + \frac{b^2}{cr} \sinh(cr) + \cosh(\beta\mu) \exp\left(-\frac{b^2}{2}\right)}, \quad (2.23 \text{ b})$$

where the abbreviations

$$b = \beta J \sqrt{\tilde{q}_0 - q} \quad \text{and} \quad c = \beta J \sqrt{q} \quad (2.24)$$

have been used. Solutions of eqs. (2.23) are presented in Sec. 2.1.3.

2.1.2 Calculation of dynamical quantities

The general dynamical approach to the quantum spin glass system presented in Chap. 1 facilitates an estimation of dynamical quantities even within the spin-static approximation. Although the dynamical part of the effective potential (2.1) is neglected it appears natural to calculate the dynamical saddle point components from eq. (1.99 b) using the spin-static weight function W_{stat} (2.11) and the auxiliary Green's function Γ_{stat} (2.3). Here the trace terms eqs. (2.14) have to be evaluated for $m \neq 0$.

As illustrated in Fig. 1.1, $A_\nu^{m \neq 0}$ vanishes due to the block diagonal structure of Γ_{stat} . The other term, however, yields a finite contribution for any m . For the sake of simplicity this discussion shall be restricted to the isotropic case. One finds

$$\begin{aligned} B_m &= \frac{1}{3} \sum_\nu B_\nu^m \\ &= \sum_{l=-\infty}^{\infty} \frac{2(i z_l + \mu)(i z_{l+m} + \mu) - \frac{2}{3} H_0^2}{\left((i z_l + \mu)^2 - H_0^2\right) \left((i z_{l+m} + \mu)^2 - H_0^2\right)} \\ &= -\frac{2}{3} \frac{\beta^2}{C(\mu, H_0)} \frac{\beta H_0 \sinh(\beta H_0)}{\beta^2 H_0^2 + \pi^2 m^2}, \end{aligned} \quad (2.25)$$

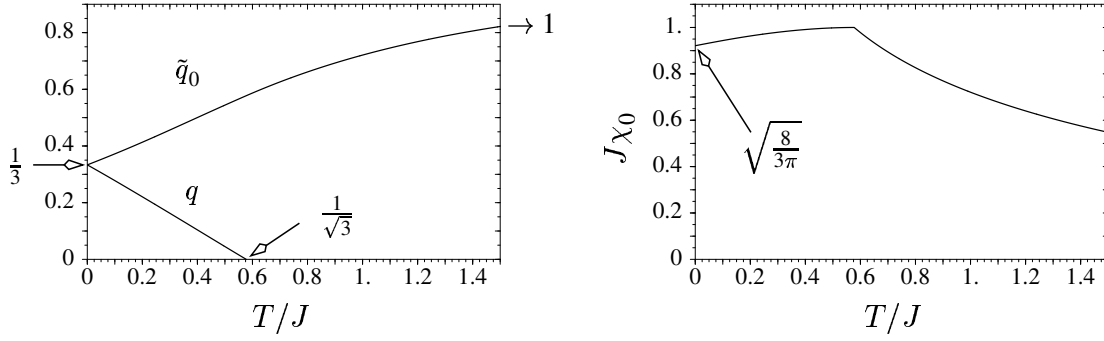


Figure 2.1: Some basic results for the isotropic Heisenberg spin glass on the spin space (HSG_S) within spin-static and replica-symmetric approximation. Right: spin-glass order parameter q and static replica-diagonal spin-spin correlation \tilde{q}_0 . Left: zero frequency part of the local susceptibility χ_0 according to eq. (1.37).

and comparison with the zero frequency component (2.19 b) leads to

$$\tilde{q}_m = \frac{1}{3} \exp(-\beta\mu) \int_z \frac{1}{\Phi_{\text{stat}}} \int_{y_0}^G \left(\frac{\beta H_0 \sinh(\beta H_0)}{\beta^2 H_0^2 + \pi^2 m^2} + \frac{\delta_{m,0}}{2} \cosh(\beta H_0) \right). \quad (2.26)$$

Recalling relation (1.37), this spin-static estimate immediately reveals the correct asymptotic behavior of the local dynamical susceptibility

$$\chi_m \propto \frac{1}{\omega_m^2}, \quad \omega_m \gg J. \quad (2.27)$$

The explicit form for the parameters \tilde{q}_m also permits the analytic continuation of the local susceptibility to the real frequency axis. Apart from the zero frequency term, the replacement $i\omega_m \rightarrow \omega + i\eta$ in eq. (2.26) yields for the imaginary part describing absorption the low frequency characteristics

$$\text{Im} \chi(\omega) \sim \omega^3, \quad \omega \rightarrow 0. \quad (2.28)$$

However, this cubic behavior seems to be an artefact of the spin-static approximation since other dynamical treatments provide evidence that $\text{Im} \chi(\omega) \sim \omega$ as $\omega \rightarrow 0$ [19, 16].

2.1.3 Selected results for the isotropic Heisenberg spin glass

2.1.3.1 The model on the spin space

In order to investigate the isotropic Heisenberg spin glass on the spin space (HSG_S) the chemical potential has to be fixed to the Popov-Fedotov potential (1.9). Consequently, the spin-static self-consistency equations eqs. (2.23) further simplify owing to the identity $\cosh(\beta\mu_{\text{PF}}) = 0$. The resulting numerical solutions are presented in Fig. 2.1. In the paramagnetic phase, where $q = 0$, eq. (2.23 b) reduces to a simple quadratic equation which has the explicit solution

$$\tilde{q}_0 = \frac{-3 + \beta^2 J^2 + \sqrt{9 + 30\beta^2 J^2 + \beta^4 J^4}}{6\beta^2 J^2}. \quad (2.29)$$

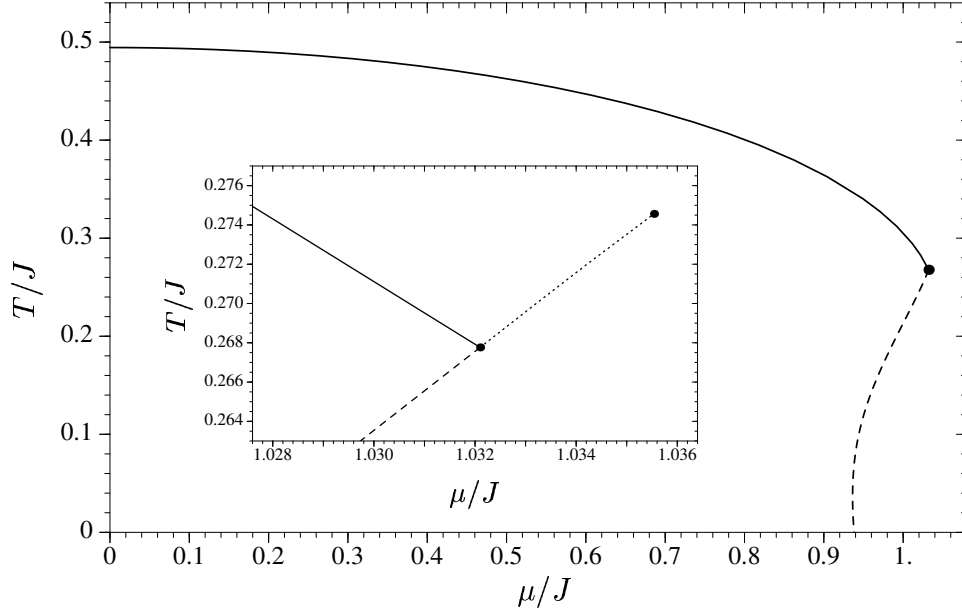


Figure 2.2: Phase diagram of the isotropic Heisenberg spin glass on the Fock space (HSG_{F}) within spin-static and replica-symmetric approximation. At the tri-critical point $\{\mu = 1.0321J, T = 0.2678J\}$ the critical behavior changes from second order (solid line) to first order (dashed line). Beyond the replica-symmetric theory the first order line is subject to small corrections due to replica symmetry breaking. Inset: vicinity of the tri-critical point. Along the dotted line, which terminates at the point $\{\mu = 1.0355J, T = 0.2746J\}$, \tilde{q}_0 changes discontinuously in the paramagnetic phase. The Ising spin glass on the Fock space possesses a very similar phase diagram [11].

The second order paramagnet to spin glass phase transition occurs at the critical temperature $T_c = 1/\sqrt{3}J$. Dynamical corrections to this spin-static result will be discussed in Sec. 2.2.3.2. Comparison with the critical temperature for the corresponding classical model, $T_c = J$ [5], already reveals the significance of quantum effects in this system.

To conclude with, an interesting feature of the spin-static approximation shall be mentioned. By way of the identity

$$\sum_{m=-\infty}^{\infty} \frac{1}{\beta^2 H_0^2 + \pi^2 m^2} = \frac{\coth(\beta H_0)}{\beta H_0} \quad (2.30)$$

one easily verifies that the parameters (2.26) exactly obey the sum rule (1.41) for the model variant on the spin space.

2.1.3.2 The model on the Fock space

The isotropic Heisenberg spin glass on the Fock space (HSG_{F}) is described by eqs. (2.23) with a real chemical potential μ . The influence of the non-magnetic states becomes apparent in the high temperature limit, where $\tilde{q}_0 \rightarrow 1/2$ contrary to the model on the spin space. For $\mu = 0$, which corresponds to half filling, the critical temperature reaches its maximum value $T_c = 0.49440J$.

Away from half filling the number of either empty or doubly occupied sites increases. In such magnetically diluted systems the spin glass freezing occurs at lower temperatures. The resulting phase diagram in the $\mu - T$ plane is presented in Fig. 2.2.

2.1.4 Some comments on other model variants

The simplest non-trivial special case of the generic model (1.1) certainly is the Ising spin glass as specified by the model parameters $J_z = J$ and $J_x = J_y = h_\nu = 0$. In this case the spin operators (1.3) for the z -components commute with the Hamilton operator (1.1), and consequently there is no quantum dynamics to be taken into account (the Grassmann spinors in the free action (1.20) nevertheless keep their auxiliary time dependence). Therefore, the spin-static approach provides an exact solution for the Ising model, and all quantum-dynamical correlations $\tilde{q}_z^{m \neq 0}$ must vanish. From the fact $H_z^0 = H_0$ consistently follows that the quantities $B_z^{m \neq 0}$ all evaluate to zero (note that in order to obtain the different result (2.25) isotropy was exploited which is not given in the Ising case). Interestingly, the spin-spin correlations in the transversal directions $\nu = \{x, y\}$ do not vanish and actually exhibit a dynamics caused by the (perpendicular) effective magnetic field in z -direction. A calculation similar to the one in Sec. 2.1.2 yields

$$\tilde{q}_\nu^m = \frac{1}{2} \exp(-\beta\mu) \int_z^G \frac{1}{\Phi_{\text{stat}}} \int_{y_0}^G \frac{\beta H_0 \sinh(\beta H_0)}{\beta^2 H_0^2 + \pi^2 m^2} \quad \text{for } \nu \neq z. \quad (2.31)$$

For the model on the spin space one easily verifies the parameters (2.31) to fulfill the sum rule (1.41).

model	T_c/J	
	spin space, $\mu = \mu_{\text{PF}}$	Fock space, $\mu = 0$
Ising	1	0.67674
isotropic XY	0.75580	0.58066
isotropic Heisenberg	$1/\sqrt{3} = 0.57735$	0.49440

Table 2.1: Critical temperatures for some spin glass models described by the general self-consistency equations (2.19). For the Ising case the spin-static approximation is exact. Estimates for T_c of the two Heisenberg model variants including dynamical corrections are given in eqs. (2.42, 2.48), respectively.

Non-trivial quantum dynamics can be generated in the Ising model by applying a transverse magnetic field $h_x = \Gamma$. This system displays a quantum phase transition located at $\Gamma_c \simeq 1.52J$ [51, 9, 43]. From the spin-static calculation one obtains $\Gamma_c = 2J$. This clear overestimate of the critical field reveals the failure of the spin-static approximation at low temperatures. This issue shall be further discussed in Sec. 3.3.3 in the context of an itinerant spin glass model.

such a sequence of improved solutions reveals sufficient convergence properties the exact full dynamical result can be inferred by extrapolation to $M \rightarrow \infty$.

The dynamical approximation scheme is applicable and useful if the finite frequency components $\tilde{q}_\nu^{m \neq 0}$ are small compared to \tilde{q}_ν^0 and fall off rapidly with increasing m . This situation is met at the relatively high temperatures in the paramagnetic phase of the HSG_S (see Fig. 2.5). This is not the case, however, at very low temperatures. The Matsubara frequencies continuously move together as the temperature decreases, and any finite number of discrete frequencies will eventually collapse into the origin of the frequency axis. Rather, a finite frequency range must be taken into account at low temperatures, for instance to investigate the quantum phase transition in the itinerant Ising spin glass studied in Chap. 3 (see Secs. 3.3.3 and A.5).

In the context of the Ising model in a transverse magnetic field a somewhat similar approximation method on the discretized imaginary time space was constructed earlier by several authors [8, 17]. In these works the full dynamical quantities were also estimated from self-consistent approximants based on a finite number of imaginary time slices. Compared to this technique it is an advantage of the dynamical approximation scheme introduced here that it takes into account all fermionic Matsubara frequencies, which corresponds to infinitely many time slices at lowest order ($M = 0$) already.

2.2.2 Implementation notes and some technical details

The dynamical results presented in this chapter apply to the isotropic HSG, and they are valid either in the paramagnetic phase, where the spin glass order parameter q vanishes, or below but sufficiently close to T_c , such that the self-consistency equations can be safely expanded in powers q . In both cases the replica-global Gaussian integrations (z -type) can be performed analytically. Hence, the technical discussion in this section shall be restricted to the special case of the isotropic system in the paramagnetic phase.

In order to actually find solutions within the dynamical approximation scheme the set of self-consistency equations (1.90 – 1.99 b) can be recast into a form more suitable for the numerical treatment by way of the substitutions

$$x_{\nu,0} = \beta J \sqrt{\tilde{q}_0} y_{\nu,0} \quad \text{and} \quad x_{\nu,m}^\pm = \beta J \sqrt{\tilde{q}_m} y_{\nu,m}^\pm. \quad (2.33)$$

Due to the assumed isotropy it is convenient to work in (hyper-)spherical coordinates. Then, the three-dimensional integration over the static variables $x_{\nu,0}$ splits into a Gaussian radial part

$$\int_{x_0}^{\tilde{G}} = (2\pi\tilde{q}_0\beta^2 J^2)^{-\frac{3}{2}} \int_0^\infty dx_0 x_0^2 \exp\left(-\frac{x_0^2}{2\beta^2 J^2 \tilde{q}_0}\right) \quad (2.34)$$

and an angular part

$$\int_{\Omega_0} = \int_0^\pi \int_0^{2\pi} d\theta_0 d\varphi_0 \sin\theta_0. \quad (2.35)$$

The six-dimensional integrations associated with each Matsubara frequency $\omega_{m \geq 1}$ comprise Gaussian radial parts

$$\int_{x_m \geq 1}^{\tilde{G}} = (2\pi\tilde{q}_m\beta^2 J^2)^{-3} \int_0^\infty dx_m x_m^5 \exp\left(-\frac{x_m^2}{2\beta^2 J^2 \tilde{q}_m}\right) \quad (2.36)$$

and the five-dimensional angular integrations

$$\int_{\Omega_{m \geq 1}} = \int_0^{\frac{\pi}{2}} \int_0^{\frac{\pi}{2}} \int_0^{2\pi} \int_0^{2\pi} \int_0^{2\pi} d\theta_m d\varphi_m d\psi_m^x d\psi_m^y d\psi_m^z \sin^3 \theta_m \cos \theta_m \sin \varphi_m \cos \varphi_m. \quad (2.37)$$

Within the dynamical approximation of order M the functional eq. (1.98) takes the form

$$\Phi(\tilde{q}_0, \dots, \tilde{q}_M) = \prod_{m=0}^M \int_{x_m}^{\tilde{G}} \int_{\Omega_m} W(\mathbf{x}_0, \dots, \mathbf{x}_M). \quad (2.38)$$

By way of the variable change (2.33) the \tilde{q}_m -dependence was transferred from the weight function W to the Gaussian factors of the integral operators (2.34, 2.36). Consequently, the extremization of the free energy with respect to the parameters \tilde{q}_m can be performed much easier than in Sec. 1.4.1. The resulting self-consistency equations for the isotropic model in the paramagnetic phase read

$$\tilde{q}_m = \frac{1}{3\alpha\beta^4 J^4 \tilde{q}_m^2} \frac{1}{\Phi} \prod_{m'=0}^M \int_{x_{m'}}^{\tilde{G}} \int_{\Omega_{m'}} (x_m^2 - 3\alpha\beta^2 J^2 \tilde{q}_m) W, \quad \alpha = \begin{cases} 1, & \text{if } m = 0, \\ 2, & \text{if } m \geq 1. \end{cases} \quad (2.39)$$

In this shape the self-consistency problem can be solved numerically much more efficiently than using eq. (1.99 b). In particular, the determinant W in eq. (2.39) can be evaluated with considerably less numerical effort than the whole integrand in eq. (1.99 b), which additionally involves a time consuming matrix inversion. Note, however, that eq. (2.39) allows for the calculation of the parameters $\tilde{q}_{m \leq M}$ only. Whenever sensible non-self-consistent estimations for the parameters $\tilde{q}_{m > M}$ are needed, e.g. in the context of the specific heat in Sec. 2.2.3.3, one has to resort to the general formulation (1.99 b).

All integrands that occur in the self-consistency equations are constructed from the matrix Γ^{-1} given by eq. (1.94). In the dynamical approximation scheme Γ^{-1} is band-diagonal and extends infinitely in the fermionic frequency space. For practical calculations this matrix was symmetrically truncated at fermionic frequencies $\pm z_{l_c}$, and hence the matrix size was $4(l_c + 1) \times 4(l_c + 1)$. Contributions from the outer regions associated with frequencies $|z_l| > z_{l_c}$ were taken into account perturbatively. The ‘‘cut-off index’’ l_c was chosen sufficiently large such that the final results did not depend on this auxiliary parameter. Most calculations discussed in this chapter were performed with $l_c = 50 - 100$.

Within the dynamical approximation of orders up to and including $M = 2$ all integrations occurring in eqs. (2.34 – 2.37) were performed virtually exactly using the highly efficient Gaussian integration method [50]. Starting with order $M = 3$, a Monte Carlo method was employed for the less important ψ -type phase integrations in eq. (2.37) to account for the increasingly high dimensionality of the integration problem.

The computer algorithm for the solution of the self-consistency problem was implemented in *Mathematica*[®], where the computationally costly matrix operations were executed by external C-routines via the *MathLink* interface. Thus, the analytical abilities and structural advantages of *Mathematica*[®] were combined with the much higher performance of compiled C-code in numerical calculations.

2.2.3 Dynamical results for the isotropic Heisenberg spin glass on the spin space

Employing the technical apparatus described in Sec. 2.2.2 and setting the chemical potential to the Popov-Fedotov potential (1.9), the self-consistency problem for the isotropic Heisenberg spin glass on the spin space (HSG_S) could be solved within the dynamical approximations up to and including order $M = 4$ [4].

An interesting feature of the dynamical approximation scheme is that for the HSG_S the sum rule (1.41) is exactly fulfilled at any order M , where the parameters $\tilde{q}_{m>M}$ are calculated in a non-self-consistent way from eq. (1.99 b). In the spin-static case $M = 0$ this fact was revealed by exact evaluation of the sum in Sec. 2.1.3.1. For $M = \{1, 2\}$ the sum rule has been verified to hold true by means of high precision numerical calculations. In spite of this strong numerical evidence no rigorous proof of eq. (1.41) for arbitrary (finite) orders M yet exists.

2.2.3.1 Solutions in the paramagnetic phase

The first quantity to discuss is the zero frequency part of the local susceptibility χ_0 , which is related to \tilde{q}_0 by (see eq. (1.37))

$$\chi_0 = \beta \tilde{q}_0. \quad (2.40)$$

Numerical results obtained in the first three dynamical approximations are presented in Fig. 2.4. The quantum-dynamical corrections to χ_0 relative to the spin-static approximation result, which is given by eq. (2.29), are quantitatively remarkably small (note the small vertical scale in fig. 2.4). This fact was already pointed out in Ref. [19].

At sufficiently high temperatures ($T > J$), quick convergence of this sequence of approximants is observed. This means that the quantum dynamics of the system is captured virtually exactly by taking into account only the effects of correlations at very few Matsubara frequencies. Naturally, as the temperature decreases the number of Matsubara frequencies required to achieve some desired level of accuracy grows, and the spacings between the individual approximants increase.

The curves in Fig. 2.4 exhibit characteristic maxima, the positions of which move to lower temperatures for higher M . A close look at the sequence of these maxima leaves room for the interesting speculation that in the limit $M \rightarrow \infty$ the position of the maximum coincides with the critical temperature.

Figure 2.5 displays the largest and most relevant among the parameters \tilde{q}_m at several temperatures for $M \leq 1$. It can be seen clearly that, at least in the paramagnetic phase, the dynamical components $\tilde{q}_{m \neq 0}$ are considerably smaller than \tilde{q}_0 and vanish quickly which justifies the dynamical approximation scheme.

2.2.3.2 Determination of the critical temperature

There exists a strikingly simple criterion for the location of the equilibrium paramagnet to spin glass phase transition, which shall be re-derived within the general formalism of Chap. 1 in

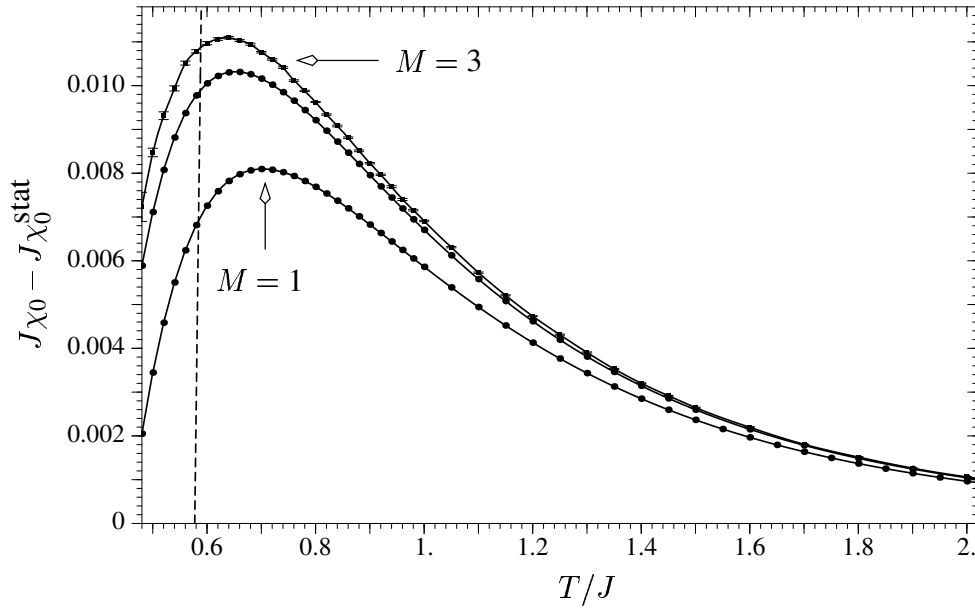


Figure 2.4: Zero frequency local susceptibility $\chi_0 = \beta\tilde{q}_0$ for the isotropic HSG_S obtained within the dynamical approximations of orders up to and including $M = 3$. Due to the smallness of the quantum-dynamical corrections only deviations from the spin-static approximation result given by eq. (2.29) are shown. The error bars indicate the statistical errors that arise from the Monte Carlo integration method employed for $M \geq 3$ (see Sec. 2.2.2). The dashed line represents $1 - J\chi_0^{stat}$. According to eq. (2.41), the intersection points mark the respective approximation to the critical temperature. To the right of the dashed line the shown paramagnetic solutions are unstable against spin glass order.

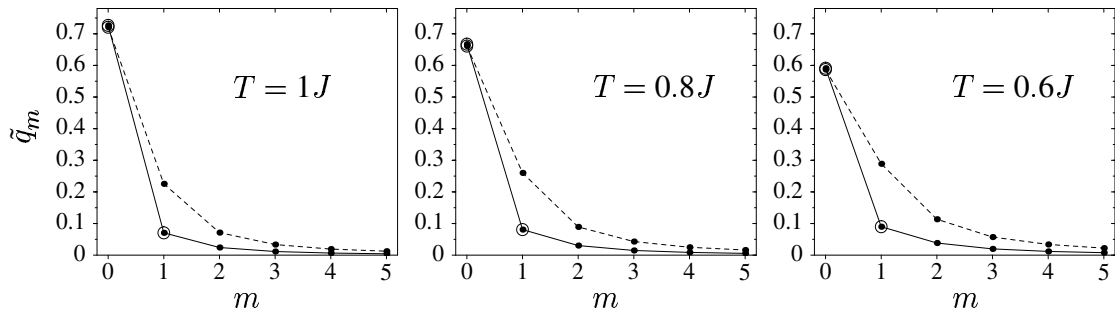


Figure 2.5: Fourier components of the replica-diagonal saddle point (1.33 b) for the isotropic HSG_S at three temperatures in the paramagnetic phase within the spin-static (dashed line) and the first order dynamical approximation (full line). Higher orders would not be distinguishable at the chosen scale and are therefore not shown. The parameters marked by the circles are taken into account self-consistently while the others were calculated from eqs. (2.26, 1.99 b).

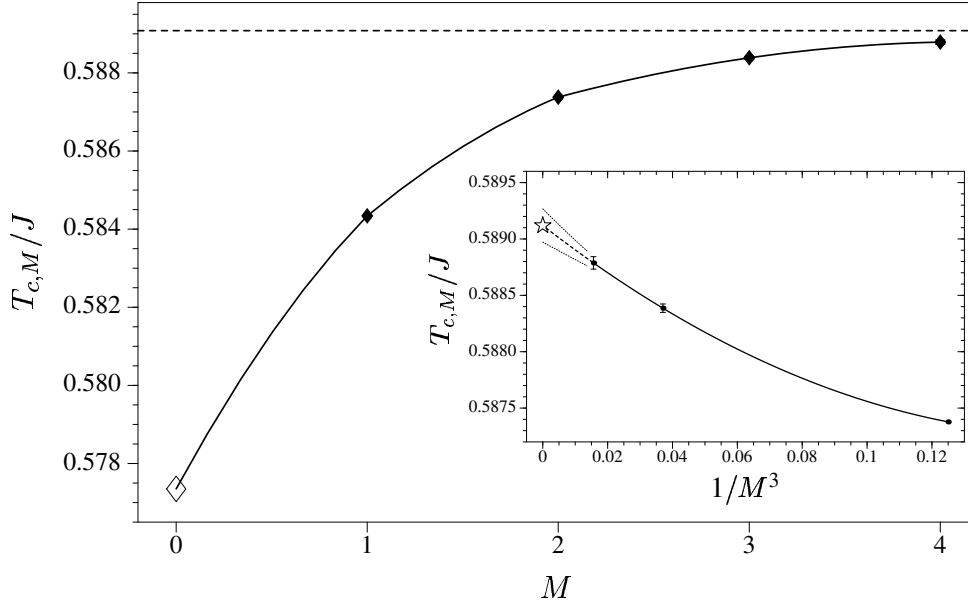


Figure 2.6: Sequence of critical temperatures for the isotropic HSG_S obtained within dynamical approximations of orders $M = \{0, \dots, 4\}$. The open diamond and the dashed line represent the spin-static and the extrapolated full quantum-dynamical result, respectively. Inset: Estimation of the full dynamical critical temperature (open star) by extrapolation of the sequence of approximants to $M = \infty$ having regard to the presumed $1/M^3$ -like convergence. The two thin lines indicate the estimate for the statistical error.

App. A.4.1. In the present isotropic case this criterion for the critical temperature reads

$$J\chi_0(T_c) = 1 \quad (2.41)$$

which holds true within the dynamical approximation of any order. In particular, relation (2.41) was used to determine the continuous transition line in the spin-static phase diagram Fig. 2.2.

The solutions of eq. (2.41) for $M = \{0, \dots, 4\}$ are presented in Fig. 2.6. From the structure of the self-consistency problem one expects a M^{-3} -like convergence of this sequence of T_c -approximants (this presumption will be justified in the context of the perturbative $\tilde{q}_{m \neq 0}$ -expansion in Sec. 2.3.2.1). Taking into account this asymptotic behavior, the data can be unambiguously extrapolated to $M \rightarrow \infty$ (see Fig. 2.6). Thus, one obtains the full quantum-dynamical critical temperature

$$T_c = (0.58912 \pm 0.00015)J. \quad (2.42)$$

This result means an increase relative to the spin-static result $T_{c,\text{stat}} = 1/\sqrt{3}J$ by about 2%. The value (2.42) can be compared to estimations of T_c obtained by other methods. Quantum Monte Carlo simulations [19] yielded $T_c \approx 0.568J$, while exact diagonalization of finite systems [1] led to $T_c \approx 0.52J^2$. However, these calculations were less accurate than the procedure

²The values for T_c found in Refs. [19, 1] have to be scaled by a factor 4 due to a slightly different definition of the spin operators (1.3)

described here, and in both cases the deviation from (2.42) can be convincingly explained by the respective statistical errors. To the authors knowledge, (2.42) is the most accurate result presently known.

2.2.3.3 The specific heat

Starting from the free energy (1.61) and using standard thermodynamic relations, a useful expression for the internal energy per site shall be derived in App. A.3. For the isotropic case, and exploiting the symmetry relation (1.36), eq. (A.24) can be cast into the form

$$U = \frac{3}{2}\beta J^2 \left(q^2 - \tilde{q}_0^2 - 2 \sum_{m=1}^{\infty} \tilde{q}_m^2 \right). \quad (2.43)$$

The specific heat is given by

$$C(T) = \frac{dU}{dT} \quad (2.44)$$

and can be calculated by numerical evaluation of the temperature derivative. As discussed in Sec. 2.2.1, within the dynamical approximation of order M only the quantities $\tilde{q}_{m \leq M}$ are part of the self-consistency problem. This opens two ways to define the approximate internal energy: on one hand, the frequency sum in eq. (2.43) can be simply restricted to $m \leq M$, on the other hand, contributions with $m > M$ can be included and calculated non-self-consistently from eq. (1.99 b), or, for $M = 0$, from eq. (2.26). At finite order M there is quite a difference between both definitions as illustrated below for the extreme case $M = 0$. Although the latter method is numerically more involved it will be adopted here since it provides better convergence of the specific heat approximants as the order M is increased.

Of particular interest is the behavior of the specific heat at the spin glass phase transition. Therefore, one is in need of solutions to the self-consistency problem in the spin glass phase. Unfortunately, a solution over the whole temperature range can be found easily only within the spin-static (and replica-symmetric) approximation from eqs. (2.23) (see Fig. 2.1). For $M > 0$, however, the full integration problem is hardly feasible due to the additional z -type integrations that occur in the spin glass phase. Therefore, the calculations were restricted to temperatures below but sufficiently close to T_c where the self-consistency equations can well be approximated by expansions in powers of $T_c - T$ which in turn allows to perform the z -integrations analytically. A detailed derivation of the following equations will be given in App. A.4. By expansion of eq. (1.99 a) one obtains for the spin glass order parameter the linear expression (see App. A.4.1)

$$q = a (T_c - T), \quad T \lesssim T_c \quad (2.45)$$

with the slope

$$a = \frac{1}{J} - \left. \frac{d}{dT} \tilde{q}_0 \right|_{T=T_c}. \quad (2.46)$$

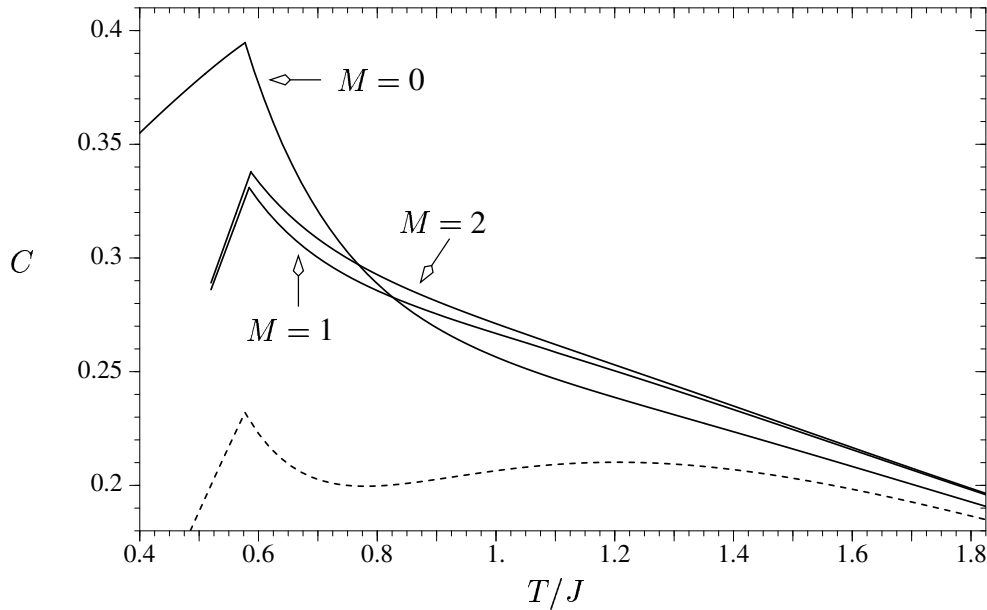


Figure 2.7: Specific heat of the isotropic HSGs obtained from numerical differentiation of the internal energy within the dynamical approximations of orders $M \leq 2$ (full lines). Contributions to eq. (2.43) with $m > M$ are taken into account non-self-consistently. The cusp of the curves indicates the respective critical temperature $T_{c,M}$. In the spin glass phase the order parameter q is taken into account perturbatively, and thus the solutions are correct close to $T_{c,M}$ only (see text). For comparison the “conventional” spin-static approximation, where the frequency sum in eq. (2.43) is restricted to the $m = 0$ term, is also shown (dashed line).

Expansion of eq. (1.99 b) in powers of q yields the simplified self-consistency equation (see App. A.4.2)

$$\tilde{q}_m = F_m|_{q=0} + c_m q^2, \quad T \lesssim T_c, \quad (2.47)$$

where F_m symbolizes the right hand side of eq. (1.99 b). The constants c_m are well defined expansion coefficients that can be calculated numerically at $T = T_c$. Substituting the solutions of eqs. (2.45, 2.47) into the formula for the internal energy, eq. (2.43), one ends up with curves for the specific heat in the ordered phase that are correct at linear order of $T_c - T$.

Instead of expanding the self-consistency equation (1.99 a), relation (2.45) can be obtained as well from an expansion of the free energy (1.61) in powers of q up to order $O(q^3)$. It is known that to this order the replica-symmetric solution is correct [13]. Effects of Parisi replica symmetry breaking first occur when the free energy is considered to quartic order in q , and therefore they will change the results for $C(T)$ only in higher than linear orders of $T_c - T$.

The resulting specific heat approximants for $M = \{0, \dots, 2\}$ are shown in Fig. 2.7. Due to the apparent quick convergence of this sequence of solutions one may safely draw qualitative conclusions for the limit $M \rightarrow \infty$. In the paramagnetic phase the full dynamical $C(T)$ -curve most probably monotonically increases as the temperature is lowered, and at T_c it exhibits a pronounced cusp.

Experiments with Heisenberg spin glass systems, such as CuMn with various Mn-concentrations [54, 7] and many more [5], have shown that in these real systems the magnetic part of the specific heat exhibits a rather broad maximum well above T_c but has virtually no fingerprints of the spin glass phase transition. Recently, such a behavior of the specific heat has been reported by other authors for the spin 1/2 infinite-range Heisenberg spin glass, too [1]. These results were obtained by way of exact diagonalization of finite clusters together with explicit disorder averages. However, due to the small cluster sizes (clusters of up to 12 spins could be dealt with) the numerical data were afflicted with strong finite size effects and poor convergence properties. Consequently, these results can not be trusted.

Contrary to the findings published in Ref. [1], in the results presented here there is no indication of a broad maximum in the full dynamical $C(T)$ -curve above T_c . Merely the “conventional” spin-static approximation, which neglects the quantum-spin dynamics altogether and omits all $m \neq 0$ terms in the internal energy formula (2.43), generates such a (artificial) maximum. Interestingly, both features of the specific heat, the absence of a broad maximum above T_c as well as the non-analytic behavior at T_c , have been observed also in a $SU(N)$ generalization of the quantum Heisenberg spin glass in the limit $N \rightarrow \infty$ and for larger spin quantum number [15, 16].

2.2.4 Dynamical results for the isotropic Heisenberg spin glass on the Fock space

This brief section temporarily departs from the HSG_S . Some basic results for the isotropic Heisenberg spin glass on the Fock space (HSG_F) at half fermion filling (i.e. $\mu = 0$) shall be presented for comparison. Solutions of the self-consistency problem within the dynamical approximation scheme were obtained with about the same numerical effort as for the model variant on the spin space.

The deviations of the χ_0 -approximants from the spin-static approximation are shown in Fig. 2.8. While the curves exhibit the same characteristic features as the ones for the HSG_S in Fig. 2.4, the absolute magnitude of these quantum-dynamical corrections is about twice as big.

Figure 2.9 displays the critical temperatures as obtained from relation (2.41) within the dynamical approximation scheme for $M = \{0, \dots, 4\}$. Extrapolation of this sequence to $M = \infty$ (see Sec. 2.2.3.2) yields the full dynamical value

$$T_c = (0.50852 \pm 0.00013)J. \quad (2.48)$$

Compared to the spin-static value (see Tab. 2.1.4) the quantum-dynamical corrections again cause a slight increase of T_c by about 3%.

2.3 The perturbative $\tilde{q}_{m \neq 0}$ -expansion

In order to consolidate the achievements of the dynamical approximation scheme discussed in the preceding sections, and particularly to support the results for the isotropic HSG_S in Sec.

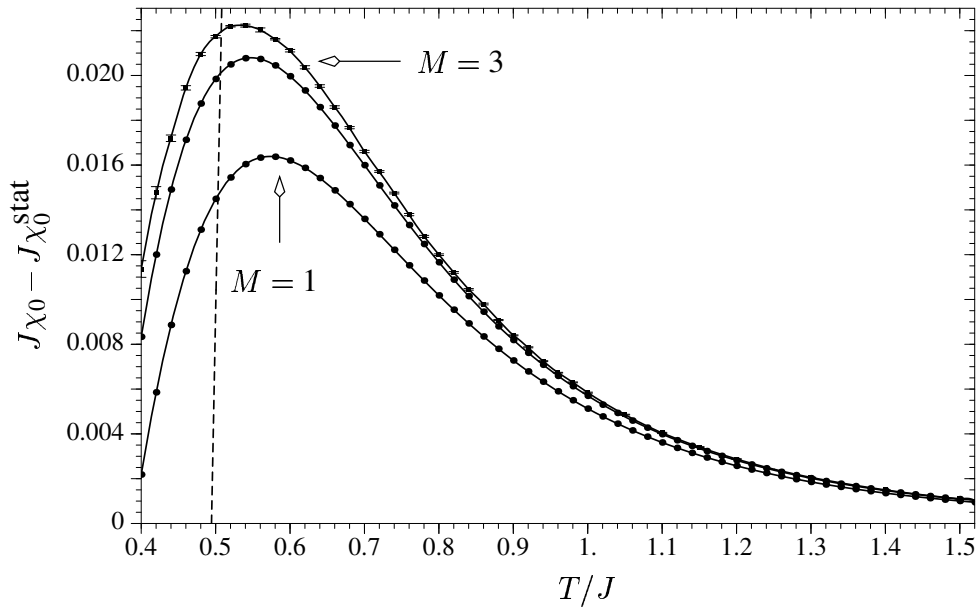


Figure 2.8: Zero frequency local susceptibility for the isotropic HSG_F obtained within the dynamical approximations of orders up to and including $M = 3$. Again, only deviations from the spin-static approximation result are shown. Compare to Fig. 2.4.

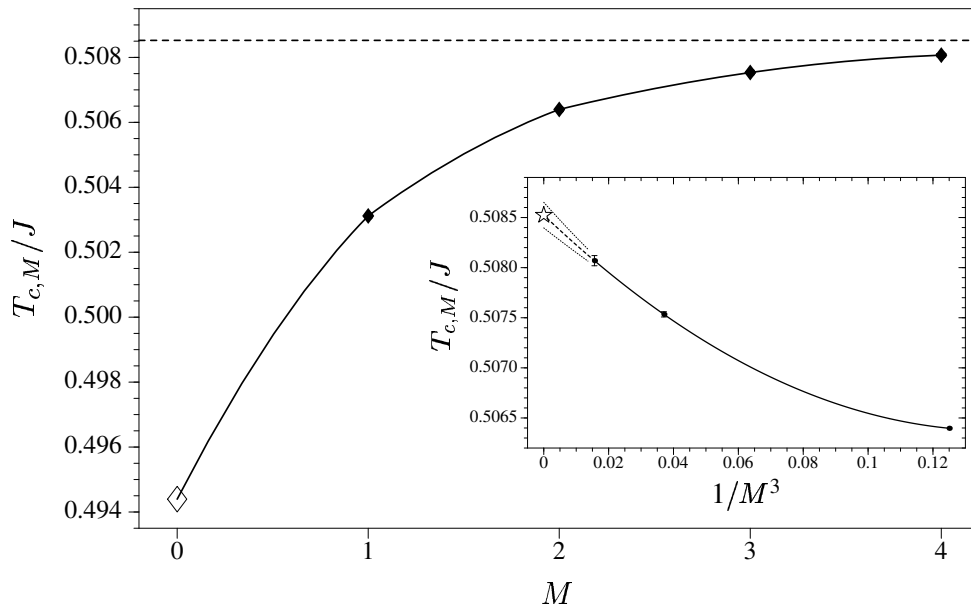


Figure 2.9: Sequence of critical temperatures for the isotropic HSG_F obtained within dynamical approximations of orders $M = \{0, \dots, 4\}$. Inset: Estimation of the full dynamical T_c by extrapolation of the sequence. Compare to Fig. 2.6.

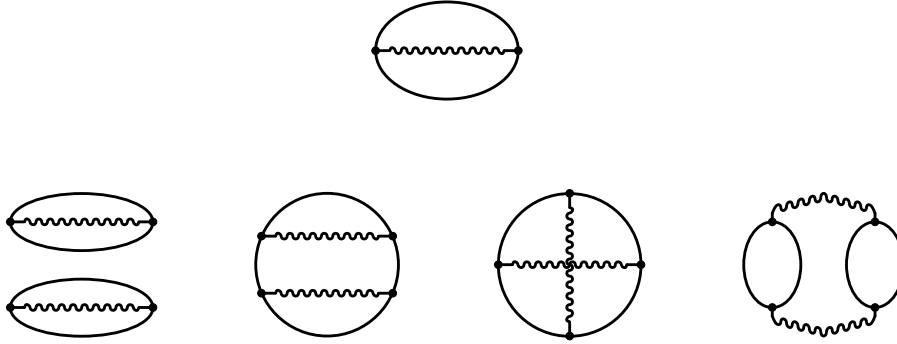


Figure 2.10: Diagrams contributing to the first (top) and second (bottom row) dynamical order of the perturbative expansion of the functional Φ defined by eqs. (1.98, 2.49) in powers of the dynamical saddle point components $\tilde{q}_\nu^{m \neq 0}$ (in the text referred to as the $\tilde{q}_{m \neq 0}$ -expansion). Straight lines represent 2×2 -blocks of the frequency-diagonal spin-static propagator matrix Γ_{stat} (2.3), and wavy lines symbolize contractions of the dynamical effective magnetic fields $H_\nu^{m \neq 0}$ (1.93) according to (2.50).

2.2.3, a completely different approximation technique was developed and applied to the self-consistency problem posed in Sec. 1.4.3. The basic idea of this method is to perturbatively expand the functional Φ (1.98) in powers of the dynamical saddle point components $\tilde{q}_\nu^{m \neq 0}$. The associated dynamical decoupling fields $y_{\nu, m}^\pm$ can then be integrated out analytically. Here, the spin-static theory of Sec. 2.1 again serves as a non-trivial starting point. Such an expansion is certainly justified at high temperatures where $\tilde{q}_\nu^{m \neq 0} \ll \tilde{q}_\nu^0 \lesssim 1$.

Substituting the $\tilde{q}_{m \neq 0}$ -expansion of Φ into eq. (1.61) one yields an approximate expression for the free energy which can be subjected to a stationarity condition similar to the procedure in Sec. 1.4.1. The resulting simplified self-consistency equations for the saddle point parameters q_ν and \tilde{q}_ν^m involve integrations over the static decoupling fields only and are therefore easily solved numerically.

2.3.1 Diagrammatic expansion of Φ

As a direct consequence of the decomposition (2.1) of the effective potential (1.90), the weight function (1.96) may be cast into the form

$$W = W_{\text{stat}} \exp \text{Tr} \ln (\mathbb{1} + \Gamma_{\text{stat}} \mathbf{V}_{\text{dyn}}), \quad (2.49)$$

where the spin-static quantities Γ_{stat} and W_{stat} have been defined by eqs. (2.3, 2.11), respectively. In the high temperature limit, the dynamical saddle point components vanish like $\tilde{q}_\nu^{m \neq 0} \sim 1/T^2$ (this asymptotic behavior can be read off already from eq. (2.26) for the spin-static and isotropic special case), whereas the zero frequency components reach unity, $\tilde{q}_\nu^0 \rightarrow 1$. Hence, at least at high temperatures it is justified to expand the logarithm in eq. (2.49) in powers of the matrix \mathbf{V}_{dyn} .

Such an expansion generates powers of the dynamical effective magnetic fields (1.93), and thus it permits the Gaussian integrations over the dynamical decoupling fields $y_{\nu, m \neq 0}^\pm$ in eq.

(1.98) to be performed exactly. With the help of a suitably defined generating functional one easily verifies the useful identity

$$\int_{\mathbf{y}}^G (H_{\nu}^m)^k (H_{\nu'}^{-m})^{k'} = J_{\nu}^{2k} (\tilde{q}_{\nu}^m)^k k! \delta_{kk'} \delta_{\nu\nu'}. \quad (2.50)$$

This contraction relation on one hand, and the trace operation in eq. (2.49) on the other, suggest to organize the expansion of the functional Φ in terms of closed diagrams. At the second dynamical order this yields the representation

$$\Phi = \Phi_{\text{stat}} + \Phi_1 + \Phi_2 + O\left(\tilde{q}_{\nu}^{m \neq 0} \tilde{q}_{\nu'}^{m' \neq 0} \tilde{q}_{\nu''}^{m'' \neq 0}\right), \quad (2.51)$$

where Φ_{stat} is given by eqs. (2.17, 2.11). All diagrams contributing to Φ_1 and Φ_2 are shown in Fig. 2.10. They can be evaluated straightforwardly exploiting formula (A.9) to perform the occurring Matsubara sums.

2.3.2 Results for the isotropic Heisenberg spin glass on the spin space

As a concrete example the case of the isotropic HSG_S shall be made explicit in this section. As the $\tilde{q}_{m \neq 0}$ -expansion is expected to be useful at high temperatures the discussion will be restricted to the paramagnetic phase (i.e. $q \equiv 0$). In the evaluation of the diagrams in Fig. 2.10 the Popov-Fedotov chemical potential (1.9) is employed again, and exploiting some symmetries the dynamical contributions to eq. (2.51) can be cast into the form (the constant b has been defined in (2.24))

$$\Phi_1 = \beta^2 J^2 \sum_{m=1}^{\infty} \tilde{q}_m \int_r^G r^2 \frac{br \sinh(br)}{b^2 r^2 + \pi^2 m^2} \quad (2.52)$$

and

$$\Phi_2 = \beta^4 J^4 \sum_{m=1}^{\infty} \sum_{m' \geq m} \tilde{q}_m \tilde{q}_{m'} \int_r^G r^2 \times \left(w\left(br, (\pi m)^2\right) \delta_{m,m'} + v\left(br, (\pi m)^2, (\pi m')^2\right) \right) \quad (2.53)$$

with the functions

$$w(x, s) = \frac{\text{sech } x}{(x^2 + s)^2} \left(-\frac{3sx^4 - s^2x^2 + 2s^3}{(x^2 + s)(x^3 + 4sx)} \sinh(2x) + \frac{x^2 - s + 4}{8} \cosh(2x) + \frac{11x^2 - 3s - 4}{8} \right) \quad (2.54)$$

and

$$v(x, s, t) = \frac{\sinh x}{(x^2 + s)(x^2 + t)} \left(\frac{x^2}{\cosh x \sinh x} + \tanh x + \frac{2sx}{x^2 + s} + \frac{2tx}{x^2 + t} - \frac{x(5x^2 + s + t)(s + t)}{(x^2 + s + t)^2 - 4st} \right). \quad (2.55)$$

Expressions (2.52 – 2.55) correctly reproduce the high temperature expansions of all considered quantities up to and including order $O(\beta^4)$.

2.3.2.1 Asymptotics of the dynamical approximation scheme at large orders M

In the context of the dynamical approximation scheme discussed in Sec. 2.2, particularly for the extrapolation to the full dynamical result of some quantity, it is important to know how this quantity varies with the order M for $M \rightarrow \infty$. This asymptotic behavior is governed by the convergence properties of the basic functional Φ which can be extracted by applying the idea of the dynamical approximation scheme to the analytical expansion (2.51). First the simplest contribution Φ_1 shall be considered. One writes

$$\Phi_1 = \Phi_{1,M} + \tilde{\Phi}_{1,M}, \quad (2.56)$$

where for $\Phi_{1,M}$ the sum in eq. (2.52) is restricted to $m = \{1, \dots, M\}$, and $\tilde{\Phi}_{1,M}$ contains the remaining high-frequency terms with indices $m > M$. The asymptotic M -dependence of the latter part, which is neglected within the dynamical approximation of order M , can be readily evaluated. Since $\tilde{q}^m \sim m^{-2}$ for large m (see, for instance, eq. (2.26)) one has the asymptotic sum

$$\tilde{\Phi}_{1,M} \sim \sum_{m=M+1}^{\infty} \frac{1}{m^4} \sim M^{-3}, \quad M \gg 1. \quad (2.57)$$

The second order contribution Φ_2 (2.53) can be treated similarly. Here the neglected high-frequency part $\tilde{\Phi}_{2,M}$ comprises all sum terms with $m' > M$. The functions (2.54, 2.55) vanish like $w \sim 1/s$ and $v \sim 1/t$. Thus, all sum terms fall off asymptotically like $(m')^{-4}$ or faster, and hence $\tilde{\Phi}_{2,M} \sim M^{-3}$ for large M . The same arguments also apply to all higher order contributions $\tilde{\Phi}_{k,M}$. Therefore, the full high-frequency part of the functional Φ , which is formally given by the k -resummation of all contributions $\tilde{\Phi}_{k,M}$, should also vanish like M^{-3} . Consequently, any quantity that is derived from Φ , e.g. the critical temperature (see Figs. 2.6 and 2.9), converges accordingly.

2.3.2.2 The static susceptibility

Simplified self-consistency equations in the paramagnetic phase were derived by combining eqs. (1.61) and (2.51 – 2.55) and requiring stationarity of the free energy with respect to variations of the parameters \tilde{q}_m . These equations were solved iteratively at the first two non-trivial orders of the $\tilde{q}_{m \neq 0}$ -expansion. The respective zero frequency parts of the local susceptibility are presented in Fig. 2.11. At temperatures $T > J$ the previous results of the dynamical approximation are reproduced very accurately (see Fig. 2.4). From this fact one can infer that the two series of approximants obtained from both approximation schemes, the dynamical approximation on one hand and the $\tilde{q}_{m \neq 0}$ -expansion on the other, are well converged in this temperature region. Going to lower temperatures, however, the perturbative solutions apparently underestimate the full dynamical curve, and higher orders of the $\tilde{q}_{m \neq 0}$ -expansion become more important.

The criterion (2.41) yields the approximate critical temperatures $T_c = 0.58557J$ and $T_c = 0.58673J$ in orders $O(\tilde{q}_{m \neq 0})$ and $O(\tilde{q}_{m \neq 0} \tilde{q}_{m' \neq 0})$, respectively. Due to the small number of available orders one can not reliably extrapolate these data to a full dynamical estimate. Nevertheless, these numbers are in good quantitative agreement with the T_c -value (2.42).

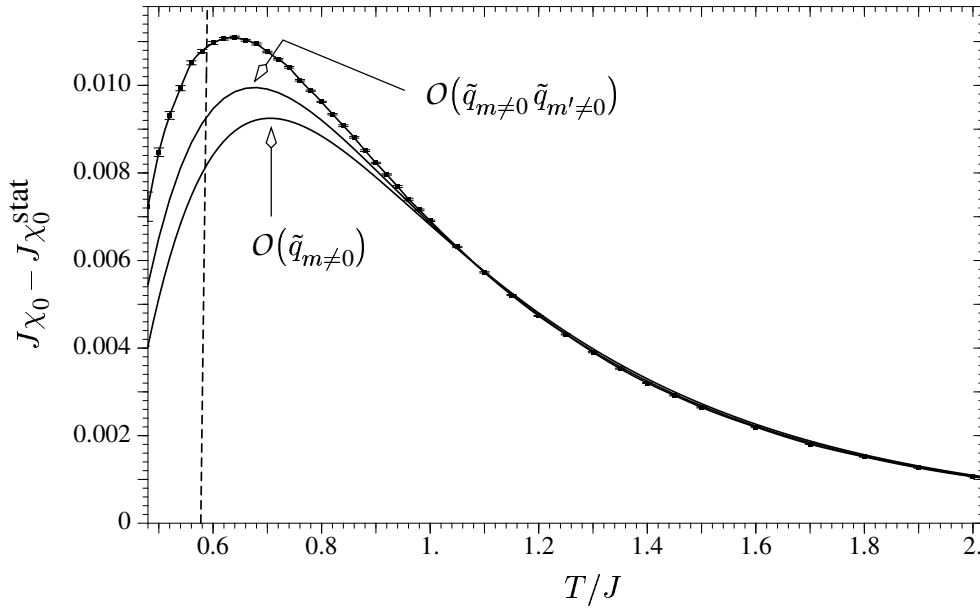


Figure 2.11: Zero frequency part of the local susceptibility $\chi_0 = \beta \tilde{q}_0$ for the isotropic HSG_S calculated within the first two non-trivial orders of the $\tilde{q}_{m \neq 0}$ -expansion (see text) and within the third order dynamical approximation for comparison (plot symbols). Only deviations from the spin-static approximation result (2.29) are shown. Compare to Fig. 2.4.

In particular, the interesting observation that the quantum-dynamical correlations increase the critical temperature compared to the spin-static approximation is strongly supported by the perturbative $\tilde{q}_{m \neq 0}$ -expansion.

2.3.2.3 The specific heat

The specific heat obtained from the $\tilde{q}_{m \neq 0}$ -expansion is presented in Fig. 2.12. Again, for $T \gtrsim J$ the approximants of orders $O(\tilde{q}_{m \neq 0})$ and $O(\tilde{q}_{m \neq 0} \tilde{q}_{m' \neq 0})$ differ only slightly from each other, and they are in good quantitative agreement with the results of Sec. 2.2.3.3. At lower temperatures the curves clearly separate which indicates poor convergence of the sequence of solutions at the highest order considered here. Consequently, it is not possible to estimate the exact $C(T)$ -curve from these data. Nevertheless, the data allow for qualitative conclusions. The maximum obtained in the “conventional” spin-static approximation (see Fig. 2.7) representing the zeroth order of the $\tilde{q}_{m \neq 0}$ -expansion is already very weak at order $O(\tilde{q}_{m \neq 0})$, and it is not present any more at order $O(\tilde{q}_{m \neq 0} \tilde{q}_{m' \neq 0})$. Hence, consistently with the findings of Sec. 2.2.3.3, no maximum can be expected in the full dynamical $C(T)$ -curve above T_c .

2.3.2.4 Fulfillment of the sum rule (1.41)

From the numerical data presented in Figs. 2.11 and 2.12 it is not obvious that the two sequences of approximations, the dynamical approximation with increasing M on one hand and the increasing orders of the $\tilde{q}_{m \neq 0}$ -expansion on the other hand, will finally converge to the same

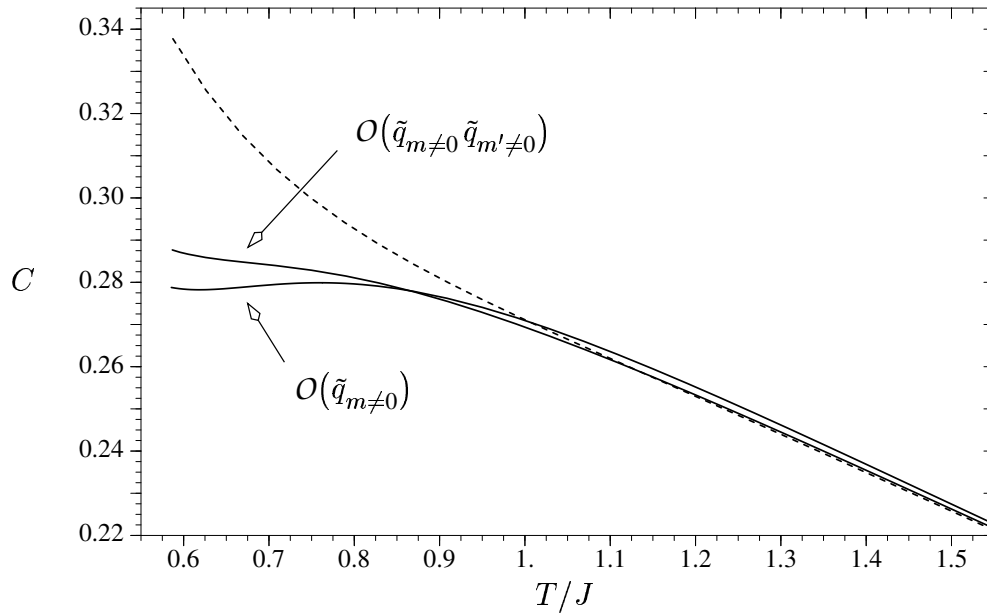


Figure 2.12: Specific heat of the isotropic HSG_S according to eqs. (2.44, 2.43) calculated within the first two non-trivial orders of the $\tilde{q}_{m \neq 0}$ -expansion. The zeroth order of this sequence of approximants is the “conventional” spin-static solution which is displayed in Fig. 2.7. For comparison the result within the second order dynamical approximation (see Fig. 2.7) is indicated (dashed line). The curves are shown in the paramagnetic phase only.

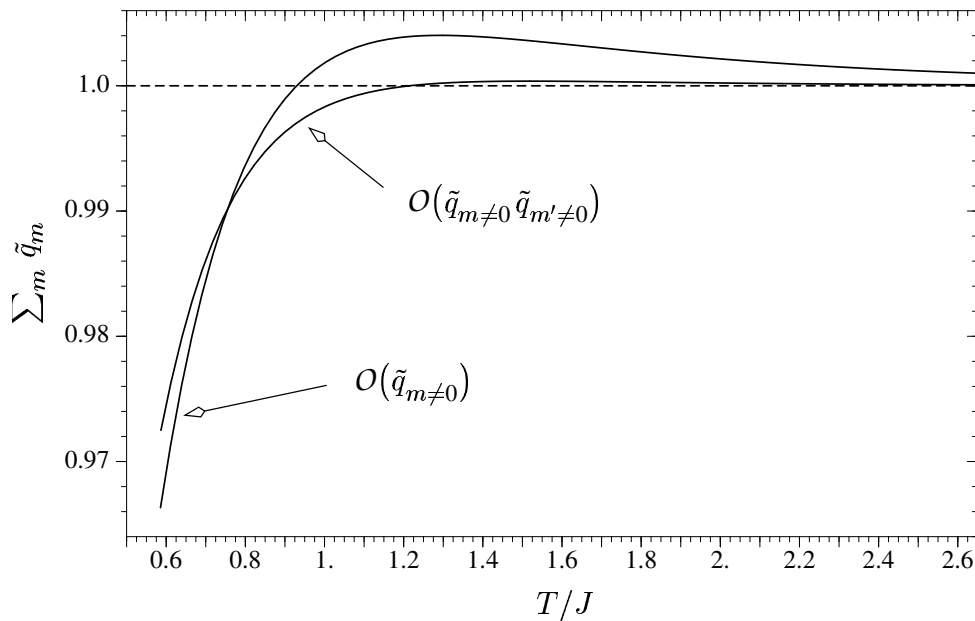


Figure 2.13: Fulfillment of the exact sum rule (1.41) for the HSG_S at the two lowest dynamical orders of the $\tilde{q}_{m \neq 0}$ -expansion providing a check of the quality of these approximations. The curves are shown down to T_c . Note that the higher order $O(\tilde{q}_{m \neq 0} \tilde{q}_{m' \neq 0})$ clearly does better for all temperatures.

full dynamical solution as required for the whole theory to be consistent and meaningful. In particular, the convergence properties of the latter perturbative series are not known. To prevent from miss-interpretations, it is illuminating to check how accurately the sum rule (1.41) is obeyed by the $\tilde{q}_{m \neq 0}$ -expansion at the two lowest dynamical orders. The results are shown in Fig. 2.13.

At high temperatures, down to $T \gtrsim J$, the sum rule is fulfilled almost exactly at order $O(\tilde{q}_{m \neq 0} \tilde{q}_{m' \neq 0})$ which reflects the good quality of the approximation. However, a substantial violation of the sum rule is observed for $T < J$, providing clear evidence that in this temperature regime the sequence of solutions obtained from the $\tilde{q}_{m \neq 0}$ -expansion is not well converged yet at the second dynamical order. As discussed in Sec. 2.3.2.2, the quantities χ_0 and T_c nevertheless give strong support to the results of the dynamical approximation scheme. The specific heat, however, directly depends on the dynamical parameters \tilde{q}_m and is therefore more sensible to the failure of the approximation to fulfill the sum rule. Hence, for $T < J$ the $C(T)$ -curves in Fig. 2.12 must be interpreted with care.

2.4 Summary and conclusion

In the present chapter the SU(2), spin 1/2 Heisenberg spin glass has been studied with the main focus being on the model variant on the spin space. Beyond the spin-static approximation two different systematic approximation schemes have been developed in order to solve the dynamical self-consistency problem posed in Chap. 1.

The dynamical approximation of order M , on one hand, describes the quantum-spin dynamics with a limited number of bosonic Matsubara frequencies, but the corresponding saddle point components $\tilde{q}_\nu^{m \leq M}$ are dealt with exactly (Sec. 2.2). The perturbative $\tilde{q}_{m \neq 0}$ -expansion, on the other hand, takes into account all frequencies but only a few powers of the parameters $\tilde{q}^{m \neq 0}$ (Sec. 2.3). In this sense the two approximation schemes are complementary to each other.

For the HSGs both approaches yield a consistent picture for the zero frequency local spin susceptibility χ_0 in the paramagnetic phase (see Figs. 2.4 and 2.11). By extrapolation of the results from the dynamical approximation scheme to $M \rightarrow \infty$ (see Fig. 2.6) the full dynamical critical temperature has been estimated to $T_c = (0.58912 \pm 0.00015)J$ which is about 2% higher than the value in the spin-static approximation. For the model on the Fock space (Sec. 2.2.4) an increase of 3% is observed.

Results for the specific heat $C(T)$ of the HSGs have been presented in Figs. 2.7 and 2.12. In the framework of the dynamical approximation scheme the calculations could be extended to the spin glass phase perturbatively. The observation of a broad maximum in the $C(T)$ -curve above T_c , which has been reported recently by other authors [1], can not be confirmed. Instead, a pronounced non-analyticity of $C(T)$ at T_c is found. The numerical method used in Ref. [1] apparently is not capable to resolve this feature, presumably due to the principal lack of sharp phase transitions in the finite size systems considered there.

The methods discussed in this chapter proved useful to qualitatively and quantitatively describe the high temperature phases of quantum spin glasses. There are many open issues that can thus be addressed in the future, e.g. the behavior in a magnetic field, questions concerning

anisotropy, or real-frequency response functions which can possibly be constructed by analytical continuation of the numerical data. For the HSG_F dynamical corrections to the spin-static phase diagram shown in Fig. 2.2 can be studied.

While the work presented here has been mainly concerned with the paramagnetic phase, it will be of high interest in the future, however, to extend the calculations to the spin glass phase and eventually to $T = 0$. As a first step it seems promising to apply the techniques developed for the Ising spin glass to analytically perform the zero-temperature limit of the self-consistency equations (2.19) (which have to be suitably generalized to allow for replica symmetry breaking). Beyond the spin-static approximation it will be a crucial question whether or not suitable new approximation schemes can be constructed which are applicable to the quantum-dynamical self-consistency problem at low temperatures.

3

The itinerant fermionic spin glass

When fermionic lattice models are investigated it appears natural to allow for mobile carriers and transport mechanisms. Therefore, the formalism developed in Chap. 1 shall be extended suitably to apply to itinerant spin glass systems.

In earlier work a metallic infinite-range Ising spin glass model was studied. Within the spin-static approximation a systematic low temperature expansion was constructed and the quantum phase transition was located [34]. Later, a more general quantum-dynamical Ginzburg-Landau theory [45] was applied to study the critical behavior. It was found that on the mean field level the effect of the dynamical spin-spin correlations changed the critical exponents obtained within the spin-static approximation (see App. A.5).

In order to account for itinerant models, the self-consistency structure summarized in Sec. 1.4.3 shall be combined with a suitable adapted coherent potential approximation (CPA) technique. Originally this powerful non-perturbative method was developed to describe non-interacting disordered electron systems [10], and in this context the CPA can be shown to become exact in the limit of infinite spatial dimensions ($d \rightarrow \infty$) [53]. Later, the CPA formalism was generalized to deal with interacting electron systems [21, 22] leading to highly non-trivial couplings of the quantum degrees of freedom. Finally, the CPA method can also be applied to dynamical disorder. Like in the present work, this situation for instance results from the dynamical decoupling of interaction terms [23, 24]. Recently, this dynamical CPA has been shown to be intimately related to the dynamical mean field theory (DMFT) [25].

After a brief introduction of the method for the general spin glass interaction (1.1), the focus shall be on the itinerant Ising system. To provide an overview of the systems' behavior the spin-static approximation will be discussed both at finite and zero temperature. In the last part the dynamical approximation scheme, which has been introduced in Sec. 2.2.1, will be applied. A sequence of dynamical approximants of the paramagnet to spin glass phase boundary in the plane of temperature and hopping strength will be presented, from which the location of the full dynamical quantum critical point can be estimated.

3.1 Model definition

In the present work a particularly simple metallic spin glass model shall be considered, which employs only on single sort of particles to provide for both local magnetic moments and mobile carriers. To this end the spin glass Hamiltonian (1.1) is augmented with a hopping term,

$$\hat{\mathcal{K}} = \hat{\mathcal{K}}_{\text{SG}} + \hat{t} \sum_{\langle ij \rangle} \sum_{\sigma} a_{i\sigma}^{\dagger} a_{j\sigma}, \quad (3.1)$$

where the sum index $\langle ij \rangle$ denotes summation over nearest-neighbor lattice sites. In distinction to previous work [35, 34, 42] there is no randomness in the kinetic term. In order to facilitate an exact treatment of the model the hopping is assumed to take place on a underlying simple cubic lattice in the limit of infinite spatial dimensions $d \rightarrow \infty$. Here the scaling of the hopping parameter according to

$$\hat{t} = \frac{1}{\sqrt{d}} t, \quad (3.2)$$

similar to the scaling of the magnetic interaction eq. (1.6), is essential to obtain physically meaningful results [55, 28].

The kinetic term in the Hamiltonian (3.1) does not interfere with the dynamical spin glass decoupling formalism as developed in Sec. 1.3. Hence the replicated and disorder averaged partition function of the itinerant model is given by eq. (1.50). The effective action (1.51) is merely modified by the hopping term and reads

$$\mathcal{A}_{\text{eff}} = -nNS(\mathbf{q}, \tilde{\mathbf{q}}) - \frac{1}{\beta} \sum_{ija} \sum_{ll'} \Psi_{ia}^l \left((iz_l + \mu) \mathbb{1}_2 \delta_{ll'} \delta_{ij} + \mathbf{v}_{ia}^{l-l'} \delta_{ij} - \hat{t} \mathbb{1}_2 \delta_{ll'} \delta_{\langle ij \rangle} \right) \Psi_{ja}^{l'}, \quad (3.3)$$

where the effective dynamical potential is defined by eq. (1.49), and the symbol $\delta_{\langle ij \rangle}$ denotes the connectivity matrix of the assumed hopping model, i.e. its matrix elements are unity for nearest neighbor sites $\{i, j\}$ and zero else.

It will be the task of the following section to properly incorporate the hopping and to formulate the generalized self-consistency problem.

3.2 The dynamical CPA approach

The effective action (3.3) describes an ensemble of non-interacting fermions moving in a complex replica- and spin-dependent effective random medium. Such a system immediately calls for the well known Coherent Potential Approximation (CPA). In the present case, the frequency dependence of the random medium requires a dynamical version of the CPA [23, 24, 25]. Following the prescription of this method the random medium is replaced exactly by a yet unknown self-energy Σ . For the present model this self-energy is frequency-diagonal,

$$(\Sigma)_{ll'} = \Sigma_l \delta_{ll'}, \quad (3.4)$$

where the diagonal elements Σ_l are in general 2×2 matrices in spin space. The full disorder averaged Green's function is then given by

$$(\mathbf{G}^{-1})_{ij}^{ll'} = \left(((iz_l + \mu) \mathbb{1}_2 - \Sigma_l) \delta_{ij} - \hat{t} \mathbb{1}_2 \delta_{\langle ij \rangle} \right) \delta_{ll'}. \quad (3.5)$$

In the chosen limit of infinite dimensions spatial fluctuations are suppressed, and the problem simplifies to a single site problem which justifies the assumption of a site-diagonal (or k -independent) self-energy [53, 14].

The effective action (3.3) is not diagonal in the frequency indices thus allowing for virtual absorption and emission of dynamical field quanta $H_{m \geq 1}^{ia}$. However, the full fermion Green's function of the original interacting problem (3.1) with any particular realization of the quenched disorder is certainly energy conserving and so is the full disorder averaged Green's function (3.5). Hence its off-diagonal elements in frequency space must vanish due to the average over the effective random medium which was explicitly checked numerically in the context of the itinerant Ising model. This fact justifies the Ansatz (3.4) of a frequency-diagonal self-energy.

Nearest-neighbor hopping of non-interacting particles on a hyper-cubic lattice in the limit of infinite spatial dimensions is described by the function (recall the scaling (3.2))

$$T_0(z, t) = \frac{\sqrt{\pi}}{2t} \exp\left(-\frac{z^2}{4t^2}\right) \left(-i \operatorname{sign}\left(\operatorname{Im}\frac{z}{t}\right) + \operatorname{erfi}\frac{z}{2t}\right). \quad (3.6)$$

Among others, one instructive way to derive this function is to expand the local Green's function in powers of the hopping parameter \hat{t} and to re-sum the arising series using Borel's method [2]. Evaluation of eq. (3.6) slightly above the real energy axis, i.e. at $z = \varepsilon + i0^+$, yields the well-known Gaussian density of states [55, 30].

The averaged Green's function \mathbf{G} can readily be expressed by

$$(\mathbf{G})_{ij} = \mathbf{T} \delta_{ij} + O\left(\frac{1}{\sqrt{d}}\right), \quad (3.7)$$

where \mathbf{T} is a site independent block-diagonal matrix in frequency and spin space given by

$$(\mathbf{T})_{ll'} = T_0((iz_l + \mu) \mathbb{1}_2 - \Sigma_l, t) \delta_{ll'}. \quad (3.8)$$

The remaining task is to determine the self-energy Σ_l . To this end Σ_l is removed and the original random medium is re-introduced at one special lattice site, say $i = s$. The resulting effective action can be cast into the form

$$\mathcal{A}_{\text{eff}}^{\text{CPA}} = -nNS(\mathbf{q}, \tilde{\mathbf{q}}) - \frac{1}{\beta} \sum_{ija} \sum_{ll'} \bar{\Psi}_{ia}^l \left((\mathbf{G}^{-1})_{ij}^{ll'} + \left(\Sigma_l \delta_{ll'} + \mathbf{v}_{sa}^{l-l'} \right) \delta_{is} \delta_{js} \right) \Psi_{ja}^{l'}. \quad (3.9)$$

For the formulation of the self-consistency equations it is useful to define as an auxiliary quantity the un-averaged local propagator at the special lattice site s and on replica a in the presence of the local effective potential,

$$(\Gamma_t^a)_{ll'}^{\sigma\sigma'} = \frac{1}{\beta} \left\langle \psi_{sa\sigma}^l \bar{\psi}_{sa\sigma'}^{l'} \right\rangle_{\mathcal{A}_{\text{eff}}^{\text{CPA}}}. \quad (3.10)$$

In the limit $d \rightarrow \infty$ one obtains from eqs. (3.7, 3.9) (dropping the site index s)

$$(\mathbf{\Gamma}_t^a)^{-1} = \mathbf{T}^{-1} + \mathbf{\Sigma} + \mathbf{V}_a \quad (3.11)$$

with the effective potential matrix \mathbf{V}_a defined in eq. (1.52). Comparison with eq. (1.53) reveals that the only difference caused by the hopping term is the replacement $\mathbf{G}_0 \rightarrow \mathbf{T}^{-1} + \mathbf{\Sigma}$. The subscript t shall remind of this modification for the itinerant model. Since

$$T_0(z, t \rightarrow 0) \rightarrow 1/z, \quad (3.12)$$

eq. (1.53) is exactly reproduced in the non-itinerant limit.

Within the CPA method the self-energy $\mathbf{\Sigma}$ is determined by the demand that the local part of the full disorder averaged homogeneous Green's function, \mathbf{T} , coincides with the explicit properly weighted average of the local propagator $\mathbf{\Gamma}_a$ over the dynamical random medium. The elements of the latter are evaluated in a way similar to the calculations in Sec. 1.4.2. One finds

$$\begin{aligned} (\mathbf{T})_{ll'}^{\sigma\sigma'} &\stackrel{!}{=} \lim_{n \rightarrow 0} \frac{1}{[Z^n]_{\text{dis}}} \int_z \int_y \int^G \mathcal{D}\psi \psi_{sa\sigma}^l \bar{\psi}_{sa\sigma'}^{l'} \exp(-\mathcal{A}_{\text{eff}}^{\text{CPA}}) \\ &= \lim_{n \rightarrow 0} \frac{1}{[Z^n]_{\text{dis}}} \int_z \int_y \int^G (\mathbf{\Gamma}_t^a)_{ll'}^{\sigma\sigma'} \int \mathcal{D}\psi \exp(-\mathcal{A}_{\text{eff}}^{\text{CPA}}) \\ &= \lim_{n \rightarrow 0} c^n \int_z \int_{y_a} \int^G W_t^a (\mathbf{\Gamma}_t^a)_{ll'}^{\sigma\sigma'} \prod_{a' \neq a} \int_{y_{a'}} \int^G W_t^{a'}, \end{aligned}$$

where the weight function W_t is given by eq. (1.96). The unimportant constant c^n in the third line comprises $[Z^n]_{\text{dis}}$ as well as all contributions from lattice sites $i \neq s$. Taking the replica limit, one obtains the conditional CPA equation for the self-energy

$$\mathbf{T} \stackrel{!}{=} \int_z \frac{1}{\Phi_t} \int_y \int^G W_t \mathbf{\Gamma}_t. \quad (3.13)$$

The quantum-dynamical nature of the model causes non-trivial couplings of the fermionic Matsubara frequencies. Although \mathbf{T} is frequency-diagonal and the off-diagonal elements on the right hand side of eq. (3.13) vanish exactly by integration, the self-energy can not be determined for one frequency at a time but only for all frequencies at once.

By explicit construction of the spin-spin correlations (1.32) at the special lattice site s the saddle point equations (1.99) can be derived analogous to the calculation for the non-itinerant model in Sec. 1.4.2. The resulting two-fold self-consistency structure for the spin glass order parameters q_ν and the dynamical saddle point components \tilde{q}_ν^m on one hand and the dynamical self-energy Σ_l on the other hand, is illustrated in Fig. 3.1.

3.3 The itinerant fermionic Ising spin glass

The CPA method formulated in Sec. 3.2 shall now be applied to the itinerant fermionic Ising spin glass (ISG_F) at half filling and in zero external magnetic field, as described by the Hamiltonian

$$\hat{\mathcal{K}} = \frac{1}{2} \sum_{i \neq j} J_{ij} \hat{S}_i^z \hat{S}_j^z + \hat{t} \sum_{\langle ij \rangle} \sum_{\sigma} a_{i\sigma}^\dagger a_{j\sigma}, \quad (3.14)$$

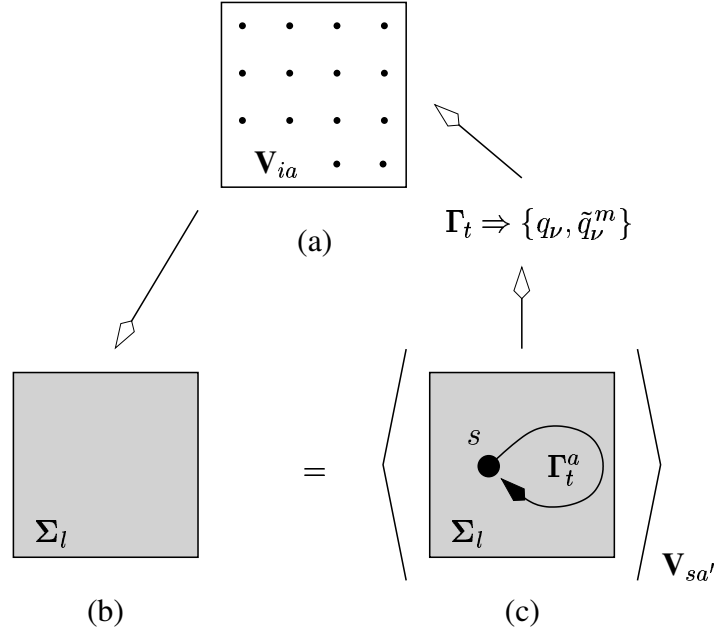


Figure 3.1: Structure of the two-fold self-consistency problem for the itinerant spin glass model (inspired by Ref. [22]). In (a) the effective dynamical random medium (1.52) is shown which depends on the spin glass order parameters q_ν and the dynamical saddle point components \tilde{q}_ν^m . In (b) the random medium is replaced by the homogeneous dynamical self-energy Σ_l (3.4). Part (c) illustrates the determination of Σ_l by means of the CPA construction at the special lattice site $i = s$. The angular brackets in (c) indicate the weighted average over the random medium that occurs in the CPA equation (3.13). From the self-consistency equations (1.99) with the local propagator matrix Γ_t (3.10), the physical quantities q_ν and \tilde{q}_ν^m are constructed, which in turn generate the self-induced random medium in (a).

where the one-component spin operators are defined by (see eq. (1.3))

$$\hat{S}_i^z = a_{i\uparrow}^\dagger a_{i\uparrow} - a_{i\downarrow}^\dagger a_{i\downarrow}. \quad (3.15)$$

Equation (3.14) represents the simplest interesting special case of the generic Hamiltonian (3.1) and corresponds to the general model with the model parameters $J_z = J$ and $J_x = J_y = h_\nu = \mu = 0$. Consequently, spin glass order can occur in z -direction only. The transversal replica-diagonal spin-spin correlations $\tilde{q}_{\nu \neq z}^m$ are finite (see Sec. 2.1.4), but they do not influence the correlations in z -direction, and thus they are irrelevant in the present context. Therefore the direction index can be dropped in this section, i.e. $q_z = q$ and $\tilde{q}_z^m = \tilde{q}_m$.

The restrictions of the model (3.14) implicate a simplified structure of the CPA self-energy. Since there is no external field considered the self-energy is independent of the spin projection, and one can write

$$\Sigma_l = \sigma_l \mathbb{1}_2. \quad (3.16)$$

In addition, the quantities σ_l are purely imaginary at half filling ($\mu = 0$) and obey the symmetry relation

$$\sigma_l = -\sigma_{-l-1}. \quad (3.17)$$

3.3.1 General solution strategies

In order to explore the quantum-dynamical behavior of the present itinerant spin glass model the dynamical approximation scheme, which has been introduced in the context of the Heisenberg spin glass in Sec. 2.2.1, was applied to the two-fold self-consistency problem sketched in Fig. 3.1. In essence, within the dynamical approximation of order M the effective potential (1.90) is constructed from the dynamical saddle point components \tilde{q}_m with frequency indices $m = \{0, \dots, M\}$ only. Contributions associated with higher bosonic Matsubara frequencies $\omega_{|m|>M}$ are neglected (see Fig. 2.3).

Within this dynamical approximation scheme the quantum-spin dynamics is treated on energy scales ranging from $\omega_0 = 0$ to $\omega_M = 2\pi TM$. To estimate the quality of this approximation one may compare the energy scales that are neglected to the hopping strength t being the model parameter that generates the dynamics. Thus one is led to

$$t \ll \omega_{M+1} \equiv 2\pi T(M+1) \quad (3.18)$$

as a simple criterion for validity of the M^{th} order dynamical approximation. Hence, although it is neither a high temperature expansion nor an expansion in small t , the method works well especially for small t/T . In those regions in parameter space the approximation already at manageable low orders M excellently captures the effects of the quantum-spin dynamics.

Another difficulty arises from the infinite extension of the matrices \mathbf{V} (1.90), \mathbf{T} (3.8), and $\mathbf{\Gamma}_t$ (3.10) in the space of the fermionic Matsubara frequencies. Naturally, a numerical analysis requires these matrices to be constructed in a limited frequency range, say z_{-l_c-1} to z_{l_c} . However, there are also important contributions from higher frequencies $\pm z_{l>l_c}$ that can not be neglected. They were rather treated perturbatively in order to permit a minimum choice for the ‘‘cut-off index’’ l_c . Particularly in the vicinity of the quantum critical point, i.e. at very low temperatures where the energetic spacings between the Matsubara frequencies are small, it was essential to take these high-frequency contributions into account as accurately as possible¹.

To this end systematic asymptotic expansions of the self-consistency equations in terms of $1/z_l$ were performed up to some feasible order $O((1/z_l)^K)$, using the high-frequency asymptotics of the self-energy

$$\sigma_l \xrightarrow{|l| \rightarrow \infty} \sum_{k=1}^K \frac{a_k}{(iz_l)^{2k-1}} + O\left(z_l^{-(2K+1)}\right) \quad (3.19)$$

which can be derived from the CPA equation (3.13). Here the expansion coefficients a_k are easy to calculate averages of polynomials of the effective magnetic fields (1.92, 1.93). The Matsubara summations which occur in the evaluation of the self-consistency equations can always be split up into a low-frequency main part and a high-frequency part separated by the cut-off index l_c . While the matrix-structured main part has to be treated numerically, the high-frequency contributions can be formulated in terms of asymptotic series expansions of docile structure that permits analytical summation.

¹This point has been less important in Sec. 2.2 because there only solutions around or above T_c have been presented.

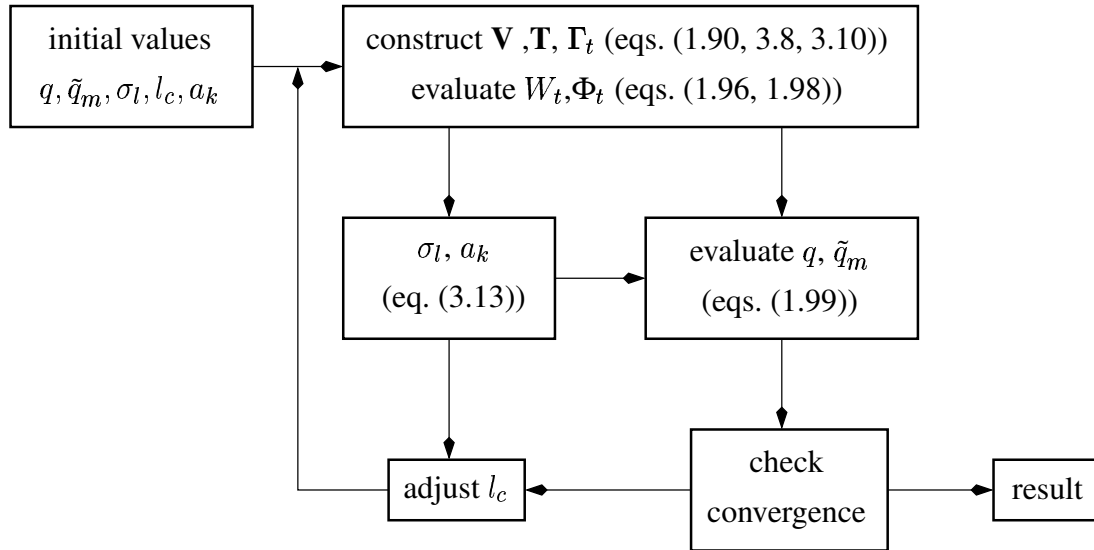


Figure 3.2: Schematic of the iterative procedure employed to solve the two-fold self-consistency problem (see Fig. 3.1) for the itinerant ISG_F defined by (3.14). The basic algorithm was implemented in the Mathematica[®] language, while all computationally expensive matrix operations were passed to external C routines making use of the MathLink interface.

The restriction of the fermionic frequency space by the numerical method introduces some error. The cut-off index l_c has to be chosen such that this error falls below some given threshold of insignificance. In practical calculations different methods were used to determine l_c . A simple way is to make trial variations of the matrix sizes at each iteration cycle and to adjust (increase or decrease) l_c according to the corresponding variations of all relevant intermediate quantities. A more direct method is to evaluate the contributions of the first neglected asymptotic order, i.e. $O((1/z_l)^{K+1})$, as a function of l_c and to apply some suitable smallness criterion. The latter method turned out to be un-practical for $M > 0$ because of the complexity of the occurring analytical expressions for the asymptotic Matsubara sums.

The final criterion for the choice of l_c is always that the physical quantities must be independent of this auxiliary parameter at some desired level of precision. The proper l_c and thereupon the computational expenses for solving the self-consistency problem strongly depend on the temperature as well as on the order K up to which the asymptotic series expansions of the equations can be driven. Parts of the low temperature data discussed below were obtained with cut-off indices up to $l_c \approx 400$.

All solutions of the self-consistency equations presented in this article were obtained by means of the principal iterative algorithm sketched in Fig. 3.2. This procedure proved to be insensitive to the initial values and also showed quite satisfying convergence properties in all regions of the parameter space explored so far.

3.3.2 Spin-static approximation

This section is devoted to a discussion of the dynamical self-consistency equations within the spin-static approximation being the first and simplest instance of the dynamical approximation scheme. The spin-static solution is not only very instructive but it also provides a reference for quantum-dynamical corrections.

The spin-static approximation has already been discussed at length in the context of the Heisenberg spin glass in Sec. 2.1. It consists in neglecting the time dependence of the saddle point (1.33 b) or, equivalently, in taking all Fourier components \tilde{q}_m with $m > 0$ to be zero in the construction of the dynamical potential (1.90). This restriction to the static component \tilde{q}_0 brings about tremendous simplifications of the self-consistency problem.

3.3.2.1 Results at finite temperature

Because the dynamical effective fields (1.93) vanish, the Gaussian integrations over the fields $y_{\nu,m}^{\pm}$ which are part of the integral operator (1.95 b) can be performed trivially. In the present Ising case one is left with only two Gaussian integrations over the static fields $y_{z,0} = y_0$ and $z_z = z$. In addition, within this approximation the occurring matrices become diagonal and thus the matrix structure of the self-consistency problem disappears. The determinant in eq. (1.96) reduces to an easily manageable Matsubara product, and hence the spin-static weight function can be evaluated to

$$W_t^{\text{stat}} = \frac{1}{2} (1 + \cosh(\beta H_0)) \exp(\beta R(H_0)). \quad (3.20)$$

Here the exponent function in the last factor is given by

$$R(\eta) = \frac{2}{\beta} \sum_{l=0}^{\infty} \ln \frac{|u_l|^2 + \eta^2}{z_l^2 + \eta^2} \quad (3.21)$$

with $H_0 = J(\sqrt{q}z + \sqrt{\tilde{q}_0 - q}y_0)$, and u_l is defined by

$$u_l = \frac{1}{T_0(iz_l - \sigma_l, t)} + \sigma_l. \quad (3.22)$$

In the present itinerant model the effect of the hopping becomes noticeable in the difference between u_l and iz_l and hence in the deviation of the function $R(H_0)$ from zero. Note that with property (3.12) in the non-itinerant limit eq. (2.11) is reproduced exactly (recall that $\mu = 0$). Since there is no explicit expression for the self-energy σ_l (and hence u_l), the l -product in eq. (3.20) can not be performed analytically but has to be evaluated numerically.

Due to the diagonality of the effective potential \mathbf{V} the matrix inversion in eq. (3.11) effectively turns into simple scalar inversion. Consequently, within the spin-static approximation the dynamical CPA equation (3.13) decouples into a set of scalar equations for each Matsubara frequency,

$$T_0(iz_l - \sigma_l, t) \stackrel{!}{=} \int_z^G \frac{1}{\Phi_t^{\text{stat}}} \int_{y_0}^G W_t^{\text{stat}} \frac{1}{u_l + H_0}, \quad (3.23)$$

which can be solved independently one at a time.

The trace terms (2.14), evaluated for the $\nu = z$ direction and at zero frequency $m = 0$, are given by

$$A_t(\eta) = 4 \sum_{l=0}^{\infty} \frac{\eta}{|u_l|^2 + \eta^2}, \quad (3.24 \text{ a})$$

$$B_t(\eta) = \frac{d}{d\eta} A_t(\eta) = 4 \sum_{l=0}^{\infty} \frac{-|u_l|^2 + \eta^2}{(|u_l|^2 + \eta^2)^2}. \quad (3.24 \text{ b})$$

Again, the Matsubara sums can not be done analytically unlike the corresponding sums in eqs. (2.15, 2.16) for the non-itinerant case. Finally, the spin-static special case of the self-consistency equations (1.99) can be written in terms of the functionals A_t and B_t :

$$q = \frac{1}{\beta^2} \int_z^G \left(\frac{1}{\Phi_t^{\text{stat}}} \int_{y_0}^G W_t^{\text{stat}} A_t(H_0) \right)^2, \quad (3.25 \text{ a})$$

$$\tilde{q}_0 = \frac{1}{\beta^2} \int_z^G \frac{1}{\Phi_t^{\text{stat}}} \int_{y_0}^G W_t^{\text{stat}} \left(A_t(H_0)^2 - B_t(H_0) \right). \quad (3.25 \text{ b})$$

Numerical solutions of the spin-static self-consistency problem given by eqs. (3.25, 3.24, 3.23) were obtained for a broad range of hopping parameters t , having regard to what was discussed in Sec. 3.3.1. The results are presented in Fig. 3.3. In the non-itinerant limit ($t = 0$) the paramagnet to spin glass transition occurs at $T_c = J / (1 + \exp(-1/(2T_c/J))) \simeq 0.6767J$. A finite hopping hampers the local freezing of the spins and thus lowers the critical temperature. The phase transition remains continuous down to zero temperature. As $T \rightarrow \infty$ all available many particle states become equally populated, and consequently $\tilde{q}_0 \rightarrow 1/2$ since two of the four local states are magnetic.

3.3.2.2 The limit of zero temperature

In the context of the non-itinerant ISG_F it was noted that the zero temperature limit brings along substantial simplifications of the self-consistency equations [37]. This is true for the itinerant case, too, and in the following the generalization to the model (3.14) shall be discussed briefly.

It is obvious from Fig. 3.3 that the spin-static solutions feature the low temperature behavior $(\tilde{q}_0 - q) \sim T$. In order to perform the zero-temperature limit it is therefore advisable to eliminate \tilde{q}_0 and to formulate the self-consistency problem in terms of q and the static part of the local susceptibility $\chi_0 = \beta(\tilde{q}_0 - q)$ (see eq. (1.37)) which remains finite as $T \rightarrow 0$.

In the zero-temperature limit the discrete fermionic Matsubara frequencies z_l merge into a continuous variable, say ζ , and the Matsubara sums have to be replaced by frequency integrations according to

$$T \sum_{l=0}^{\infty} f(z_l) \xrightarrow{T \rightarrow 0} \frac{1}{2\pi} \int_0^{\infty} d\zeta f(\zeta). \quad (3.26)$$

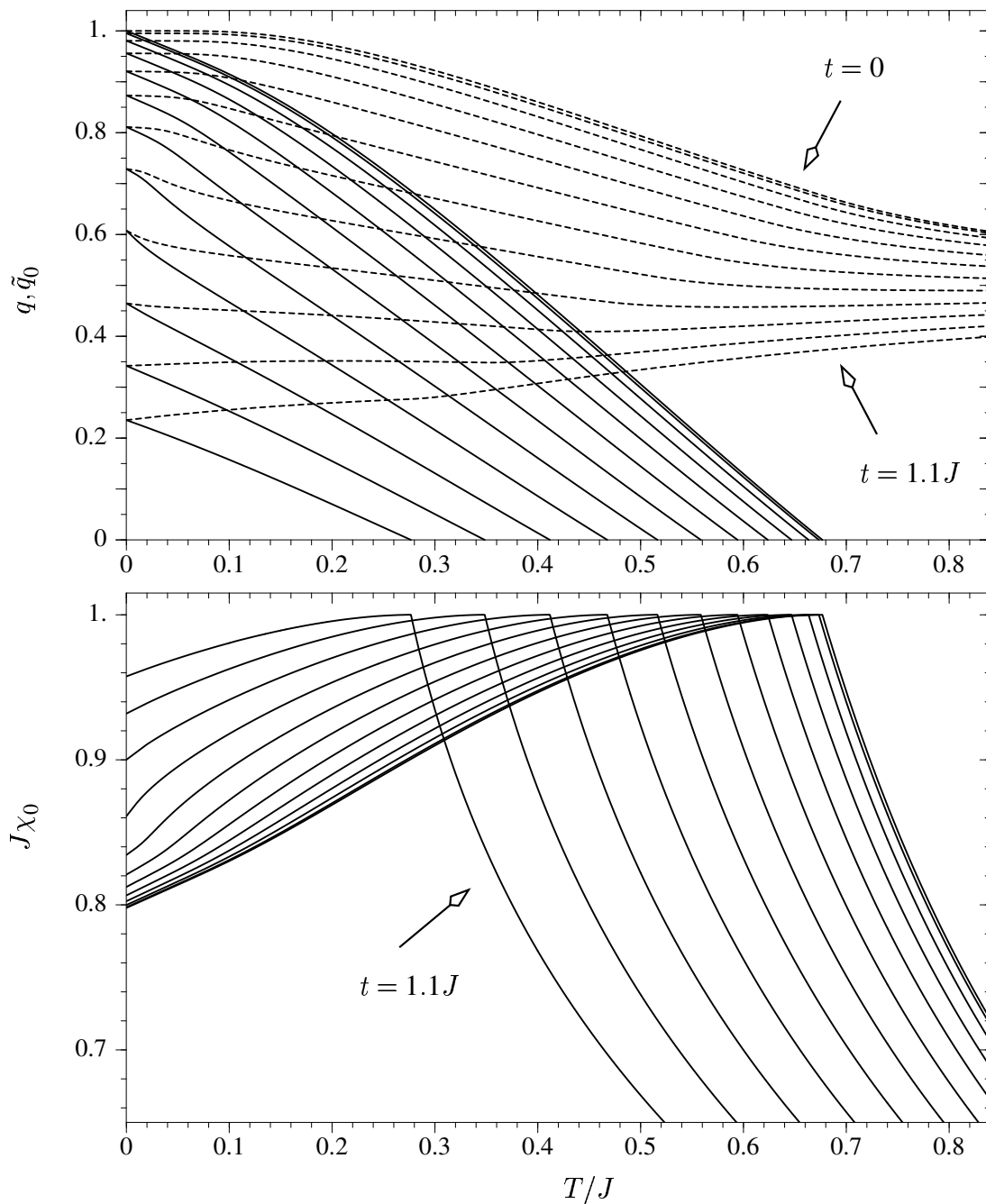


Figure 3.3: Numerical results for the itinerant ISG_F defined by (3.14) within the replica-symmetric and spin-static approximation for hopping parameters $t = \{0, \dots, 1.1J\}$ in steps of $0.1J$. All energies are measured in units of the average magnetic coupling J . The upper plot shows the spin glass order parameter q (full lines) and the zero frequency component of the replica-diagonal spin-spin correlation \tilde{q}_0 (dashed lines). Both lines merge at $T = 0$. The \tilde{q}_0 -curves approach $1/2$ as $T \rightarrow \infty$. A continuous spin glass to paramagnet phase transition occurs for all $t < 1.406J$ (see Sec. 3.3.2.2). The lower plot shows the corresponding local static susceptibility $\chi_0 = \beta(\tilde{q}_0 - q)$ which remains finite as $T \rightarrow 0$ and always reaches unity at the phase transition.

In particular, the sums (3.24) turn into

$$\bar{A}_t(\eta) = \frac{2}{\pi} \int_0^\infty d\zeta \frac{\eta}{|u(\zeta)|^2 + \eta^2}, \quad (3.27 \text{ a})$$

$$\bar{B}_t(\eta) = \frac{d}{d\eta} \bar{A}_t(\eta) = \frac{2}{\pi} \int_0^\infty d\zeta \frac{-|u(\zeta)|^2 + \eta^2}{(|u(\zeta)|^2 + \eta^2)^2}. \quad (3.27 \text{ b})$$

Here $u(\zeta)$ denotes the continuous version of the definition (3.22).

Saddle point integration of y_0 . In order to demonstrate the procedure the quantity $\Phi_t^{\text{stat}}(z)$ shall be evaluated explicitly for low temperature. To this end one may write

$$\begin{aligned} \Phi_t^{\text{stat}}(z) &= \int_{y_0}^G W_t^{\text{stat}}(H_0) \\ &= \underbrace{\int_{y_0}^G \frac{\exp(\beta(R+H_0))}{4}}_{\Phi_{t,a}^{\text{stat}}} + \underbrace{\int_{y_0}^G \frac{\exp(\beta(R-H_0))}{4}}_{\Phi_{t,b}^{\text{stat}}} + \underbrace{\int_{y_0}^G \frac{\exp(\beta R)}{2}}_{\Phi_{t,c}^{\text{stat}}}, \end{aligned} \quad (3.28)$$

where $R(\bar{H}_0)$ has been defined in eq. (3.21). These three contributions arise from the exponential representation of the cosh and the remaining constant part in eq. (3.20). Employing the variable transformation

$$y_0 \longrightarrow x = \frac{1}{\sqrt{\beta J}} y_0, \quad H_0 \longrightarrow \bar{H}_0 = J(\sqrt{q}z + \sqrt{J\chi_0}x) \quad (3.29)$$

the first term can be expressed by

$$\Phi_{t,a}^{\text{stat}}(z) = \sqrt{\frac{\beta}{J}} 16\pi \exp\left(\beta J \left(\sqrt{q}z + \frac{J\chi_0}{2}\right)\right) \int_{-\infty}^{\infty} dx \exp(-\beta J g(x, z)), \quad (3.30)$$

where the dimensionless exponent function is given by

$$g(x, z) = \frac{1}{2} (x - \sqrt{J\chi_0})^2 - \frac{1}{J} R(\bar{H}_0). \quad (3.31)$$

Further progress is based on the observation that $R(\bar{H}_0)$ remains finite as $T \rightarrow 0$. This allows the x -integration in eq. (3.30) to be performed by means of the saddle point method which yields

$$\Phi_{t,a}^{\text{stat}}(z) = \sqrt{\frac{1}{16 \partial_x^2 g(x_{\text{sp}}(z), z)}} \exp\left(\beta J \left(\sqrt{q}z + \frac{J\chi_0}{2} - g(x_{\text{sp}}(z), z)\right)\right). \quad (3.32)$$

Here $x_{\text{sp}}(z)$ denotes the z -dependent saddle point, i.e. the minimum of $g(x, z)$ at fixed z , that has to be determined numerically. Note that the saddle point integration becomes exact in the zero-temperature limit. The second contribution to eq. (3.28) is related to the first by symmetry,

$$\Phi_{t,b}^{\text{stat}}(z) = \Phi_{t,a}^{\text{stat}}(-z), \quad (3.33)$$

while $\Phi_{t,c}^{\text{stat}}$ can be shown to be exponentially small compared to the other terms and can therefore be neglected safely (away from half filling, i.e. for $\mu \neq 0$, this is not true any more).

The other y_0 -integrations that occur in eqs. (3.23, 3.25) can be done in the same fashion as demonstrated above for the simplest case. Without further going into detail, this saddle point method results in the simplified self-consistency problem posed below.

Self-consistency equations. The effective magnetic field is given by

$$\bar{H}_{0,\text{sp}}(z) = J(\sqrt{q}z + \sqrt{J\chi_0}x_{\text{sp}}(z)), \quad (3.34)$$

where x_{sp} is subject to the saddle point condition

$$x_{\text{sp}}(z) \stackrel{!}{=} \sqrt{J\chi_0} \bar{A}_t(\bar{H}_{0,\text{sp}}(z)), \quad (3.35)$$

and \bar{A}_t has been defined in eq. (3.27 a). The CPA-equation which determines the continuous self-energy $\sigma(\zeta)$ acquires the form

$$T_0(i\zeta - \sigma_l(\zeta), t) = \int_z^G \frac{-u(\zeta)}{|u(\zeta)|^2 + \bar{H}_{0,\text{sp}}(z)^2}. \quad (3.36)$$

Finally, the self-consistency equations for the spin glass order parameter and the static local susceptibility evaluate to

$$q = \tilde{q}_0 = \int_z^G \bar{A}_t(\bar{H}_{0,\text{sp}}(|z|))^2, \quad (3.38 \text{ a})$$

$$\chi_0 = \sqrt{\frac{2}{\pi q J^2}} \bar{A}_t(\bar{H}_{0,\text{sp}}(0^+)) + \int_z^G \frac{\bar{B}_t(\bar{H}_{0,\text{sp}}(|z|))}{1 - J^2 \chi_0 \bar{B}_t(\bar{H}_{0,\text{sp}}(|z|))}, \quad (3.38 \text{ b})$$

respectively.

Results at zero temperature. Numerical solutions of the set of self-consistency equations (3.35 – 3.38) are presented in Fig. 3.4. In the non-itinerant limit ($t = 0$) the well known results $q = 1$, $J\chi_0 = \sqrt{2/\pi}$ are reproduced correctly. A finite hopping delocalizes the particles and reduces the local spin-spin correlations. Thus, with increasing hopping strength t the spin glass order parameter q decreases monotonically. Within the spin-static approximation the spin glass to paramagnet quantum phase transition occurs at the critical hopping strength

$$t_{c,\text{stat}} = \frac{2\gamma}{\pi} J \simeq 1.406 J. \quad (3.39)$$

The constant γ is given by

$$\gamma = \int_0^\infty d\xi \exp(2\xi^2) \Gamma\left(\frac{1}{2}, \xi^2\right)^2, \quad (3.40)$$

where Γ denotes the incomplete Gamma function defined by

$$\Gamma(a, \xi) = \int_\xi^\infty ds s^{a-1} e^{-s}. \quad (3.41)$$

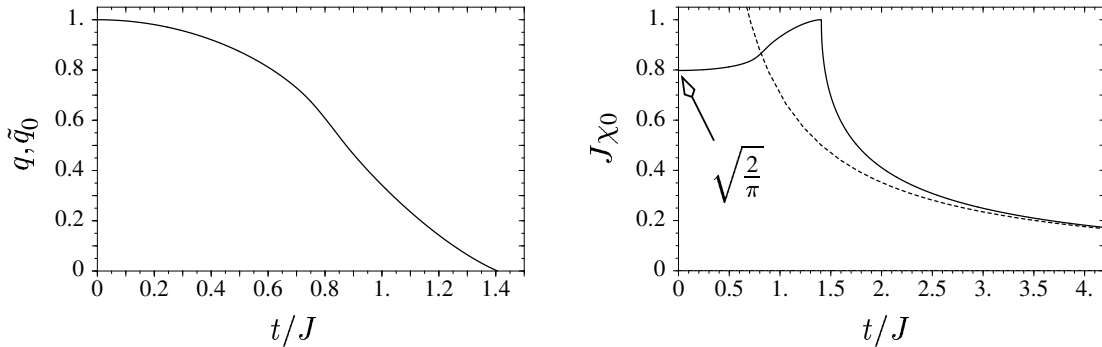


Figure 3.4: Zero-temperature results for the itinerant ISG_F within the replica-symmetric and spin-static approximation. The spin glass order is depressed Left: An increasing hopping strength t continuously depletes the spin glass order and eventually drives a zero temperature spin glass to paramagnet phase transition at $t_{c,\text{stat}} \simeq 1.406J$ (see eq. (3.39)). Right: The static part of the local susceptibility (full line) reaches the value $1/J$ at $t_{c,\text{stat}}$ and in the disordered phase it vanishes asymptotically like $\chi_0 \sim 1/t$ (see eq. (3.42)). For comparison the non-interacting limit $J \rightarrow 0$ (dashed line) is also shown.

The critical value (3.39) very well agrees with the corresponding result obtained in [34] for a similar model with a semi-elliptic (instead of a Gaussian) free density of states. The static local susceptibility reaches the value $1/J$ at $t_{c,\text{stat}}$. In the zero-temperature disordered phase, i.e. for $t > t_{c,\text{stat}}$, one finds

$$\chi_0 = \frac{\pi t - \sqrt{\pi^2 t^2 - 4\gamma^2 J^2}}{2\gamma J^2}, \quad t > t_{c,\text{stat}}. \quad (3.42)$$

Its deviation from the corresponding quantity in the non-magnetic limit, $\chi_0|_{J=0} = \gamma/(\pi t)$ (see Fig. 3.4), signals the vicinity of the spin glass phase.

3.3.3 Dynamical solutions

While exact in the non-itinerant limit, the spin-static approximation discussed in Sec. 3.3.2 turns out to provide a very good description of the model (3.14) for weak hopping according to the rough criterion (3.18). In the opposite limit $t \gg J$ the kinetic term dominates the behavior of the system and the quantum-spin dynamics loses importance, too, as can be seen from Fig. 3.4. For intermediate hopping, however, the spin-static approximation becomes inaccurate and particularly fails in the vicinity of the quantum critical point (QCP). In the present section systematically improved dynamical solutions of the self-consistency problem shall be discussed.

3.3.3.1 The phase diagram in the T - t plane

By means of the iterative scheme of Fig. 3.2 and the general condition for the phase transition, eq. (2.41), the phase diagram in the plane of temperature T and hopping strength t was evaluated within the dynamical approximation of orders up to and including $M = 3$. Since at criticality

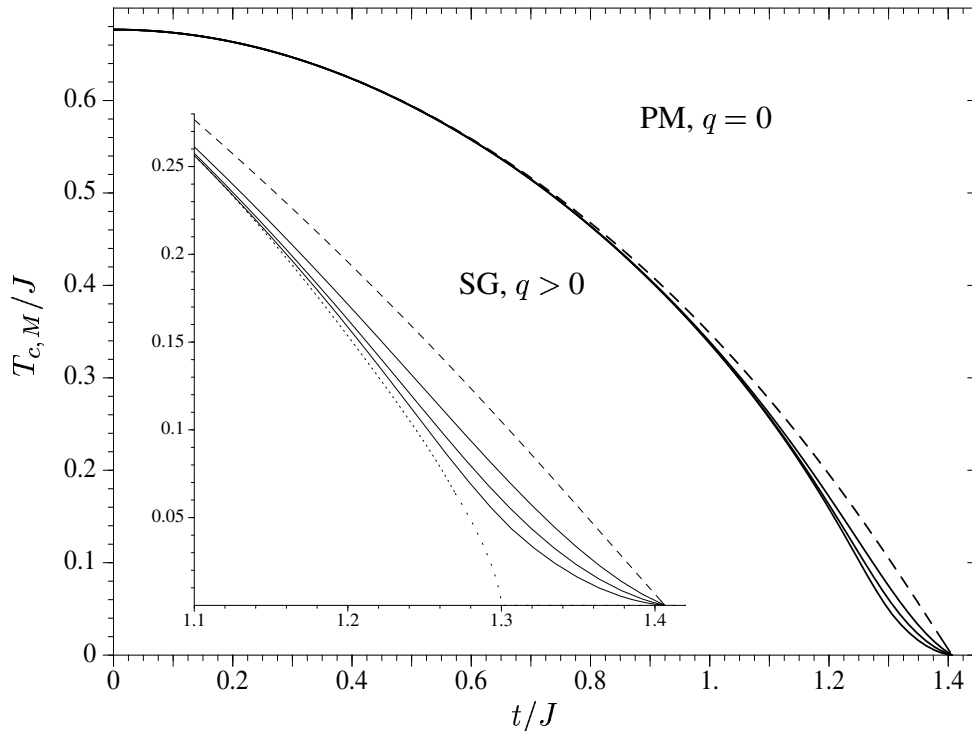


Figure 3.5: The critical line of the second order spin glass (SG) to paramagnet (PM) phase transition in the itinerant ISG_F within the spin-static approximation (dashed line, see Sec. 3.3.2) and within the dynamical approximations (full lines) of first ($T_{c,1}$, uppermost) to third ($T_{c,3}$, undermost) order M as discussed in Sec. 3.3.1. The dotted line indicates the expected course of the full dynamical phase boundary in the limit $M \rightarrow \infty$; the light-dotted part displays the leading critical behavior (3.43) with exponent $\phi = 2/3$. The presumed location of the QCP, $t_c \simeq 1.30J$, will be estimated in Sec. 3.3.3.2.

there is no issue of replica symmetry breaking the choice of the replica-symmetric saddle point (1.33 a) is justified in these calculations. In solving the conditional equation (2.41) it is sufficient to fix the spin glass order parameter to $q = 0$ thus rendering the z -integrations in the CPA equation (3.13) and in the self-consistency equation (1.99 b) trivial.

The sequence of dynamical approximants to the critical line $T_c(t)$ is shown in Fig. 3.5. With increasing hopping strength t and decreasing temperature the growing influence of the discrete dynamic saddle point components $\tilde{q}_{m>0}$ is getting more and more apparent. It can be seen clearly from Figs. 3.5 and 3.6 that with increasing order M of the dynamical approximation two successive solutions start to separate at larger t . One observes a rapid convergence of this sequence of solutions except for the region where the QCP is expected. As $T_c \rightarrow 0$ all curves collapse into the static critical point at $t_{c,\text{stat}}$ given by eq. (3.39).

It is important to note that the self-consistent inclusion of any finite number of the \tilde{q}_m can not affect neither the position of the QCP nor the critical exponents. In order to capture the quantum-dynamical character of the problem it is rather necessary to take into account the parameters \tilde{q}_m over a finite range of Matsubara frequencies ω_m around $\omega_0 = 0$ (see App. A.5). In the disordered phase the parameters \tilde{q}_m vanish linearly with temperature, i.e. the dynamical

susceptibility $\chi_m = \tilde{q}_m/T$ has a finite zero-temperature limit. Consequently, the effective potential matrix (1.90) is proportional to \sqrt{T} , and hence the leading quadratic term in a formal expansion of the un-averaged local propagator Γ_t (3.11) in powers of \mathbf{V} also falls off linearly with temperature (odd terms generally vanish by the Gaussian \mathbf{y} -integrations in all equations Γ_t appears in). However, matrix powers of \mathbf{V} involve internal frequency summations. Thus, the linear temperature decrease of the parameters \tilde{q}_m is exactly compensated by their increasing number within a fixed frequency range. As a consequence, the location of the zero temperature critical point is shifted towards smaller hopping strength compared to the result obtained within the spin-static approximation.

Close to zero temperature the critical line behaves like

$$T_c \sim (t_c - t)^\phi, \quad t < t_c, \quad (3.43)$$

where the critical exponent changes from $\phi = 1$ in the spin-static approximation to $\phi = 2/3$ [45] due to the quantum-spin dynamics (see App. A.5). Figure 3.5 gives an impression of how this non-analytical behavior emerges from the sequence of the (analytical) approximate solutions in the limit $M \rightarrow \infty$.

3.3.3.2 Location of the quantum critical point

In order to estimate the location of the QCP one may consider the differences between the T_c -curves within two successive dynamical approximations, defined by

$$\Delta_M = \frac{1}{J} (T_{c, M-1} - T_{c, M}). \quad (3.44)$$

As can be seen in Fig. 3.6, the functions $\Delta_M(t)$ exhibit pronounced maxima. While the positions of these maxima vary only very little, they become lower in height but sharper with increasing order M . The critical lines $T_{c, M}$ are monotonically decreasing functions of t . Hence, the distance between $T_{c, M}$ and the full dynamical critical line, defined by

$$\tilde{\Delta}_M = \frac{1}{J} (T_{c, M} - T_{c, \infty}), \quad (3.45)$$

possesses a non-analytical maximum exactly at t_c for any M . Since

$$\tilde{\Delta}_M = \sum_{M'=M+1}^{\infty} \Delta_{M'}, \quad (3.46)$$

this non-analyticity must coincide with the position of the maxima of the Δ_M as $M \rightarrow \infty$. This simply means that the sequence of the critical lines $T_{c, M}$ converges slowest in the very proximity of the QCP. Based on this scenario the critical hopping strength can be estimated by plotting the maxima's positions vs. their heights (see Fig. 3.6) and extrapolation of these points to zero height. This simple procedure yields the final result

$$t_c \simeq 1.30J. \quad (3.47)$$

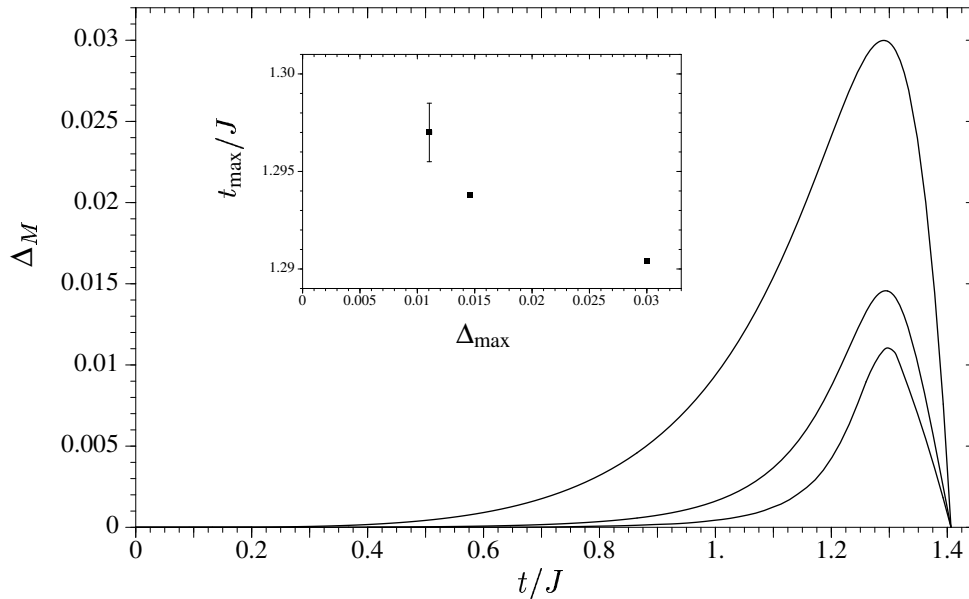


Figure 3.6: Differences between the critical lines within two successive orders of the dynamical approximation, Δ_1 (uppermost) to Δ_3 (undermost), as defined in eq. (3.44). As explained in the text, the location of the dynamical QCP is expected to coincide with the maxima positions in the limit $M \rightarrow \infty$. Inset: plot of the positions vs. heights of the maxima. The error in the $M = 3$ data is due to numerical problems at low temperatures.

3.3.4 Summary and conclusion

In the last part of this thesis the technical framework of Chap. 1 has been generalized to account for itinerant spin glass models. By means of a dynamical CPA method an effective single-site problem could be constructed, and the corresponding extended two-fold self-consistency structure has been formulated (see Fig. 3.1).

As the simplest example the ISG_F with nearest-neighbor hopping in $d \rightarrow \infty$ at half fermion filling has been studied. Beyond the spin-static approximation, the dynamical approximation scheme, introduced in Sec. 2.2, has led to an estimation of the second order SG to PM phase boundary in the T - t plane including the location of the QCP. The obtained sequence of improved dynamical solutions nicely illustrates the emergence of quantum critical behavior (see Figs. 3.5 and 3.6).

This work has concentrated on the spin sector of the model and left out the properties in the charge sector, such as the fermionic density of states. In the future it will be of high interest to investigate the effect of the hopping on the band structure of the system, particularly on the spin glass gap at zero temperature [36]. In this context an extension of the solutions to non-zero chemical potential μ [41] is also desirable.

A

Appendix

A.1 Derivation of a general formula for a class of Matsubara frequency sums

In Chap. 2 there occur several Matsubara sums of expressions of rational form, e.g. in eqs. (2.16, 2.25). This physically important type of sums can easily be evaluated by virtue of a general formula which shall be derived in this appendix.

Consider the polynomial

$$P(z) = \prod_{i=1}^n (z - c_i)^{m_i}, \quad (\text{A.1})$$

where the m_i are positive integers and the complex zeros c_i are non-integers and pairwise different, i.e. $c_i \neq c_j$ for $i \neq j$. One further requires $P(z)$ to be of degree two at least. With these assumptions the series

$$S = \sum_{l=-\infty}^{\infty} \frac{1}{P(l)} \quad (\text{A.2})$$

is well defined and converges. S can be represented by

$$S = \sum_{l=-\infty}^{\infty} \operatorname{Res}_{z=l} \frac{r(z)}{P(z)}. \quad (\text{A.3})$$

In this expression $r(z)$ is an arbitrary function which is analytic for all non-integer arguments and has the property

$$\operatorname{Res}_{z=l} r(z) = 1 \quad \text{for integer } l. \quad (\text{A.4})$$

Possible choices are

$$r(z) = \left\{ \frac{-2\pi i}{1 - \exp(2\pi i z)}, -\pi \tan(\pi(z + 1/2)), \pi \cot(\pi z), \text{etc.} \right\}. \quad (\text{A.5})$$

The function $r(z)/P(z)$ has n additional poles at the zeros c_i . According to the residue theorem the sum of all residua in the whole complex plane is exactly zero. As polynomials of degree one have been excluded there is no residue at infinity. Consequently, S is given by

$$S = - \sum_{i=1}^n \operatorname{Res}_{z=c_i} \frac{r(z)}{P(z)}. \quad (\text{A.6})$$

By means of the well known relation

$$\operatorname{Res}_{z=z_0} \frac{g(z)}{(z-z_0)^p} = \frac{1}{(p-1)!} \left. \frac{d^{p-1}}{dz^{p-1}} g(z) \right|_{z=z_0}, \quad (\text{A.7})$$

and employing the auxiliary polynomial

$$\bar{P}_i(z) = \prod_{\substack{j=1 \\ i \neq j}}^n (z - c_j)^{m_j} = (z - c_i)^{m_i} P(z), \quad (\text{A.8})$$

one finally finds the formula

$$S = - \sum_{i=1}^n \frac{1}{(m_i - 1)!} \left. \frac{d^{m_i-1}}{dz^{m_i-1}} \frac{r(z)}{\bar{P}_i(z)} \right|_{z=c_i}. \quad (\text{A.9})$$

A.2 Derivatives of the weight function W

The aim of this appendix is to establish formulae which are useful for the evaluation of arbitrary multiple derivatives of the weight function (1.96) with respect to the effective magnetic fields (1.92, 1.93). The basic idea has been sketched already in Sec. 1.4.1.4.

To condense the notation, the magnetic fields shall be given a collective index for frequency and direction, i.e.

$$H_{\nu_r}^{m_r} \longrightarrow H_r. \quad (\text{A.10})$$

According to eqs. (1.96, 1.94, 1.73) the weight function can be written as

$$W = \det \left(\mathbf{G}_0^{-1} / \mathbf{G}_{\text{reg}}^{-1} \right) \exp(\Theta), \quad (\text{A.11})$$

where the exponent is given by

$$\Theta = \operatorname{Tr} \ln(\mathbb{1} + \mathbf{G}_0 \mathbf{V}). \quad (\text{A.12})$$

A sequence of magnetic field derivatives applied to W can be expressed in a first step by derivatives of Θ only. It takes a little combinatorics to arrive at the expression

$$\begin{aligned} \frac{\partial}{\partial H_1} \cdots \frac{\partial}{\partial H_k} W &= \det \left(\mathbf{G}_0^{-1} / \mathbf{G}_{\text{reg}}^{-1} \right) \frac{\partial}{\partial H_1} \cdots \frac{\partial}{\partial H_k} \exp(\Theta) \\ &= W \sum_{\text{partitions}} \prod_{\text{subsets}} \left(\frac{\partial}{\partial H_{s_1}} \cdots \frac{\partial}{\partial H_{s_r}} \Theta \right). \end{aligned} \quad (\text{A.13})$$

Given a set of indices the sum in eq. (A.13) extends over all set partitions representing the ways to group these distinct elements into subsets¹. For each partition the product runs over all of these subsets, where a sequence of field derivatives is applied to Θ according to the indices in the respective subset.

The remaining task is to evaluate the multiple field derivatives of Θ . A single derivative yields (compare to eq. (1.76))

$$\frac{\partial}{\partial H_r} \Theta = \text{Tr} \Lambda_r \Gamma. \quad (\text{A.14})$$

In a similar fashion one calculates a single field derivative of the matrix Γ :

$$\begin{aligned} \frac{\partial}{\partial H_r} \Gamma &= \sum_{n=0}^{\infty} (-1)^n \frac{\partial}{\partial H_r} (\mathbf{G}_0 \mathbf{V})^n \mathbf{G}_0 \\ &= \sum_{n=1}^{\infty} \sum_{k=0}^{n-1} (-1)^n (\mathbf{G}_0 \mathbf{V})^k \left(\mathbf{G}_0 \underbrace{\frac{\partial}{\partial H_r} \mathbf{V}}_{\Lambda_r} \right) (\mathbf{G}_0 \mathbf{V})^{n-1-k} \mathbf{G}_0 \\ &= \sum_{n=1}^{\infty} \sum_{k=0}^{\infty} \sum_{m=0}^{\infty} \delta_{m, n-k-1} (-1)^n (\mathbf{G}_0 \mathbf{V})^k \mathbf{G}_0 \Lambda_r (\mathbf{G}_0 \mathbf{V})^{n-1-k} \mathbf{G}_0 \\ &= \sum_{k=0}^{\infty} \sum_{m=0}^{\infty} (-1)^{k+m+1} (\mathbf{G}_0 \mathbf{V})^k \mathbf{G}_0 \Lambda_r (\mathbf{G}_0 \mathbf{V})^m \mathbf{G}_0 \\ &= -(\mathbb{1} + \mathbf{G}_0 \mathbf{V})^{-1} \mathbf{G}_0 \Lambda_r (\mathbb{1} + \mathbf{G}_0 \mathbf{V})^{-1} \mathbf{G}_0 \\ &= -\Gamma \Lambda_r \Gamma. \end{aligned} \quad (\text{A.15})$$

This result immediately leads to

$$\frac{\partial}{\partial H_r} \prod_{i=1}^k (\Lambda_{s_i} \Gamma) = - \sum_{i=1}^k \left(\prod_{j=1}^{i-1} (\Lambda_{s_j} \Gamma) \right) \Lambda_{s_i} \Gamma \Lambda_r \Gamma \left(\prod_{j=i+1}^k (\Lambda_{s_j} \Gamma) \right), \quad (\text{A.16})$$

where the products on the right hand side are understood to be one if $j > i - 1$. Relation (A.16) expresses the fact that, according to the product rule of differentiation, the derivative with respect to H_r has to be applied to each of the factors $\Lambda_{s_i} \Gamma$ strictly keeping their order. By repeated use of eq. (A.16) one finally constructs the compact formula

$$\frac{\partial}{\partial H_1} \cdots \frac{\partial}{\partial H_k} \Theta = (-1)^{k+1} \sum_{\substack{\text{non-cyclic} \\ \text{permutations} \\ \{1, \dots, k\}}} \text{Tr} \prod_{i=1}^k (\Lambda_{p_i} \Gamma). \quad (\text{A.17})$$

Here the sum extends over all non-cyclic permutations of the set of indices, i.e. cyclic permutations contribute only once. The product arranges the matrix factors according to the respective permutation p .

Equation (A.17) is used in combination with eq. (A.13). It can be shown that a k -fold field derivative of the weight function W generates exactly $k!$ terms.

¹The corresponding *Mathematica*[®] function is SetPartitions[[]].

A.3 Derivation of an expression for the internal energy

In Secs. 2.2.3.3 and 2.3.2.3 the specific heat of a Heisenberg spin glass model was investigated by numerically evaluating the temperature derivative of the internal energy. In this appendix a useful expression for the latter shall be derived.

According to the basics of statistical physics [40] the internal energy per site U is related to the free energy by

$$U = \frac{d}{d\beta} (\beta f). \quad (\text{A.18})$$

In the present context the total rather than the partial β -derivative is appropriate. This is because the saddle point values q_ν and \tilde{q}_ν^m appearing in the expression for the free energy are not fixed model parameters, but they are functions of the temperature themselves. Thus, starting from eq. (1.61) one finds

$$U = -\frac{d}{d\beta} S - \frac{d}{d\beta} \int_z^G \ln \Phi, \quad (\text{A.19})$$

where the quadratic form S has been defined in eq. (1.40). The first term in eq. (A.19) is readily evaluated to

$$\frac{d}{d\beta} S(\beta, \mathbf{q}, \tilde{\mathbf{q}}) = \frac{2}{\beta} S + \frac{\beta^2}{2} \sum_\nu J_\nu^2 \left(q_\nu \frac{d}{d\beta} q_\nu - \sum_{m=-\infty}^{\infty} \tilde{q}_\nu^m \frac{d}{d\beta} \tilde{q}_\nu^m \right). \quad (\text{A.20})$$

For the sake of simplicity the discussion shall be restricted to the case where there is neither an external magnetic field nor a finite real chemical potential applied. With these assumptions the inverse temperature enters the functional Φ (eq. (1.98)) through the combinations βH_ν^m only or, if the factor β is pulled under the square roots in eqs. (1.92, 1.93), through

$$\eta_\nu := \beta^2 q_\nu \quad \text{and} \quad \tilde{\eta}_\nu^m := \beta^2 \tilde{q}_\nu^m. \quad (\text{A.21})$$

Exploiting this fact the total β -derivative of Φ can be expressed in terms of derivatives with respect to the saddle point parameters q_ν and \tilde{q}_ν^m . Having regard to the symmetry relation eq. (1.36) one finds

$$\frac{d}{d\beta} \Phi = \sum_\nu \frac{d\eta_\nu}{d\beta} \underbrace{\frac{\partial}{\partial \eta_\nu} \Phi}_{\beta^{-2} \partial \Phi / \partial q_\nu} + \sum_\nu \sum_{m \geq 0} \frac{d\tilde{\eta}_\nu^m}{d\beta} \underbrace{\frac{\partial}{\partial \tilde{\eta}_\nu^m} \Phi}_{\beta^{-2} \partial \Phi / \partial \tilde{q}_\nu^m}. \quad (\text{A.22})$$

Now the second contribution in eq. (A.19) can be evaluated making use of the saddle point conditions (1.62, 1.67, 1.70):

$$\begin{aligned} \frac{d}{d\beta} \int_z^G \ln \Phi &= \int_z^G \frac{1}{\Phi} \frac{d}{d\beta} \Phi \\ &= \sum_\nu \left(\left(\frac{2}{\beta} + \frac{d}{d\beta} q_\nu \right) \overbrace{\int_z^G \frac{1}{\Phi} \frac{\partial}{\partial q_\nu} \Phi}^{-\frac{1}{2} \beta^2 J_\nu^2 q_\nu} + \right. \end{aligned}$$

$$\begin{aligned}
& + \sum_{m \geq 0} \left(\frac{2}{\beta} + \frac{d}{d\beta} \tilde{q}_\nu^m \right) \overbrace{\int_z^G \frac{1}{\Phi} \frac{\partial}{\partial \tilde{q}_\nu^m} \Phi}^{(1 - \frac{1}{2} \delta_{m,0}) \beta^2 J_\nu^2 \tilde{q}_\nu^m} \\
& = -\frac{4}{\beta} S - \frac{\beta^2}{2} \sum_\nu J_\nu^2 \left(q_\nu \frac{d}{d\beta} q_\nu - \sum_{m=-\infty}^{\infty} \tilde{q}_\nu^m \frac{d}{d\beta} \tilde{q}_\nu^m \right). \tag{A.23}
\end{aligned}$$

Comparison of eqs. (A.20, A.23) reveals that all remaining terms involving β -derivatives cancel each other. Thus, one is left with the simple relation $U = 2S/\beta$ or

$$U = \frac{1}{2} \beta \sum_\nu J_\nu^2 \left(q_\nu^2 - \sum_{m=-\infty}^{\infty} (\tilde{q}_\nu^m)^2 \right). \tag{A.24}$$

As mentioned before, this simple formula is valid for the HSG_S and for the HSG_F at half filling, both without an external magnetic field.

A.4 Expansions of the self-consistency equations in powers of small q_ν

The purpose of this appendix is to derive the condition (2.41) for the critical temperature and to justify the expansions (2.45, 2.47) which led to the specific heat curves in the spin glass phase shown in Fig. 2.7. To this end systematic expansions of the general self-consistency equations (1.99) in powers of small spin glass order parameters q_ν shall be presented briefly.

In order to improve readability the short hand notation

$$\bar{\Phi}_{\nu_1, \dots, \nu_k}^{m_1, \dots, m_k} := \int_y^G \frac{\partial}{\partial H_{\nu_1}^{m_1}} \cdots \frac{\partial}{\partial H_{\nu_k}^{m_k}} W \tag{A.25}$$

shall be employed throughout this appendix.

A.4.1 The q_ν -equation and critical temperatures

Using the definition (A.25) the self-consistency equation (1.69) can be written as

$$q_\nu = \frac{1}{\beta^2} \int_z^G \frac{(\bar{\Phi}_\nu^0)^2}{\Phi^2} =: \frac{1}{\beta^2} R_\nu. \tag{A.26}$$

In the general anisotropic case there exist individual critical points for each spatial direction. Immediately below T_c^ν the order parameter q_ν is very small, while the $q_{\mu \neq \nu}$ in the other two directions could be exactly zero still or finite already. One is interested in the series expansion of eq. (A.26) in powers of the corresponding small parameter q_ν only:

$$\beta^2 q_\nu = \frac{\partial}{\partial q_\nu} R_\nu \Big|_{q_\nu=0} q_\nu + \frac{\partial^2}{\partial q_\nu^2} R_\nu \Big|_{q_\nu=0} q_\nu^2 + O(q_\nu^3). \tag{A.27}$$

The first order term can be manipulated into

$$\begin{aligned} \frac{\partial}{\partial q_\nu} R_\nu &= J_\nu^2 \int_z^G \left(-\frac{2}{\Phi^3} (\bar{\Phi}_\nu^0)^2 \frac{\partial}{\partial q_\nu} \Phi + \frac{2}{\Phi^2} \bar{\Phi}_\nu^0 \frac{\partial}{\partial q_\nu} \bar{\Phi}_\nu^0 \right) \\ &= J_\nu^2 \int_z^G \left(3 \frac{(\bar{\Phi}_\nu^0)^2 \bar{\Phi}_{\nu,\nu}^{0,0}}{\Phi^3} - 4 \frac{(\bar{\Phi}_\nu^0)^4}{\Phi^3} + \frac{(\bar{\Phi}_{\nu,\nu}^{0,0})^2}{\Phi^2} \right). \end{aligned} \quad (\text{A.28})$$

In the second line the q_ν -derivatives have been expressed in terms of derivatives with respect to the respective static magnetic field by taking the same steps as in Sec. 1.4.1.2 ($y_{\nu,0}$ - and z_ν -integration by parts).

Next the quantity $\bar{\Phi}_\nu^0$ must be considered a little closer. For the physically interesting choices for the chemical potential, i.e. $\mu = \mu_{\text{PF}}$ (eq. (1.9)) and $\text{Im} \mu = 0$ the weight function W obeys the symmetry relation

$$W(-\mathbf{V}) = W(\mathbf{V})^* \quad (\text{A.29})$$

which follows from its definition (1.96). As a direct consequence of eq. (A.29) one may easily verify the statement

$$\bar{\Phi}_\nu^0 \Big|_{q_\nu=0} = 0 \quad (\text{A.30})$$

which can be generalized to any odd number of identical direction indices. Using this result in eq. (A.28) leads to

$$\frac{\partial}{\partial q_\nu} R_\nu \Big|_{q_\nu=0} = J_\nu^2 \underbrace{\int_z^G \frac{(\bar{\Phi}_{\nu,\nu}^{0,0})^2}{\Phi^2}}_{\beta^2 \tilde{q}_\nu^0} \Big|_{q_\nu=0}. \quad (\text{A.31})$$

Having regard to the saddle point condition for \tilde{q}_ν^0 in the shape of eq. (1.66) the integral on the right hand side can be identified with $\beta^2 \tilde{q}_\nu^0$. The same arguments also apply to the second order term in eq. (A.27). A tedious but straightforward calculation finally yields the expansion

$$q_\nu = \beta^2 J_\nu^2 \left(\tilde{q}_\nu^0 \Big|_{q_\nu=0} \right)^2 q_\nu - 2\beta^4 J_\nu^4 \left(\tilde{q}_\nu^0 \Big|_{q_\nu=0} \right)^3 q_\nu^2 + O(q_\nu^3). \quad (\text{A.32})$$

By comparison of the $O(q_\nu)$ terms one immediately reads off the simple condition

$$J_\nu \tilde{q}_\nu^0 (T_c^\nu) = T_c^\nu \quad (\text{A.33})$$

for the equilibrium critical point in ν -direction. The solution of eq. (A.32) reveals that the spin glass order parameter emerges linearly with decreasing temperature below T_c^ν according to

$$q_\nu = a_\nu (T_c^\nu - T), \quad T \lesssim T_c^\nu, \quad (\text{A.34})$$

where the coefficient is given by

$$a_\nu = \frac{1}{J_\nu} - \frac{d}{dT} \tilde{q}_\nu^0 \Big|_{T=T_c^\nu}. \quad (\text{A.35})$$

A.4.2 The \tilde{q}_ν^m -equation

In terms of the abbreviation (A.25) the self-consistency equation (1.72) which includes the static special case eq. (1.66) reads

$$\tilde{q}_\nu^m = \frac{1}{\beta^2} \int_z^G \frac{\bar{\Phi}_{\nu,\nu}^{m,-m}}{\Phi} =: \frac{1}{\beta^2} F_\nu^m. \quad (\text{A.36})$$

In the expansion of the right hand side F_ν^m all directions have to be taken into account. Making use of eq. (A.30) one obtains at second order

$$\beta^2 \tilde{q}_\nu^m = F_\nu^m|_{q=0} + \frac{1}{2} \sum_\mu J_\mu^4 \int_z^G \left(\frac{(\bar{\Phi}_{\mu,\mu}^{0,0})^2 \bar{\Phi}_{\nu,\nu}^{m,-m}}{\Phi^3} - \frac{\bar{\Phi}_{\mu,\mu}^{0,0} \bar{\Phi}_{\mu,\mu,\nu,\nu}^{0,0,m,-m}}{\Phi^2} \right) \Big|_{q=0} q_\mu^2 + O(q^3). \quad (\text{A.37})$$

Here the Gaussian z -integration is trivial since the integrand of the second term has no z -dependence any more.

Exploiting the saddle point condition (1.72) and assuming the isotropic special case, for which this expansion has been applied in Sec. 2.2.3.3, eq. (A.37) simplifies to

$$\tilde{q}_m = F_m|_{q=0} + \underbrace{\frac{1}{2} \beta^4 J^4 \tilde{q}_0 (3\tilde{q}_0 \tilde{q}_m - d_m)}_{C_m} \Big|_{q=0} q^2 + O(q^3), \quad (\text{A.38})$$

where the coefficients d_m are given by

$$d_m = \frac{1}{3\beta^4} \sum_{\mu\nu} \frac{\bar{\Phi}_{\mu,\mu,\nu,\nu}^{0,0,m,-m}}{\Phi} \Big|_{q=0}. \quad (\text{A.39})$$

These coefficients can be calculated numerically, for instance with the help of the formulas derived in Sec. A.2.

A.5 Computation of the critical exponent (3.43)

In Sec. 3.3.3.1 the phase diagram of the itinerant Ising spin glass (3.1) has been presented (Fig. 3.5). In this appendix the critical exponent of the phase boundary, as defined by eq. (3.43), shall be calculated.

Starting point is an expansion of the self-consistency equation (1.99 b) in powers of the effective potential matrix (1.90) in the paramagnetic phase (this expansion is similar to the $\tilde{q}_{m \neq 0}$ -expansion of Sec. 2.3, but in the present context the separation of static and dynamical components would be senseless). The Gaussian integrations over all y -fields can be performed according to eq. (2.50), and the internal summations due to the occurring matrix multiplications compensate the linear temperature decrease of the dynamical saddle point components \tilde{q}_m . A

tedious but straightforward calculation yields the following self-consistency equation for the dynamical susceptibility $\chi_m = \beta \tilde{q}_m$:

$$\chi_m = P_m (1 + \chi_m^2) - (1 - P_m \chi_m) T \sum_{m'=-\infty}^{\infty} \frac{Q_{m,m'} \chi_{m'}}{1 - P_{m'} \chi_{m'}} + \mathcal{O}(\chi^3). \quad (\text{A.40})$$

Using the abbreviation $X_l = 1/u_l$ (see eq. (3.22)) the coefficients read

$$P_m = P(\omega_m) = -2T \sum_{l=-\infty}^{\infty} X_l X_{l+m}, \quad (\text{A.42 a})$$

$$Q_{m,m'} = Q(\omega_m, \omega_{m'}) = T \sum_{l=-\infty}^{\infty} X_l X_{l+m} X_{l+m'} (2X_l + X_{l+m+m'}), \quad (\text{A.42 b})$$

and the self-energy is given explicitly by

$$\sigma_l = \frac{1}{2} X_l^2 T \sum_{m=-\infty}^{\infty} \frac{\chi_m X_{l+m}}{1 - P_m \chi_m}. \quad (\text{A.43})$$

The set of equations (A.40 – A.43) can be solved easily in the limit of zero temperature, and one determines the critical hopping strength $t_c = 1.372J$, which lies well between the spin-static result (3.39) and the expected full dynamical value (3.47).

Important now is the behavior of the coefficient functions (A.42) at low temperature and low frequencies. A closer study reveals the leading terms

$$P_m = P_0 + a|\omega_m| + bT^2 + \dots \quad (\text{A.44})$$

The linear frequency dependence of P_m is characteristic for metallic spin glasses [44]. Having regard to eq. (A.44), the solution of the quadratic equation (A.40) for low frequencies can be written as

$$\chi_m = \chi_{\text{nc}}^m - \sqrt{|\omega_m| + r(t, T)}. \quad (\text{A.45})$$

Here χ_{nc}^m denotes the uninteresting non-critical part and $r(t, T)$ comprises the remaining contributions to eq. (A.40) including the m' -sum. The condition for criticality is

$$r(t, T) \stackrel{!}{=} 0, \quad (\text{A.46})$$

and the shape of the critical line can be obtained by expanding $r(t, T)$ in both the hopping parameter t and temperature around the quantum critical point. Here the hopping function (3.6) varies linearly with t , and consequently so does $r(t, T)$. The temperature dependence is a much more delicate question. It turns out that the leading contribution arises from the frequency sum. Back-substitution of the solution into eq. (A.40) yields at lowest order the essential terms

$$r(t, T) = \alpha_1 + \alpha_2 t + \alpha_3 S(T) + \dots, \quad (\text{A.47})$$

where the α_i are constants and

$$S(T) = T \sum_{m=-\infty}^{\infty} \sqrt{|\omega_m|} f(\omega_m). \quad (\text{A.48})$$

An auxiliary soft cut-off function $f(\omega)$ has been introduced to guarantee convergence in explicit calculations. Taking the difference of expression (A.47) at finite and zero temperature together with the criterion (A.46) define

$$t_c(T) - t_c(0) \sim S(T) - S(0) \quad (\text{A.49})$$

as the condition for the phase boundary.

The remaining task is to evaluate the frequency sums. For the cut-off function one may choose, for instance,

$$f(\omega) = \frac{i^n}{(\omega + i)^n}, \quad n \geq 2. \quad (\text{A.50})$$

Since $f(\omega)$ has no poles for $\text{Im}\omega \geq 0$ the first sum can be transformed into a contour integral enclosing the upper half plane by standard techniques. Further manipulation leads to

$$S(T) = \frac{1}{\pi} \int_0^\infty d\omega \sqrt{\omega} \left(-\frac{(1+i)}{\sqrt{2}} \frac{f(-i\omega)}{\exp(\beta\omega) - 1} + \frac{(1-i)}{\sqrt{2}} \frac{f(i\omega)}{\exp(-\beta\omega) - 1} \right). \quad (\text{A.51})$$

The second sum at $T = 0$ is understood as an integration analogous to the prescription (3.26). For the difference one finds

$$\begin{aligned} S(T) - S(0) &= \frac{-1}{\sqrt{2}\pi} \int_0^\infty d\omega \frac{\sqrt{\omega}}{\exp(\beta\omega) - 1} ((1+i)f(-i\omega) + (1-i)f(i\omega)) \\ &= -\frac{1}{\sqrt{2}\pi} \zeta\left(\frac{3}{2}\right) T^{3/2} + O\left(T^{5/2}\right), \end{aligned} \quad (\text{A.52})$$

where $\zeta(x)$ is the Riemann ζ -function. Substitution into eq. (A.49) finally yields the result $\phi = 2/3$ in (3.43).

Bibliography

- [1] L. Arrachea and M. J. Rozenberg. Infinite-range quantum random Heisenberg magnet. *Phys. Rev. B*, 65:224430–224441, 2002.
- [2] M. Bechmann. Ordered and disordered systems in high spatial dimensions. Diploma thesis, Universität Würzburg, 2000.
- [3] M. Bechmann and R. Oppermann. Dynamical CPA approach to an itinerant fermionic spin glass model. *Eur. Phys. J. B*, 35:223–232, 2003.
- [4] M. Bechmann and R. Oppermann. Dynamical solutions of a quantum Heisenberg spin glass model. *Eur. Phys. J. B*, 41:525–533, 2004.
- [5] K. Binder and A. P. Young. Spin glasses: Experimental facts, theoretical concepts, and open questions. *Rev. Mod. Phys.*, 58(4):801–976, 1986.
- [6] A. J. Bray and M. A. Moore. Replica theory of quantum spin glasses. *J. Phys. C*, 13:L655–L660, 1980.
- [7] G. E. Brodale, R. A. Fisher, W. E. Fogle, N. E. Phillips, and J. van Curen. The effect of spin-glass ordering on the specific heat of CuMn. *J. Magn. Magn. Mater.*, 31–34:1331–1333, 1983.
- [8] G. Büttner and K. D. Usadel. Replica-symmetry breaking for the Ising spin glass in a transverse field. *Phys. Rev. B*, 42(10):6385–6395, 1990.
- [9] B. K. Chakrabarti, A. Dutta, and P. Sen. *Quantum Ising phases and transitions in transverse Ising models*. Lecture notes in physics. Springer-Verlag, Berlin, 1996.
- [10] R. J. Elliot, J. A. Krumhansl, and P. L. Leath. The theory and properties of randomly disordered crystals and related physical systems. *Rev. Mod. Phys.*, 46:465–543, 1974.
- [11] H. Feldmann. *Disorder versus Quantum Coherence. Examples from Condensed Matter*. PhD thesis, Universität Würzburg, 2000.

- [12] A. L. Fetter and J. D. Walecka. *Quantum Theory of Many-Particle Systems*. International Series in Pure and Applied Physics. McGraw-Hill, Inc., New York, 1971.
- [13] K. H. Fischer and J. A. Hertz. *Spin glasses*. Cambridge University Press, Cambridge, 1991.
- [14] A. Georges, G. Kotliar, W. Krauth, and M. Rozenberg. Dynamical mean-field theory of strongly correlated fermion systems and the limit of infinite dimensions. *Rev. Mod. Phys.*, 68(1):13–125, 1996.
- [15] A. Georges, O. Parcollet, and S. Sachdev. Mean field theory of a quantum Heisenberg spin glass. *Phys. Rev. Lett.*, 85(4):840–843, 2000.
- [16] A. Georges, O. Parcollet, and S. Sachdev. Quantum fluctuations of a nearly critical Heisenberg spin glass. *Phys. Rev. B*, 63:134406–134422, 2001.
- [17] Y. Y. Goldschmidt and P.-Y. Lai. Ising spin glass in a transverse field: Replica-symmetry-breaking solution. *Phys. Rev. Lett.*, 64(21):2467–2470, 1990.
- [18] Y. Y. Goldschmidt and P.-Y. Lai. Quantum vector spin-glass models in an applied field. *Phys. Rev. B*, 43(13):11434–11437, 1991.
- [19] D. R. Grempel and M. J. Rozenberg. Solution of the quantum Sherrington-Kirkpatrick model. *Phys. Rev. Lett.*, 80(2):389–392, 1998.
- [20] J. Hertz, A. Krogh, and R. G. Palmer. *Introduction to the theory of neural computation*. Addison-Wesley, Redwood City, 1991.
- [21] V. Janiš. Free-energy functional in the generalized coherent-potential approximation. *Phys. Rev. B*, 40(16):11331–11334, 1989.
- [22] V. Janiš and D. Vollhardt. Coupling of quantum degrees of freedom in strongly interacting disordered electron systems. *Phys. Rev. B*, 46(24):15712–15715, 1992.
- [23] Y. Kakehashi. Monte Carlo approach to the dynamical coherent-potential approximation in metallic magnetism. *Phys. Rev. B*, 45(13):7196–204, 1992.
- [24] Y. Kakehashi. Dynamical coherent-potential approximation to the magnetism in a correlated electron system. *Phys. Rev. B*, 65:184420–184435, 2002.
- [25] Y. Kakehashi. Many-body coherent potential approximation, dynamical coherent potential approximation, and dynamical mean-field theory. *Phys. Rev. B*, 66:104428–104436, 2002.
- [26] S. Kirkpatrick and D. Sherrington. Infinite-ranged models of spin-glasses. *Phys. Rev. B*, 17(11):4384–4403, 1978.
- [27] T. K. Kopeć, G. Büttner, and K. D. Usadel. Quantum Heisenberg spin glasses: Anisotropy effects and field dependence. *Phys. Rev. B*, 41(13):9221–9227, 1990.

- [28] W. Metzner and D. Vollhardt. Correlated lattice fermions in $d = \infty$ dimensions. *Phys. Rev. Lett.*, 62(3):324–327, 1989.
- [29] M. Mezard, G. Parisi, and M. A. Virasoro. *Spin glass theory and beyond*. Lecture notes in physics vol. 9. World Scientific Publishing, Singapore, 1987.
- [30] E. Müller-Hartmann. Correlated fermions on a lattice in high dimensions. *Z. Phys. B*, 74:507–512, 1989.
- [31] J. A. Mydosh. *Spin Glasses. An experimental introduction*. Taylor & Francis, London, 1993.
- [32] J. W. Negele and H. Orland. *Quantum Many-Particle Systems*. Advanced Book Classics. Perseus Books, Reading, Massachusetts, 1998.
- [33] H. Nishimori. *Statistical physics of spin glasses and information processing*. International Series of Monographs on Physics. Oxford University Press, Oxford, 111 edition, 2001.
- [34] R. Oppermann and M. Binderberger. Solutions for the $T = 0$ quantum spin glass transition in a metallic model with spin-charge coupling. *Ann. Physik*, 3:494–511, 1994.
- [35] R. Oppermann and A. Müller-Groeling. From localized to itinerant spin glasses: Grassmann field theory and mean-field solutions. *Nucl. Phys. B*, 401:507–547, 1993.
- [36] R. Oppermann and B. Rosenow. Magnetic gaps related to spin glass order in fermionic systems. *Phys. Rev. Lett.*, 80(21):4767–4770, 1998.
- [37] R. Oppermann and B. Rosenow. Parisi symmetry of the many-body quantum theory of randomly interacting fermionic systems. *Phys. Rev. B*, 60(14):10325–10361, 1999.
- [38] R. Oppermann and D. Sherrington. Fermionic Sherrington-Kirkpatrick models with Hubbard interaction: Magnetism and electronic structure. *Phys. Rev. B*, 67:245111–245135, 2003.
- [39] V. N. Popov and S. A. Fedotov. The functional-integration method and diagram technique for spin systems. *Sov. Phys. JETP*, 67(3):535–541, 1988.
- [40] F. Reif. *Fundamentals of statistical and thermal physics*. McGraw-Hill Book Co, Singapore, international edition edition, 1985.
- [41] B. Rosenow and R. Oppermann. Tricritical behavior of Ising spin glasses with charge fluctuations. *Phys. Rev. Lett.*, 77(8):1608–1611, 1996.
- [42] B. Rosenow and R. Oppermann. Metal-insulator transition in randomly interacting systems. cond-mat/9811174, 1998.
- [43] M. J. Rozenberg and D. R. Grempel. Dynamics of the infinite-range Ising spin-glass model in a transverse field. *Phys. Rev. Lett.*, 81(12):2550–2553, 1998.

- [44] S. Sachdev. *Quantum Phase Transitions*. Cambridge University Press, 1999.
- [45] S. Sachdev, N. Read, and R. Oppermann. Quantum field theory of metallic spin glasses. *Phys. Rev. B*, 52(14):10286–10294, 1995.
- [46] S. Sachdev and J. Ye. Gapless spin-fluid ground state in a random quantum Heisenberg model. *Phys. Rev. Lett.*, 70(21):3339–3342, 1993.
- [47] D. Sherrington and S. Kirkpatrick. Solvable model of a spin-glass. *Phys. Rev. Lett.*, 35(26):1792–1796, 1975.
- [48] H.-J. Sommers. Theory of a Heisenberg spin glass. *J. Magn. Magn. Mater.*, 22:267–270, 1980.
- [49] H.-J. Sommers and K. D. Usadel. Theory of an induced-moment spin glass. *Z. Phys. B*, 47:63–69, 1982.
- [50] J. Stoer. *Numerische Mathematik*, volume 1. Springer-Verlag, Berlin, 7 edition, 1994.
- [51] K. D. Usadel, G. Büttner, and T. K. Kopeć. Phase diagram of the quantum Ising spin glass in a transverse field. *Phys. Rev. B*, 44(22):12583–12585, 1991.
- [52] O. Veits, R. Oppermann, M. Binderberger, and J. Stein. Extension of the Popov-Fedotov method to arbitrary spin. *Journal de Physique I*, 4:493–497, 1994.
- [53] R. Vlaming and D. Vollhardt. Controlled mean-field theory for disordered electronic systems: Single-particle properties. *Phys. Rev. B*, 45(9):4637–4649, 1992.
- [54] L. E. Wenger and P. H. Keesom. Calorimetric investigation of a spin-glass alloy: CuMn. *Phys. Rev. B*, 13(9):4053–4059, 1976.
- [55] U. Wolff. Saddle point mean field calculation in the Hubbard model. *Nucl. Phys. B*, 225:391–408, 1983.

Lebenslauf

Persönliches

Name:	Michael Bechmann
Geboren:	10. Mai 1973 in Berlin, Vater Dipl. Ing., Mutter Dipl. Ing. Päd.
Familienstand:	ledig, zwei Kinder

Ausbildung

1979 – 1989	Polytechnische Oberschule in Berlin (Mittlere Reife)
Sep 1989	Beginn einer Berufsausbildung zum Elektromonteur mit Abitur in Neubrandenburg
Jan 1990 – Jun 1992	Abitur am A.v.Humboldt Gymnasium in Schweinfurt
Nov 1994 – Okt 2000	Studium der Physik an der Uni Würzburg, (Röntgen-Studienpreis der Uni Würzburg)
Aug 1997 – Aug 1998	Integriertes Auslandsstudium an der State University of New York (SUNY) at Buffalo
Nov 1996	Vordiplom
Sep 1998	Master of Arts
Dez 2000	Diplom
Seit Nov 2000	Promotionsstudium an der Uni Würzburg, zeitweilig Universitätsstipendiat

Berufliche Tätigkeiten

Dez 1992 – Feb 1994	Zivildienst im Pflegedienst am Leopoldina-Krankenhaus, Schweinfurt
Apr 1999 – Jul 2004	Umfangreiche Tätigkeit als Lehrassistent (Mechanik, Quantenmechanik, Differentialgleichungen etc.)
Nov 2000 – Dez 2004	Diverse Zeitverträge als Wissenschaftl. Angestellter am Inst. f. Theoretische Physik der Uni Würzburg